
Universität Hamburg
DER FORSCHUNG | DER LEHRE | DER BILDUNG

# ASSESSMENT OF STORM SURGE RISK IN THE GERMAN BIGHT: MODELING PAST EVENTS AND PROJECTING FUTURE CHANGES

Dissertation

with the aim of achieving a doctoral degree

at the Faculty of Mathematics, Informatics and Natural Sciences

Department of Earth System Sciences

at University of Hamburg

submitted by

**LAURA SCHAFFER**

Hamburg, November 2025

Department of Earth System Sciences

| | |
|---|---|
| Date of Oral Defense: | 09.02.2026 |
| Reviewers: | Prof. Dr. Johanna Baehr |
| | Dr. Tim Kruschke |
| Members of the examination commission: | Prof. Dr. Felix Ament |
| | Prof. Dr. Eleanor Frajka-Williams |
| | Prof. Dr. Beate M.W. Ratter |

Chair of the Subject Doctoral Committee

| | |
|---|---|
| Earth System Sciences: | Prof. Dr. Dirk Notz |
| Dean of Faculty MIN: | Prof. Dr.-Ing. Norbert Ritter |

The truth is: the natural world is changing. And we are totally dependent on that world. It provides our food, water and air. It is the most precious thing we have and we need to defend it.

— David Attenborough

This document was typeset using the typographical look-and-feel `classicthesis` developed by André Miede and Ivo Pletikosić. The template is openly available at:
https://bitbucket.org/amiede/classicthesis/

## ABSTRACT

Storm surges represent a persistent and growing challenge for coastal populations. These extreme events can cause severe flooding, substantial damage to property and critical infrastructure, and endanger human lives. The German Bight, located in the southeastern North Sea, is a region frequently affected by storm surges. With ongoing climate change, the frequency and intensity of extreme weather events are expected to increase, while rising sea levels further amplify the potential impact of storm surges. In this context, reliable information of future storm surge risk is essential for effective coastal planning and adaptation strategies.

From a scientific perspective, however, significant challenges remain, particularly in translating wind conditions into storm surge heights. This difficulty arises because the response of coastal waters to wind forcing is highly variable and influenced by multiple interacting physical factors. Current approaches rely on either computationally intensive regional or global climate models or highly complex statistical models, neither of which allow for comprehensive multi-model assessments based on climate projections. Consequently, projections of storm surge heights for the German Bight based on multi-model assessments do not yet exist. However, such assessments are essential for providing reliable and robust information on future storm surge risk. Moreover, the few existing projections of storm surge heights, which are based on a single climate model or scenario, do not incorporate sea-level rise, even though it plays a critical role in elevating the baseline water level. Rising sea levels make even moderate storm events increasingly dangerous. Despite its importance, the integration of sea-level rise into storm surge modeling remains an open issue.

As existing modeling approaches do not allow for projecting storm surge heights based on a multi-model ensemble of climate simulations, the first part of this dissertation focuses on developing a statistical storm surge model suitable for this purpose. The statistical model is based on a multiple linear regression approach that uses wind as the only predictor. By systematically tuning the model settings, the final model comprises only five terms – squared wind values at four lead times and an intercept as the fifth term. Despite its simplicity, it has a predictive skill comparable to more complex approaches. Moreover, the storm surge model delivers robust predictions for moderate and extreme storm surges. Its minimal input requirements and computational efficiency make it well suited for using large ensembles of climate model data, providing a valuable tool for projecting future storm surge heights.

Next, I explore the impacts of climate change on storm surge frequency and height in the German Bight. For this purpose, I apply the statistical model to a multi-model ensemble of climate simulations and present projections of storm surge heights for the German Bight across multiple emission scenarios. Based on changes in wind patterns alone I find an increase in the frequency of potential winter storm surge events by around 10% by 2100. Supported by recent studies, this increase is attributed to

a higher frequency of westerly and northwesterly winds, linked to shifts in storm tracks under future climate conditions. When additionally accounting for sea-level rise, moderate and severe present-day storm surge thresholds in the German Bight are projected to be exceeded three to five times more often by the end of the century than historically.

Overall, in this thesis, I introduce a new statistical storm surge model for the German Bight. Its simplicity and efficiency make it a novel tool for investigating storm surge heights across a range of timescales. Moreover, the underlying modeling approach is transferable to coastal regions worldwide where wind is the dominant driver for storm surge development. I demonstrate the statistical model's capabilities by applying it to a multi-model ensemble of climate projections to investigate future storm surge heights in the German Bight. The resulting projections across multiple emission scenarios provide robust insights into how storm surge risk in the German Bight may evolve under a changing climate.

# ZUSAMMENFASSUNG

Sturmfluten stellen für die Bevölkerung in Küstenregionen eine anhaltende und zunehmende Herausforderung dar. Diese Extremereignisse können schwere Überschwemmungen, erhebliche Schäden an Eigentum und kritischer Infrastruktur verursachen und Menschenleben gefährden. Die Deutsche Bucht, im südöstlichen Teil der Nordsee gelegen, ist eine Region, die häufig von Sturmfluten betroffen ist. Mit dem fortschreitenden Klimawandel wird erwartet, dass die Häufigkeit und Intensität extremer Wetterereignisse zunehmen, während der Anstieg des Meeresspiegels die potenziellen Auswirkungen von Sturmfluten zusätzlich verstärkt. In diesem Zusammenhang sind zuverlässige Informationen über das zukünftige Sturmflutrisiko für eine effektive Küstenplanung und Anpassungsstrategien unerlässlich.

Aus wissenschaftlicher Sicht bestehen jedoch nach wie vor erhebliche Herausforderungen, insbesondere bei der Umrechnung von Windverhältnissen in Sturmfluthöhen. Diese Schwierigkeit entsteht, da die Auswirkungen von Wind auf Küstengewässer sehr unterschiedlich sind und von mehreren miteinander interagierenden physikalischen Faktoren beeinflusst werden. Aktuelle Ansätze beruhen entweder auf rechenintensiven regionalen oder globalen Klimamodellen oder auf hochkomplexen statistischen Modellen, wobei keiner dieser Ansätze umfassende Multi-Modell-Bewertungen auf Grundlage von Klimaprojektionen ermöglicht. Folglich gibt es bislang noch keine Projektionen der Sturmfluthöhen für die Deutsche Bucht, die auf Multi-Modell-Beweretungen basieren. Solche Bewertungen sind jedoch unerlässlich, um zuverlässige und fundierte Informationen über das zukünftige Sturmflutrisiko zu liefern. Darüber hinaus beinhalten die wenigen vorhandenen Projektionen der Sturmfluthöhen, die auf einem einzigen Klimamodell oder Szenario basieren, nicht den Anstieg des Meeresspiegels, obwohl dieser eine entscheidene Rolle bei der Ehöhung des Ausgangswasserstandes spielt. Der Anstieg des Meeresspiegels macht selbst moderate Sturmereignisse zunehmend gefährlicher. Trotz seiner Wichtigkeit bleibt die Einbeziehung des Meeresspiegelanstiegs in die Sturmflutmodellierung eine noch zu lösende Aufgabe.

Da bestehende Modellierungsansätze keine Projektionen von Sturmfluthöhen auf der Grundlage eines Multi-Modell-Ensembles von Klimasimulationen ermöglichen, konzentriert sich der erste Teil dieser Dissertation auf die Entwicklung eines statistischen Sturmflutmodells, das für diesen Zweck geeignet ist. Das statistische Sturmflutmodell basiert auf dem Ansatz der multiplen linearen Regression, bei dem Wind als einziger Prädiktor verwendet wird. Durch systematische Anpassung der Modelleinstellungen besteht das endgültige Modell lediglich aus fünf Termen – quadrierte Windwerten zu vier Vorlaufzeiten sowie einem Achsenabschnitt als fünften Term. Trotz seiner Einfachheit hat es eine Vorhersagegenauigkeit, die mit komplexeren Ansätzen vergleichbar ist. Darüber hinaus liefert das Sturmflutmodell robuste Vorhersagen sowohl für moderate als auch für extreme Sturmfluten. Aufgrund seiner minimalen Eingabevorgaben und seiner Recheneffizienz eignet es sich gut zur Verwendung

großer Ensembles von Klimamodelldaten und stellt ein wertvolles Instrument zur Bewertung der zukünftigen Sturmfluthöhen dar.

Als Nächstes untersuche ich die Auswirkungen des Klimawandels auf die Häufigkeit und Höhe von Sturmfluten in der Deutschen Bucht. Dafür wende ich das statistische Modell auf ein Multi-Modell-Ensemble von Klimasimulationen an und stelle Projektionen der Sturmfluthöhen in der Deutschen Bucht unter verschiedenen Emissionsszenarien vor. Allein aufgrund der sich verändernden Windverhältnisse stelle ich bis 2100 eine Zunahme der Häufigkeit potenzieller Wintersturmfluten um etwa 10% fest. Gestützt durch aktuelle Studien wird dieser Anstieg auf eine höhere Häufigkeit von West- und Nordwestwinden zurückgeführt, die mit Verschiebungen der Sturmbahnen unter zukünftigen Klimabedingungen zusammenhängen. Unter zusätzlicher Berücksichtigung des Meeresspiegelanstiegs wird projiziert, dass die heutigen Grenzwerte für moderate und schwere Sturmfluten in der Deutschen Bucht bis zum Ende des Jahrhunderts drei- bis fünfmal häufiger überschritten werden als in der Vergangenheit.

In dieser Arbeit stelle ich ein neues statistisches Sturmflutmodell für die Deutsche Bucht vor. Seine Einfachheit und Effizienz machen es zu einem neuen Instrument zur Untersuchung von Sturmfluthöhen über verschiedene Zeiträume hinweg. Darüber hinaus lässt sich der zugrunde liegende Modellierungsansatz auf Küstenregionen weltweit übertragen, bei denen Wind der dominierende Faktor für die Entstehung von Sturmfluten ist. Ich veranschauliche die Leistungsfähigkeit des statistischen Modells, indem ich es auf ein Multi-Modell-Ensemble von Klimaprojektionen anwende, um zukünftige Sturmfluthöhen in der Deutschen Bucht zu untersuchen. Die daraus resultierenden Projektionen für verschiedenen Emissionsszenarien liefern robuste Erkenntnisse darüber, wie sich das Sturmflutrisiko in der Deutschen Bucht unter sich ändernden Klimabedingungen entwickeln könnte.

# PUBLICATIONS RELATED TO THIS DISSERTATION

Appendix A:

Schaffer, L., Boesch, A., Baehr, J., and Kruschke, T. (2025). "Development of a wind-based storm surge model for the German Bight." *Natural Hazards and Earth System Sciences* 25.6, pp. 2081–2096. DOI: 10.5194/nhess-25-2081-2025.

Appendix B:

Schaffer, L., Baehr, J., and Kruschke, T. (in prep.). "Future Storm Surge Risk in the German Bight."

# ACKNOWLEDGMENTS

What a journey! When I started the position at BSH three and a half years ago, I would have never imagined that I would one day be writing these lines. Actually finishing this thesis means a lot to me, and it would not have been possible without the support, guidance, and company of so many wonderful people along the way.

First of all, I would like to express my heartfelt thanks to my supervisors, Johanna Baehr and Tim Kruschke, for their guidance throughout this PhD journey. Johanna, thank you for welcoming me back into the group, shaping the framework of this PhD, and making me feel as though I had never left. Thank you for your constant support, encouragement, empathy, and for always being there to listen when things got complicated. Thank you for all your advice – both scientific and personal – for your guidance, and for helping me view things from new angles when I felt stuck. Tim, thank you for countless hours of brainstorming, for always keeping your door open, and for helping me stay on track whenever I got lost in the details. I am grateful for your patience in answering my endless questions and for reminding me to zoom out and see the bigger picture when I couldn't see the forest for the trees. Thank you also for celebrating even the small milestones, and for handling the many bureaucratic challenges at BSH – often making things possible that could not be taken for granted. Moreover, I would like to thank Kerstin Jochumsen for being a wonderful panel chair. I truly appreciated our panel meetings and your honest, thoughtful advice, which have greatly contributed to shaping this work.

I would also like to thank the Climate Modeling Group – such a great group of people! Thank you all for welcoming me back so warmly into the team. Even though I was only at the university on Mondays, I truly enjoyed our time together – the chats over lunch, the talks in the kitchen, and the days we spent during the group retreat. I am also grateful for the valuable advice and discussions during our group meetings, which helped me improve my work and see my research from new perspectives. A special thanks to Marlene for welcoming me into her office and for being such a wonderful Monday office-mate. I really enjoyed all our conversations – whether about science or about life in general. Thanks also to Edu for patiently answering all my formal thesis-related questions, especially in the last few months.

A huge thank you to the members of the Marine Climate group at BSH, especially Claudia, Corinna, Frank and Jens, for the many scientific discussions and valuable advice. I truly enjoyed our exchanges – they were inspiring, motivating and always left me with new ideas and energy for my work. A very special thanks goes to Corinna, the best office-mate I could have imagined. Thank you for all the joint brainstorming sessions, for helping me in interpret results and for motivating me. Thank you for the endless supply of snacks when my brain needed extra sugar and for all the chatting and laughing that made every day in the office a joy.

Many thanks to Claudia, Frank, Jens, Daniel, Arne, Lena and Patricia for taking the time to proofread my thesis. Your comments and feedback were invaluable and greatly helped to improve the quality and clarity of this work.

Finally, I would like to thank my family and my partner, Arne. To my family, thank you for you support and for never giving up on trying to understand what I am actually doing every day. Arne, thank you for sharing all the ups and downs of this journey with me, for always cheering me up, and for standing by my side with your support and patience.

# CONTENTS

# LIST OF FIGURES

# LIST OF TABLES

| | |
|---|---|
| BSH | Bundesamt für Seeschifffahrt und Hydrographie<br>German Federal Maritime and Hydrographic Agency |
| CDF | Cumulative Distribution Function |
| CMIP | Coupled Model Intercomparison Project |
| DJF | December-February |
| ECMWF | European Centre for Medium-Range Weather Forecasts |
| ERA5 | European Centre for Medium-Range Weather Forecasts Reanalysis v5 |
| hwss | High-water skew surge |
| JJA | June-August |
| MHW | Mean High Water |
| NAO | North Atlantic Oscillation |
| OLS | Ordinary Least Squares |
| PDF | Probability Density Function |
| RMSE | Root-Mean-Square Error |
| SLR | Sea-Level Rise |
| SSPs | Shared Socioeconomic Pathways |

# UNIFYING ESSAY

# 1 INTRODUCTION

## 1.1 STORM SURGES: NATURE'S NEVER-ENDING CHALLENGE TO COASTS

The ocean is never still. Its constant motion – tides, waves and surges – has fascinated observers for centuries. For as long as humans have lived near the coast, the sea has been both a vital source of sustenance and a subject of enduring fascination, but also of awe and respect for its power (O'Halloran and Silver, 2022). Storm surges – sudden increases of coastal water levels driven by strong winds – are among the most striking expressions of the ocean's force. They are capable of reshaping coastlines within hours, making them a critical challenge for coastal regions worldwide, as they are more exposed to natural hazards than any other region (Kron, 2013). Storm surges can cause severe flooding and erosion, leading to widespread damage to infrastructure and property. They may also result in loss of life and injury, making them one of the most destructive coastal hazards (von Storch, 2014). In 2018, about 10% of the global population resided within 5 km of the shoreline and nearly 25% within 50 km (Cosby et al., 2024). As the population in coastal areas continue to grow faster than in inland regions, both the exposure and vulnerability to storm surges are steadily increasing (Cosby et al., 2024).

Among the regions worldwide that are exposed to the risk of extreme water levels, the German Bight (Fig. 1.1) in the southeastern North Sea is particularly prone to storm surges. Its location at the narrow, funnel-shaped end of the North Sea amplifies surge levels as wind-driven water masses are pushed toward the shallow southeastern corner. Especially, strong northwesterly winds coinciding with high tide can lead to extreme water levels along the German Bight coast (Gönnert, 2003; Jensen and Müller-Navarra, 2008). An example of the destructive potential of storm surges in the German Bight is the storm surge of 16 February 1962. Most affected was the city of Hamburg which is located at the end of the Elbe estuary, about 100 km inland from the North Sea Coast (Fig. 1.1). During storm surges, water accumulates there as the North Sea is forced inland through the estuary. The event was the most deadly in the city's 20th-century history, claiming more than 300 lives, and the most costly, with damages of 1.6 billion EUR (de Guttry and Ratter, 2022; Jochner et al., 2013). It also ranks as the biggest natural disaster in Germany during this period. The flooding caused dikes to breach and inundated large parts of the city, destroying 6,000 buildings and leaving 20,000 people homeless (de Guttry and Ratter, 2022; Jochner et al., 2013; Meyer and Gaslikova, 2024). The storm surge of 1962 served as an alarm bell, demonstrating the urgent need for a fundamental renewal of storm surge protection. In response, massive investments were made in coastal defense. The design water levels were recalculated, and dikes were subsequently widened, raised, and in many sections completely rebuilt. In addition, disaster plans were established and public information measures were improved (de Guttry and Ratter, 2022; Meyer and Gaslikova, 2024; von Storch et al., 2008; von Storch and Woth, 2008). The effective-

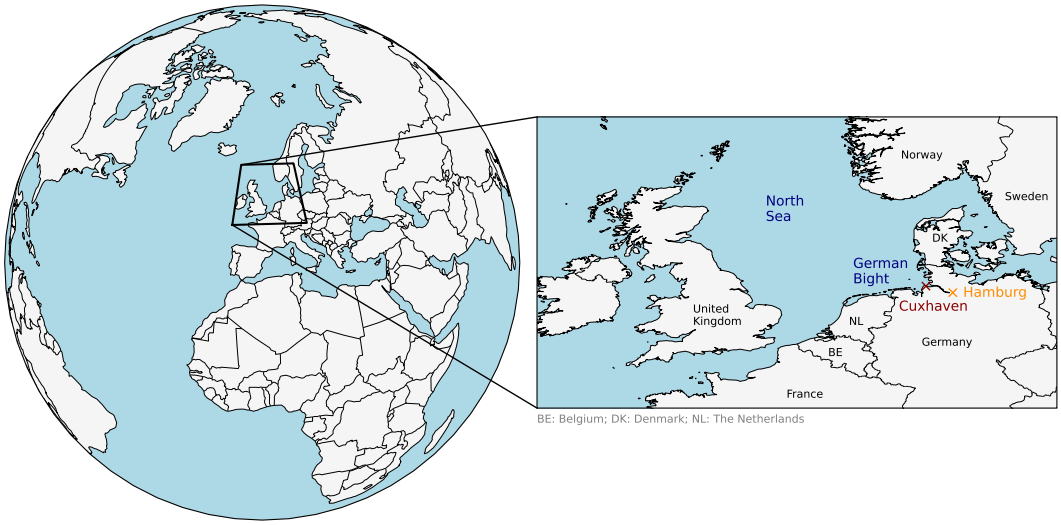


Figure 1.1: Map showing the German Bight and the cities of Hamburg and Cuxhaven.

ness of these efforts became evident during the storm surge of 3 January 1976. This event produced the highest water levels ever recorded in the German Bight, well above those of 1962. Nevertheless, the newly reinforced coastal defenses withstood the surge, resulting in insignificant damages in Hamburg and, crucially, no loss of life in the city (de Guttry and Ratter, 2022; Meyer and Gaslikova, 2024; von Storch and Woth, 2008).

Over the past century, coastal protection along the German Bight has continuously improved considerably, with dikes, seawalls, beach nourishment, and wetlands providing a combination of hard and nature-based defenses. At the same time, the population along the German Bight coast has grown, placing more people and critical infrastructure in areas vulnerable to flooding and storm surges. To inform coastal planning and enable authorities to anticipate future hazards and implement effective protection measures, research providing reliable projections of storm surge heights is essential. However, substantial uncertainties remain regarding future storm surge behavior. The magnitude and direction of change in storm surge heights depend on several interacting factors. In particular, potential changes in wind patterns over the North Sea could significantly alter storm surge heights in the German Bight. Accelerating sea-level rise (SLR) will further influence surge levels by increasing the baseline water level (Fox-Kemper et al., 2021). Understanding the extent to which these factors will affect future storm surge heights in the German Bight is a key challenge.

To address this challenge and to estimate future storm surge heights in the German Bight, it is first necessary to define what constitutes a storm surge (Sect. 1.2). Furthermore, it is important to outline the primary drivers behind these events (Sect. 1.3) and to describe projected changes in these drivers under future climate conditions (Sect. 1.4). Finally, reviewing how storm surges have been modeled in past studies and evaluating the applicability of these approaches for projecting future storm surge heights is essential (Sect. 1.5).

A storm surge is the ocean's response to certain meteorological conditions and occurs only when these conditions coincide with high tide. Strong winds during a storm can elevate water levels along coastlines and estuaries above the expected tidal heights. However, not every increase in water level qualifies a storm surge – it has to surpass a specific threshold. If this threshold is not exceeded, the wind-induced water level change is referred to as a wind surge. Wind surges can be either positive, causing higher water levels than expected, or negative, causing lower water levels than expected, depending on the wind forcing. These wind surges are superimposed on the regular tides, and when the combined water level exceeds a defined threshold, it is classified as a storm surge. The definition of the storm surge threshold varies between different coastal regions and responsible authorities, as it depends strongly on local tidal dynamics. In areas with large tidal ranges, the reference values for identifying a storm surge are generally higher than in regions with little or no tidal influence. In the German Bight and its connected estuaries, the wind-driven component of storm surges can reach several meters – comparable to the tidal cycle itself. The German Federal Maritime and Hydrographic Agency (Bundesamt für Seeschiffahrt und Hydrographie, BSH) classifies storm surges in the North Sea relative to Mean High Water (MHW), which is the average high tide level calculated from several years of observations. MHW serves as a reference level around which individual high tides fluctuate due to the regular spring-neap cycle (BSH, 2025b). Based on this reference, storm surges along the German Bight coastline are defined according to their intensity: water levels exceeding 1.5 m above MHW are considered storm surges, those above 2.5 m are severe storm surges, and those exceeding 3.5 m are classified as very severe storm surges (Fig. 1.2) (BSH, 2025a).

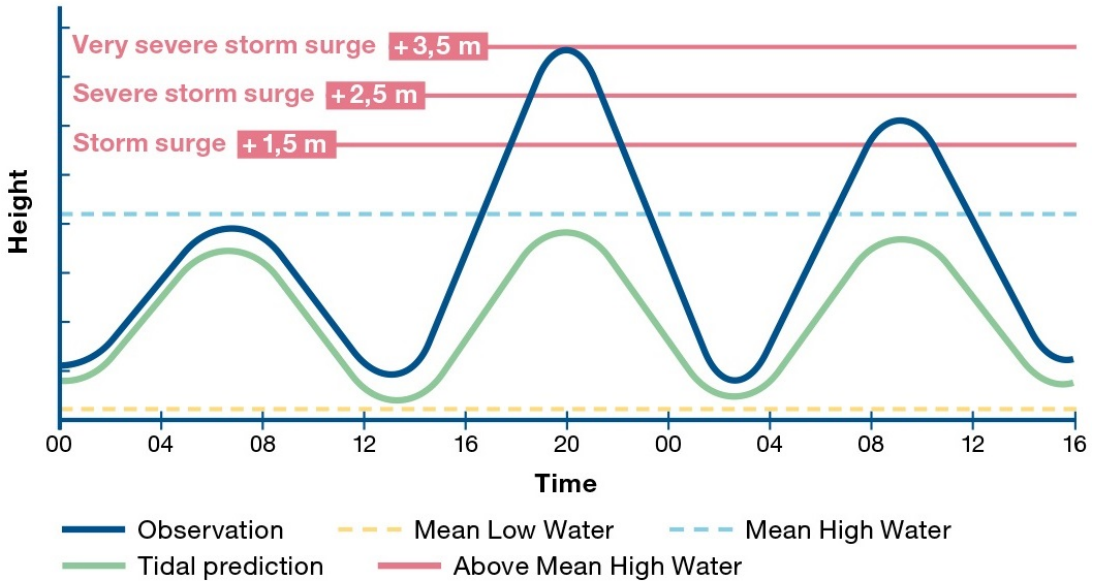


Figure 1.2: Simplified representation of storm surge thresholds for the German Bight. Adapted from BSH (2024).

Storm surges in the German Bight only develop when storm events coincide with high tide. Under these conditions, the height of the surge depends on several interacting factors – such as wind speed and direction, atmospheric pressure, external surges, and coastal geometry – which together control how much water is pushed toward the coast. Hence, research on storm surges in the German Bight necessarily require an understanding of the governing large-scale atmospheric processes. The German Bight, together with the wider North Sea, lies within the North Atlantic storm track. Spanning from the western North Atlantic Ocean into northwestern Europe, the storm track constitutes the principal pathway for extratropical cyclones and is associated with high wind speeds (Blender et al., 1997; Dacre et al., 2012). Storm surges in the German Bight are closely linked to the position, intensity and frequency of extratropical cyclones traveling along this track. The location of the storm track is not stationary. It undergoes meridional and zonal shifts in response to modes of climate variability, especially the North Atlantic Oscillation (NAO) (Hurrell et al., 2003).

The NAO describes variations in the sea-level pressure gradient between the Icelandic Low and the Azores High, commonly expressed through the NAO index. A positive NAO phase reflects an enhanced pressure gradient, characterized by a deepened Icelandic Low and a strengthened Azores High. Under NAO+ conditions, the storm track shifts northward, while stronger and more persistent westerly winds prevail over Northern Europe (Hurrell and Deser, 2010; Hurrell et al., 2003; Mathis et al., 2015; Wakelin et al., 2003). These westerly winds are a key driver for elevated water levels in the German Bight, as their persistent occurrence pushes water masses into the shallow, funnel-shaped southeastern part of the North Sea (Fig. 1.1). Conversely, a negative NAO phase is characterized by a weakened pressure gradient, with the storm track shifting southward and westerly winds over Northern Europe becoming weaker (Hurrell and Deser, 2010; Hurrell et al., 2003; Wakelin et al., 2003).

Extratropical cyclones traveling along the North Atlantic storm track are primary drivers of extreme storm surges in the German Bight. They can form locally from small atmospheric disturbances, such as weak lows, or originate as tropical cyclones in the subtropics and transform as they move north into cooler regions. Their intensification is driven by strong temperature contrasts between air masses, which are typically found along the polar jet stream – a fast upper-level current that guides cyclones along the storm track. The impact of extratropical cyclones and their associated high wind speeds on storm surges in the German Bight depends primarily on the cyclones' trajectory, as this determines the direction and intensity of the wind forcing (Gerber et al., 2016). In particular, strong westerly to northwesterly winds over the North Sea region, often associated with cyclones passing over Scandinavia, are the most effective drivers for storm surges in the German Bight (Meyer and Gaslikova, 2024). In addition to generating high winds, these extratropical cyclones are low-pressure systems, which cause an extra rise in sea level through the inverse barometer effect: as atmospheric pressure drops, the weight of the air on the sea surface decreases, allowing the water level to rise (Böhme et al., 2023; Koopmann, 1962).

Another important contributor to extreme water levels along the North Sea Coast are external surges. These originate from storms over the North Atlantic and are amplified as they propagate onto the continental shelf. They can raise sea levels by over one meter along the British, Dutch and German coasts (Böhme et al., 2023). When they coincide with locally generated surges, the combined effect can produce extreme water levels. In the German Bight, for instance, their average contribution during storm surges is about 50 cm (Böhme et al., 2023).

The primary drivers of storm surges in the German Bight operate across multiple scales. They range from the position, intensity, and frequency of extratropical cyclones traveling along the North Atlantic storm track to the orientation of local wind conditions, both shaped by modes of climate variability. The local geography of the German Bight further modulates the magnitude of surge events, while external surges highlight the interplay between remote and local processes in generating extreme water levels. Understanding storm surges in this region therefore requires a holistic perspective that links large-scale atmospheric variability with regional meteorology and coastal dynamics. This also includes the fact that storm surges only develop when storm conditions coincide with high tide. Looking ahead, future storm surge heights in the German Bight will depend on how these interacting drivers evolve under climate change, apart from the overarching influence of sea-level rise.

## 1.4 Storm surges and their drivers in a changing climate

Climate change is expected to increase the frequency and severity of extreme events, including extreme sea levels driven by storm surges (Bernier et al., 2024; Dangendorf et al., 2025). This is of particular concern for low-lying coastal regions, with the German Bight coastline being one of them. Therefore, developing robust projections of future storm surge heights is essential, as they provide the scientific basis for coastal risk management, adaptation strategies, spatial planning and the design of resilient infrastructure in this region (Bernier et al., 2024). A central aspect of these projections is the influence of large-scale atmospheric patterns, which are expected to change under global warming (Bernier et al., 2024).

In the German Bight, storm surges are predominantly induced by extra-tropical cyclones, which, depending on their trajectory, can generate strong westerly and northwesterly winds over the North Sea. These winds act as the main drivers of surge events. Consequently, projected changes in cyclone frequency, intensity and tracks are central to any assessment of future storm surge heights. Numerous studies have investigated how climate change may affect storms and storm tracks over the North Atlantic (e.g. Harvey et al., 2020, 2014, 2015; Lee et al., 2021; Lehmann et al., 2014; Priestley and Catto, 2022). According to the IPCC's 6th assessment report, multimodel analyses indicate that the total number of cyclones over the North Atlantic is projected to decrease by the end of the century (Priestley and Catto, 2022; Seneviratne et al., 2021). Despite the overall decrease in cyclone numbers, the frequency of intense cyclones affecting Northern Europe during winter is projected to increase (Priestley and Catto, 2022; Seneviratne et al., 2021). During the Northern Hemisphere winter, the North Atlantic storm track is expected to strengthen and extend further

into Europe, accompanied by a reduction in cyclone activity over the Mediterranean (Harvey et al., 2020; Priestley and Catto, 2022; Seneviratne et al., 2021). In contrast, during the summer months, storm track density is projected to decline across Northern Europe, leading to reduced cyclone activity (Priestley and Catto, 2022). These global-warming-induced changes are most pronounced under higher emission scenarios (Harvey et al., 2020; Priestley and Catto, 2022). Even minor shifts may trigger substantial changes in the frequency and intensity of extreme events at particular locations (Seneviratne et al., 2021). This is particularly relevant for the German Bight, where winds from extra-tropical cyclones largely control storm surge magnitudes. Recent studies provide consistent evidence that rising greenhouse gas concentrations may alter both the frequency and intensity of wind regimes, with direct implications for storm surge characteristics in the German Bight. For instance, Schade et al. (2025) project a higher frequency of westerly wind patterns over the North Sea toward the end of the century. Moreover, Krieger and Weisse (2025) report an increasing frequency of northwesterly winds over the German Bight, both developments enhancing the occurrence of storm surge events. Krieger and Weisse (2025) further indicate that the most extreme storms in the region may become both stronger and more frequent under future climate conditions. In addition, Ortega et al. (2025) highlight an increasing frequency and intensity of westerly winds over the German Bight during the winter months, potentially associated with a predominance of the positive NAO phase. This is in line with Mitevski et al. (2025), who show that under higher $CO_2$ concentrations the NAO is projected to shift toward more positive and less variable phases, in both winter and summer. Such a shift includes more frequent extreme NAO+ events and a decline in extreme NAO- events, particularly in winter. These changes ultimately promote stronger and more frequent westerly winds across Europe and the North Atlantic (Mitevski et al., 2025).

Although future changes in wind conditions have been widely studied, few investigations address how these changes translate into storm surge heights, leaving comprehensive surge projections limited (Bernier et al., 2024). Nevertheless, existing approaches rely on future projections from global or regional climate models. For instance, using a regionally coupled climate system model, Lang and Mikolajewicz (2020) report an increased frequency, height and duration of storm surges in the German Bight under rising $CO_2$ conditions, even without accounting for mean sea-level rise. They explain these findings by enhanced storm track activity combined with more extreme westerly winds over the region. These results are later supported by Mayer et al. (2022), who, using a dynamically downscaled global single model ensemble, investigate climate-induced changes in height, duration and frequency of storm surges in the German Bight. Their analysis confirms that storm surge characteristics are projected to intensify toward the end of the century, resulting in a higher frequency of storm surge events. Recent work by Irazoqui Apecechea et al. (2025), conducted in parallel to this dissertation, presents a hybrid statistical downscaling model that uses a large ensemble of climate model simulations to project future extreme storm surges across Europe. In contrast to the aforementioned studies, they find no robust change in storm surge intensity for the southern North Sea by 2100.

While wind-driven water level elevations that coincide with high tide contribute substantially to extreme coastal water levels, they only represent one component of the overall picture. Another critical factor, however, is the ongoing and long-term rise in mean sea level. It is well established that global mean sea level is rising as a result of global warming, primarily due to a combination of ice melting and thermal expansion. Regionally, changes in sea level have historically been the main driver for variations in extreme sea levels, as observed across the global tide gauge network during the 20th century (Fox-Kemper et al., 2021). Looking ahead, the IPCC's 6th assessment report highlights that sea-level rise is projected to remain the dominant factor behind the substantial increase in the frequency of extreme sea levels throughout the next century (Fox-Kemper et al., 2021). Given the accelerating rise in sea level in the North Sea (Steffelbauer et al., 2022), the storm intensity required to reach critical flood levels is reduced, meaning that even moderate storm events may pose a significant risk. Consequently, assessments of future coastal hazards and the design of adaptation measures must account for changes in both wind conditions and mean sea level simultaneously.

In summary, recent research shows substantial progress in examining climate change-induced changes to the North Atlantic storm track and wind conditions over the North Sea. These developments suggest shifts in the frequency and intensity of storm surges in the German Bight. However, challenges remain in translating these projected changes in wind conditions into corresponding storm surge heights. As a result, the number of available surge projections remains limited. Moreover, incorporating sea-level rise into surge projections is crucial, since it raises the baseline for storm surges, making even moderate storm events more dangerous, yet this remains an open issue. The limited availability of storm surge projections and the lack of sea-level rise inclusion, highlight the need for further research.

## 1.5 Storm surge modeling: applications and limitations

The German Bight has long been a focus of storm surge research, with approaches ranging from hydrodynamic models to statistical methods and, more recently, machine learning (e.g., Befort et al., 2015; Dangendorf et al., 2014; Harter et al., 2024; Jensen et al., 2013; Krieger et al., 2025; Lang and Mikolajewicz, 2020; Mayer et al., 2022; Müller-Navarra and Giese, 1999; Müller-Navarra et al., 2003; Niehüser et al., 2018). For both, previous studies and in this dissertation, Cuxhaven, a city located centrally along the German Bight coast (Fig. 1.1) often serves as a proxy for the entire German Bight. Cuxhaven plays a crucial role for Hamburg, as storm surge heights observed there provide an early indication of how high the surge could be in Hamburg several hours later. Moreover, Cuxhaven has an extensive historical tide gauge record, offering important data for the analysis and modeling of storm surges.

Hydrodynamic models are the most advanced and reliable tools for translating atmospheric forcing into surge estimates. They are capable of reproducing the complex physical processes that drive coastal water level extremes and can provide detailed simulations of surge events. However, this strength comes at a cost: they require extensive input data and significant computational resources, especially for large do-

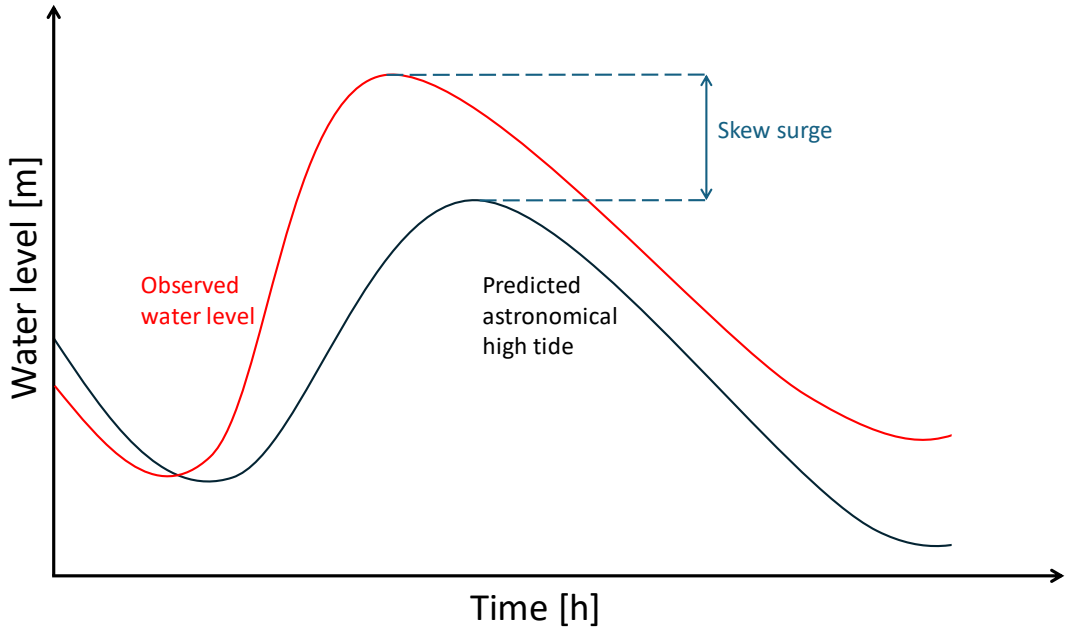


Figure 1.3: Simplified schematic of the skew surge. Adapted from Williams et al. (2016).

mains or high-resolution studies. These limitations reduce their suitability for long-term climate projections, where multiple simulations are necessary, highlighting the need for simpler, more efficient approaches.

Statistical methods provide a practical alternative to hydrodynamical modeling. In this context, a useful metric for storm surge research in the German Bight is the skew surge (Williams et al., 2016). It is defined as the difference between the observed water level and the expected astronomical high water, independent of the time (Fig. 1.3). This measure effectively removes the tidal component, highlighting the meteorological contribution to surges. One common statistical approach to predict skew surges is multiple linear regression, which requires suitable variables as input, referred to as predictors. Early work by Müller-Navarra and Giese (1999) incorporates a range of predictors to capture the main drivers of skew surges, including wind speed and direction, air and sea surface temperature, air pressure and its three-hourly change, water levels at Wick on the Scottish east coast 12 hours earlier, and the immediately preceding low and high water levels at Cuxhaven. This results in an empirical model with 14 basic functions capable of reproducing skew surge height at Cuxhaven. Subsequent studies refined this approach by, for example, excluding external surges to focus on atmospheric forcing (Dangendorf et al., 2014), reconstructing historical surges (Dangendorf et al., 2014; Jensen et al., 2013), or adjusting predictor locations and time lags (Niehüser et al., 2018). Despite these variations, the statistical models consistently show comparable predictive skill. While they offer valuable insights, the statistical models are comparatively complex due to the large number of location- or region-specific input variables they require. These models are primarily designed for detailed, event-specific storm surge prediction where such tailored inputs are essential. In this dissertation, however, the focus is on projecting future storm surge heights rather than predicting individual events. Consequently, these models are not

well suited for use with climate projection data, where only a few variables are available. In addition, climate projection data are provided at a coarse spatial resolution, which further limits the usefulness of the above mentioned statistical modeling approaches for assessing future storm surge heights. In order to incorporate necessary climate projection data, a less complex statistical model is needed.

Another statistical method and useful proxy for assessing storm surge conditions in the German Bight is the effective wind. The effective wind consists of wind speed and direction, reflecting the wind contribution most favorable for generating storm surges at a given location (Jensen et al., 2006; Müller-Navarra et al., 2003). Based on a regression analysis, for Cuxhaven the effective wind corresponds to the fraction of the 10 m wind blowing from 295°. This direction was empirically determined to be the one causing the strongest wind-induced increases in water levels in the German Bight (Jensen et al., 2006; Müller-Navarra et al., 2003). When averaged over the region, the effective wind thus provides a quantitative measure of the wind contribution to surge development and serves as an indicator of the storm surge potential of a given weather situation (Jensen et al., 2006). Different studies further demonstrate that combining the effective wind with a storm tracking algorithm improves the identification of storm surge events compared to relying on the effective wind alone (Befort et al., 2015; Ganske et al., 2018).

In addition to statistical models, neural networks have been applied to storm surge reconstruction, providing a flexible alternative capable of capturing more complex, nonlinear relationships. A comparison by Harter et al. (2024) shows that statistical models using multiple linear regression and neural networks demonstrate comparable overall performance and share a common tendency to underestimate extreme events. Neural networks can, however, reconstruct surges even when local wind data are missing by learning from large-scale sea level pressure patterns (Harter et al., 2024). Neural networks are effective at capturing complex, nonlinear relationships, but they are also far more complex than traditional statistical models and operate as "black boxes", making it difficult to interpret how input variables influence predictions. In contrast, statistical models based on multiple linear regression require less data and are computationally efficient. Moreover, they provide a simple, transparent framework, where the contribution and significance of each predictor to the outcome can be clearly understood and quantified. This interpretability is crucial for understanding causal mechanisms and communicating results.

## 1.6 How my research fits in

Previous research has advanced our understanding of projected changes in the key drivers of storm surges in the German Bight. In particular, studies highlight shifts in wind conditions over the North Sea and changes in the characteristics of extratropical cyclones along the North Atlantic storm track. However, relatively few studies have translated such atmospheric changes directly into projections of future storm surge heights. Existing analyses for the German Bight rely on a single emission scenario (Irazoqui Apecechea et al., 2025; Mayer et al., 2022) or are based on a single climate model (Lang and Mikolajewicz, 2020; Mayer et al., 2022). This limits the ro-

bustness of the results and makes it difficult to assess the range of possible outcomes. To strengthen confidence in future projections, it is essential to use multi-model ensembles, which account for uncertainties in climate projections. Equally important is the consideration of a broader range of climate change emission scenarios, as they represent a range of possible futures and form a crucial basis for assessing future coastal risk. However, projecting storm surge heights in the German Bight under different climate change emission scenarios using multi-model ensembles remains a challenge. Applying a hybrid statistical downscaling model to climate projections, Irazoqui Apecechea et al. (2025) find large disagreement among climate models regarding potential changes in storm surge intensity in the southern North Sea. These results underscore the need for region-specific models or methods applicable to climate projections to better capture local storm surge dynamics in the southern North Sea. Additionally, while it is well established that sea-level rise raises the baseline for storm surges, its explicit incorporation into surge projections remains a key challenge that has not yet been addressed.

Against this background, and motivated by the need to understand how storm surge heights in the German Bight may change under different climate pathways, the overarching research question guiding this work is:

**How will climate change affect storm surge risk in the German Bight?**

Answering the research question using a multi-model ensemble of climate simulations presents methodological challenges. Most statistical storm surge models available for the German Bight are designed for detailed, event-specific storm surge prediction and require numerous input variables for very specific locations or regions (Dangendorf et al., 2014; Jensen et al., 2013; Müller-Navarra and Giese, 1999; Niehüser et al., 2018). Consequently, they are not suitable for use with climate projection data, as climate models operate at coarse spatial resolution and provide only a limited number of variables. This leaves a key challenge unaddressed: the development of a storm surge model that can work with such sparse input. This gap motivates the development of a simple statistical storm surge model for the German Bight that relies on a single variable and can be applied to climate projections. In this dissertation, I focus on statistical modeling approaches rather than hydrodynamic or machine learning methods, as they offer a simpler, more practical, and computationally efficient pathway. Given that wind is the primary driver of storm surges in the German Bight, and that corresponding data is consistently available from climate model simulations, I aim to first address the following research question:

1. **How well can a simple wind-based regression model predict storm surges in the German Bight?**

In Paper A (Chapter 2; Schaffer et al., 2025), I develop a statistical storm surge model for the German Bight using a multiple linear regression approach with wind-based predictors. The aim is to provide a simple and climate-projection-suitable alternative to existing statistical models. The statistical model is based on the concept of the effective wind. At any point in the North Sea, the effective wind is defined as

the fraction of the wind from directions most favorable for generating surges in the German Bight. These effective wind values serve as predictors at multiple locations and lead times within the North Sea region, thereby capturing both the temporal and spatial evolution of storm systems. To ensure robustness and avoid overfitting, I employ a regularization method in the regression, allowing the model to objectively select the most relevant predictors to improve prediction accuracy while maintaining simplicity. Trained and validated against long tide gauge records from Cuxhaven, the model achieves predictive skill comparable to more complex statistical approaches, despite its simplicity.

Encouraged by the model's strong performance and its applicability to climate projections, I aim to answer the following research questions:

2. **How will future storm surge heights in the German Bight evolve solely due to potential changes in wind patterns, based on a multi-model assessment?**

3. **How will the combined effect of future wind-driven changes in storm surge heights and projected sea-level rise impact extreme water levels in the German Bight?**

In Paper B (Chapter 3; Schaffer et al., in prep.), I investigate future storm surge heights in the German Bight by applying the statistical storm surge model developed in Paper A to wind data from a multi-model ensemble from the sixth phase of the Coupled Model Intercomparison Project (CMIP6) under three different emission scenarios. I analyze how changes in large-scale atmospheric conditions may influence the frequency and height of storm surges during winter (December-February, DJF) and summer (June-August, JJA). Additionally, I combine projected wind-driven surges with sea-level rise projections for Cuxhaven to estimate future winter coastal water levels at high tide.

# 2

# WIND-BASED STORM SURGE PREDICTION: A SIMPLE STATISTICAL MODEL

Projecting storm surge heights in the German Bight is of major importance in the context of climate change, as potential shifts in the atmospheric drivers could significantly intensify coastal hazards. Existing statistical approaches for modeling storm surges in the region often rely on large numbers of location-specific input variables and are typically based only on observational data or atmospheric reanalysis. Developed for detailed, event-specific storm surge prediction, these approaches offer valuable insights but are too complex to be applied directly to climate projection data. To overcome this gap, there is a clear need for robust statistical storm surge models that are applicable to climate model outputs, thereby enabling projections of future storm surge heights in the German Bight. In Paper A, I therefore develop a wind-based statistical storm surge model for the German Bight, incorporating regularization techniques to simplify the model. The study thus addresses the following research question:

**How well can a simple wind-based regression model predict storm surges in the German Bight?**

## 2.1 MODEL DEVELOPMENT AND TRAINING FRAMEWORK

The statistical storm surge model developed in Paper A is set up for the tide gauge station at Cuxhaven, which provides a long-term and reliable observational record representative of storm surge conditions in the German Bight. I develop the model using the multiple linear regression approach. For this, both a target variable and a predictor variable are required. In the following, I describe the target variable in detail. Given that the skew surge in Cuxhaven serves as an useful metric for storm surge research (Sect. 1.5), I select it as the target variable. Since the focus lies on storm surge conditions, I only consider positive skew surges during high tide. To determine an appropriate training subsample, I test several thresholds as the lower boundary for defining the subsample ranging from a skew surge of 50 cm to 150 cm and ultimately select a threshold of 80 cm. This choice is based on three findings, which are elaborated in Paper A: (1) model performance does not differ significantly from other thresholds, (2) the selected threshold provides a sufficient large dataset for efficient model training, and (3) it ensures a satisfactory representation of extreme events. The resulting skew surge distribution is not normally distributed. Since multiple linear regression performs best when the target variable is close to a normal distribution, I apply a logarithmic transformation to normalize the data. Consequently, the model is trained using log-transformed skew surge values of greater than or equal to 80 cm as the target variable.

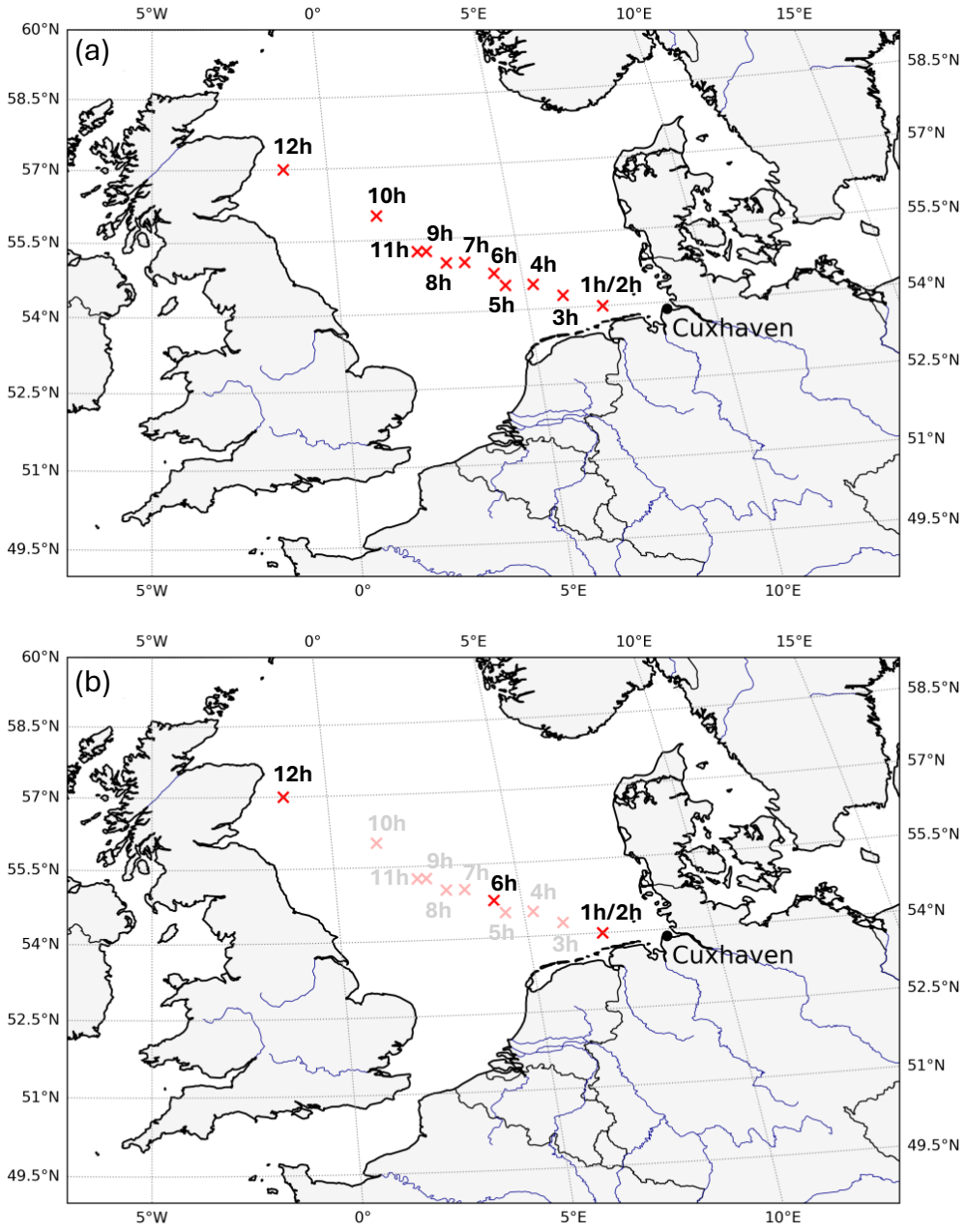


Figure 2.1: Predictor locations across the North Sea for high water skew surge events $\geqslant$ 80 cm. (a) Red crosses mark the selected grid cells, with the corresponding lead times (in hours) indicated above each location. (b) Grid cells retained after applying the elastic net regression, with non-selected grid cells shown in a faded background. Adapted from Paper A Fig. A.3.

As the predictor variable, I use the effective wind (Sect. 1.5), as wind has proven to be the primary driver of storm surges in the German Bight. To derive this variable, I identify the wind direction most relevant for generating high water skew surges at or above the 80 cm training threshold. I determine this wind direction separately for every grid cell in the North Sea region (longitudes -5 to 10.5°E, latitudes 51 to 59°N) using hourly wind data from the European Centre for Medium-Range

Weather Forecasts Reanalysis version 5 (ERA5; Hersbach et al., 2020) for the period 1959-2022. By projecting the actual wind components onto the corresponding relevant wind directions, I obtain the effective wind for each grid cell within the North Sea region in hourly resolution for the same period. Before training the statistical model, I first identify the most relevant predictor locations across the North Sea region. Thus, unlike static predictor approaches (Dangendorf et al., 2014; Jensen et al., 2013; Müller-Navarra and Giese, 1999), I apply the method of non-static predictors, accounting for temporal and spatial variations in the wind forcing. This method only considers predictor locations relevant to the observed skew surge variability in Cuxhaven. To identify these locations, I use effective wind data up to 12 hours before the skew surge events. At each lead time, I select the grid cell across the entire North Sea region that is most strongly associated with skew surge events during high tide of at least 80 cm in Cuxhaven (details are provided in Paper A). The temporal evolution of the selected grid cells follows a clear northwest-to-southeast progression (Fig. 2.1 a). This pattern aligns with typical storm situations driving storm surges in the German Bight. The effective wind values at these specific grid cells, together with their corresponding lead times, serve as predictors in the statistical model.

Subsequently, I perform multiple linear regression to relate the selected predictors to observed high water skew surges greater or equal to 80 cm in Cuxhaven. To reduce model complexity and improve robustness, I incorporate regularization techniques, which prevent overfitting and enhance the model's reliability. Among the three regularization methods tested, I select the elastic net regression (Zou and Hastie, 2005) which combines the advantages of the other approaches. Elastic net regression simultaneously shrinks coefficients and eliminates irrelevant predictors, resulting in a simple model. The outcome is a statistical storm surge model comprising only five terms: the squared effective wind in certain grid cells (Fig. 2.1 b) at four lead times (12, 6, 2 and 1 hour prior to the skew surge event) as robust predictors, along with an intercept.

## 2.2 MODEL PERFORMANCE

To verify the storm surge model, I apply it to predict all high water skew surge events in Cuxhaven from 1959 to 2022. This also includes events below the 80 cm training threshold, enabling an assessment of the model's capability to predict skew surge events on which it was not trained. The model is trained on all years (high water skew surge $\geqslant$ 80 cm) except the one being predicted. For example, to predict the skew surges in the year 2000, the statistical model is trained using all high water skew surge values $\geqslant$ 80 cm from the years 1959-1999 and 2001-2022. This procedure is repeated for each year from 1959-2022. A comparison between observed and predicted skew surges shows a strong correlation of 0.867 and an $R^2$ of 0.751, indicating good overall model performance (Fig. 2.2 a). However, the model tends to overestimate events with observed surges below 80 cm and underestimate those with observed surges exceeding 150 cm. The underestimation of extreme surges is likely related to the limited number of extreme events in the dataset, whereas the overestimation of low or negative skew surges results from training the model on logarithmic values.

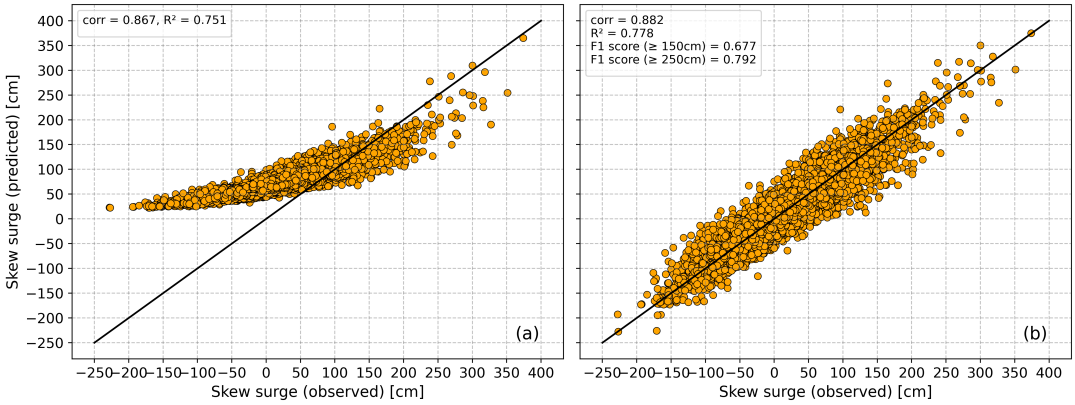


Figure 2.2: Scatter plots comparing observed and predicted skew surge heights from 1959 to 2022 before (a) and after (b) applying quantile mapping bias correction. The black diagonal line indicates perfect agreement between observed and predicted skew surges. The model is trained on events with high water skew surges $\geqslant$ 80 cm using elastic net regularization, excluding the year being predicted from the training. Taken from Paper A Fig. A.7.

This arises from the fact that logarithmic functions are only defined for positive real numbers. To correct this bias, I apply a quantile mapping technique following Cannon et al. (2015) to align the distributions of predicted and observed skew surges. After applying the bias correction, the correlation and $R^2$ values improve to 0.882 and 0.778, respectively (Fig. 2.2 b). The quantile mapping method successfully reduces both the overestimation of lower surges and the underestimation of higher surges, resulting in improved agreement with the observed surges. Despite its simplicity, the storm surge model achieves predictive skill comparable to the more complex statistical models developed in previous studies (Dangendorf et al., 2014; Jensen et al., 2013; Niehüser et al., 2018).

To assess the storm surge model's ability to predict extreme storm surge events, it is useful to perform a classification evaluation at two thresholds defined by the BSH: $\geqslant$ 150 cm for a storm surge and $\geqslant$ 250 cm for a severe storm surge (Sect. 1.2). Using the model predictions, I construct a contingency table with true positives, false positives and false negatives to calculate precision and recall. Precision tells us how many of the predicted events were actually correct, whereas recall tells us how many of the real events the model managed to detect. Subsequently, I calculate the F1 Score, which balances these two metrics to provide an overall measure of predictive performance. The F1 Score has its best value at 1 (perfect precision and recall) and its worst at 0 (Sect. A.6.2.2). After applying bias correction, the F1 Score improves to 0.677 and 0.792 for the 150 cm and 250 cm thresholds, respectively, compared to 0.64 and 0.387 before correction (Fig. 2.2). These results indicate excellent model performance, particularly for larger skew surges, although the small sample size for events $\geqslant$ 250 cm introduces higher uncertainty. Overall, the analysis highlights that bias correction enhances the model's ability to predict extreme events, improving both precision and recall.

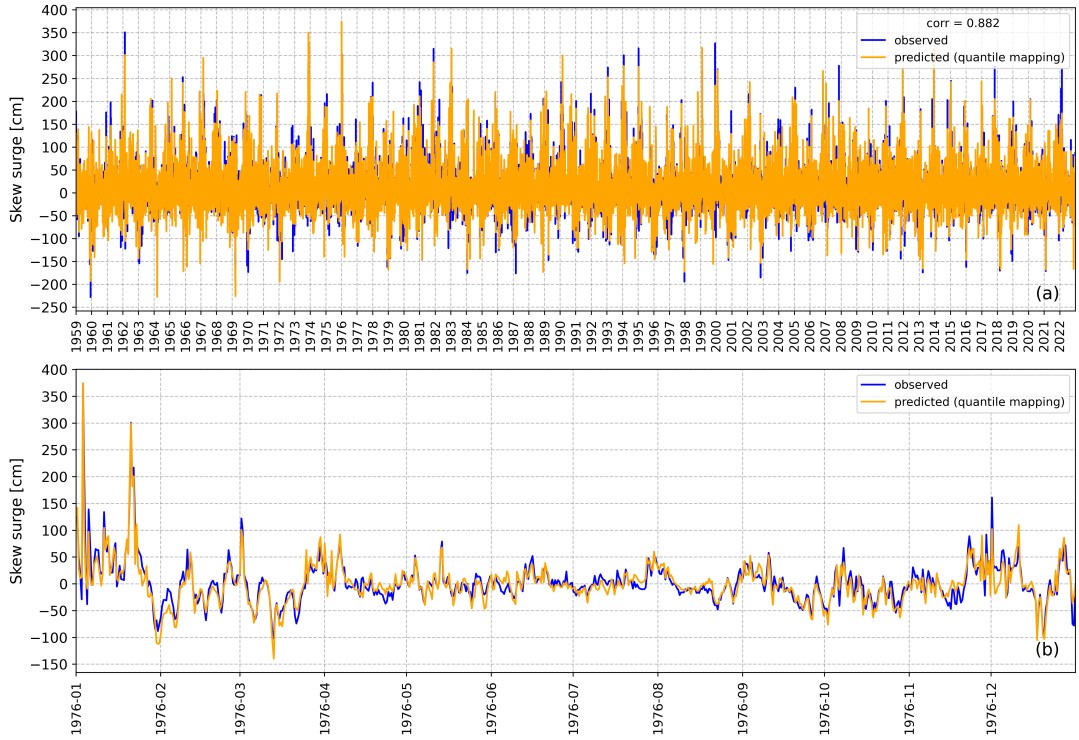


Figure 2.3: Time series of observed and bias-corrected predicted skew surges from 1959 to 2022, shown for the full period (a) and for a detailed view of 1976 (b), which includes the highest storm surge ever measured in Cuxhaven. The model is trained on events with high water skew surges $\geqslant$ 80 cm using elastic net regularization, excluding the year being predicted from the training. Taken from Paper A Fig. A.8.

In contrast to other studies, which often underestimate extreme surges (Dangendorf et al., 2014; Müller-Navarra and Giese, 1999; Niehüser et al., 2018), the statistical storm surge model captures these events while remaining remarkably simple. Its predictive skill aligns closely with northwesterly wind conditions, the primary driver of severe storm surges in the German Bight (Gerber et al., 2016). The majority of severe events caused by northwest-type weather patterns, such as the storm surges in February 1962 and late January 1976 (Gerber et al., 2016), are well reproduced (Fig. 2.3). However, some of the less typical west and southwest-type storm surge events are predicted with mixed success: the storm surge model successfully captures the storm surge of early January 1976, but underestimates the event of February 2022 (Fig. 2.3). The underestimation is primarily due to low effective winds in the northwestern North Sea and the pre-filling of the basin by previous storms (Mühr et al., 2022), which amplified the observed surge. Nevertheless, even in this case, the predicted skew surge exceeds 150 cm (Fig. 2.3 a), meeting the operational warning threshold. Furthermore, external surges from North Atlantic low-pressure systems can additionally elevate water levels. Their combined occurrence with storm surges, as in February 1962 and December 2013 (Böhme et al., 2023), explains the residual underestimation. Importantly, for these events, the storm surge model predicted a skew surge of more than 150 cm in December 2013 and over 250 cm in February 1962 (Fig. 2.3 a), successfully reaching operational storm surge and severe storm

surge warning thresholds. Despite the aforementioned limitations, the model shows strong performance in predicting both moderate and extreme storm surges in the German Bight.

## 2.3 ANSWERING THE RESEARCH QUESTION

The main findings of Paper A show that a simple, purely wind-based statistical model can reliably predict storm surges in the German Bight using only effective wind as input. Through systematic testing of predictor locations, training thresholds, and regularization methods, the final model comprises just five terms – squared effective wind values at four lead times and an intercept. Despite its simplicity, the statistical model achieves predictive skill comparable to more complex approaches and performs particularly well for extreme storm surges ($\geqslant$ 250 cm). The results emphasize the dominant influence of westerly and northwesterly winds on storm surge generation in the German Bight. Due to its minimal input requirements and computational efficiency, the statistical storm surge model is a valuable tool to investigate future storm surge heights using data from climate projections. Encouraged by the statistical model's suitability and predictive accuracy, in the following I apply it to climate projection data to estimate storm surge heights under changing climate conditions (Chapter 3).

# 3

# WIND-DRIVEN STORM SURGES AND THEIR INTERACTION WITH SEA-LEVEL RISE IN A CHANGING CLIMATE

Projecting storm surge heights in the German Bight is crucial for effective coastal management and long-term adaptation planning under changing climate conditions. Owing to methodological limitations, existing projections of wind-driven storm surge heights for the German Bight rely on a single model or scenario (Irazoqui Apecechea et al., 2025; Lang and Mikolajewicz, 2020; Mayer et al., 2022). So far, no multi-model assessment of storm surge heights in the German Bight has been conducted across different climate change scenarios, nor has any study incorporated the accelerating rise in sea level in the North Sea (Steffelbauer et al., 2022), which elevates the storm surge baseline. A multi-model approach is essential in this context, as it accounts for uncertainties arising from differences in model structure, individual model biases, and climate sensitivity. Moreover, considering multiple future scenarios captures the range of possible socio-economic and emission pathways that shape future climate conditions. Addressing this gap, in Paper B I employ a CMIP6 multi-model ensemble in combination with the statistical storm surge model developed in Paper A to estimate future storm surge heights in the German Bight. I select the climate models based on two criteria: the availability of three-hourly wind data for both historical and scenario simulations, and the use of identical realizations across historical and future periods. This selection results in nine different climate models with in total 25 ensemble members. From the available Shared Socioeconomic Pathways (SSPs; O'Neill et al., 2016), I consider three scenarios representing moderate (SSP2-4.5; middle-of-the-road), high (SSP3-7.0, regional rivalry), and very high (SSP5-8.5; fossil fuel-rich development) emission futures. This framework forms the basis for addressing the following research question:

**How will future storm surge heights in the German Bight evolve solely due to potential changes in wind patterns, based on a multi-model assessment?**

To address the gap in incorporating sea-level rise into storm surge projections, I use sea-level rise projections for Cuxhaven under the three selected emission scenarios. These projections are based on the newly developed dataset by Jensen et al. (2025). This dataset integrates IPCC projections of total sea-level change (Garner et al., 2022) with a high-resolution land elevation model for Fennoscandia (Vestøl et al., 2019), resulting in an optimized set of relative sea-level projections for the North and Baltic Sea regions. By combining these sea-level projections with the wind-driven surge projections from the aforementioned multi-model assessment, I aim to answer the following research question:

**How will the combined effect of future wind-driven changes in storm surge heights and projected sea-level rise impact extreme water levels in the German Bight?**

The statistical storm surge model I developed in Paper A is based on hourly data, while climate model outputs are typically available in only three-hourly or even coarser temporal resolution. To overcome this difference in temporal resolution, I re-trained the statistical storm surge model using three-hourly instantaneous ERA5 reanalysis data from 1959 to 2022, following the same statistical approach as the original. The updated statistical model demonstrates comparable performance, achieving a high correlation of 0.88 with only two predictors: squared effective wind speeds at two locations within the North Sea (with 12-hour and 3-hour lead times) along with an intercept (Fig. 3.1). Subsequently, I apply the revised statistical storm surge model to climate projections using the corresponding historical and future effective wind data. To account for the differing spatial resolutions of the climate models, I select the grid cells nearest to the original predictor locations in the North Sea. This approach yields wind surge projections for Cuxhaven under the SSP2-4.5, SSP3-7.0, and SSP5-8.5 scenarios, representing the wind-driven component of coastal water elevation during high tide. As tidal data are not included in climate models, I compute wind surges independently at three-hour intervals.

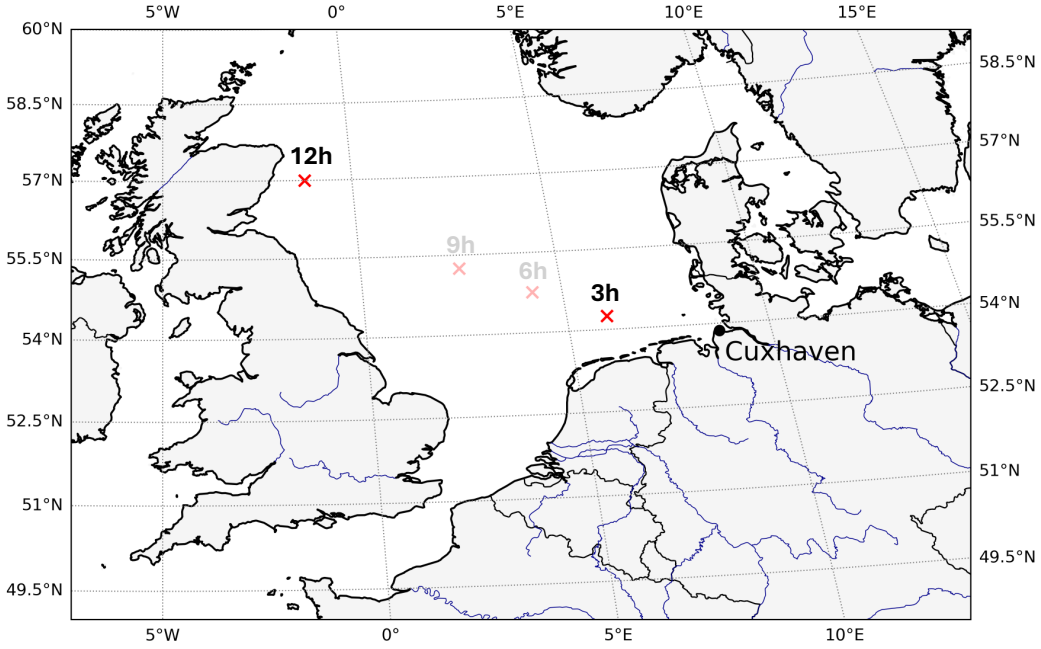


Figure 3.1: Predictor locations of the statistical storm surge model trained on three-hourly data for high water skew surges ($\geqslant$ 80 cm) across the North Sea. Red crosses mark grid cells retained after elastic net regression, with lead times (in hours) shown above each location and non-selected grid cells shown faded. Taken from Paper B Fig. S1.

Focusing exclusively on positive wind surges, Figure 3.2 shows the frequency of such events for the end of the historical period (1985-2014) and the projections for the late 21st century (2071-2100). I find a significant increase in positive winter wind

surge events across all SSP scenarios (Fig. 3.2 a, b). This includes events exceeding the 150 cm threshold that are classified as storm surges by the BSH if they coincide with tidal high water. Under the SSP5-8.5 emission scenario I find an increase in the frequency of potential storm surge situations of more than 10% (Fig. 3.2 b). In contrast, summer projections show a significant decline in positive wind surge events, which intensifies with higher forcing levels (Fig. 3.2 c, d).

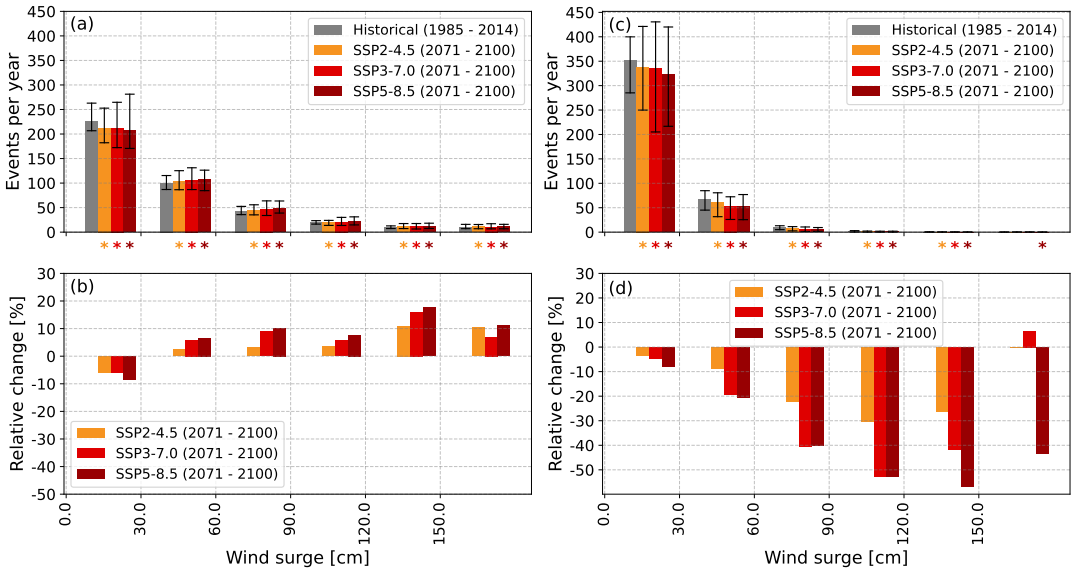


Figure 3.2: **Top panel:** Annual counts of positive wind surge events in 30 cm bins from the statistical storm surge model applied to the CMIP6 multi-model ensemble. Results are shown for winter (DJF, a) and summer (JJA, c) during the historical period (1985-2014; gray) and for the late century (2071-2100; reddish) under different SSP scenarios. Vertical error bars indicate ensemble spread; stars mark statistically significant changes compared to the historical period. **Bottom panel:** Projected changes in frequency by bin relative to the historical period for winter (b) and summer (d). Taken from Paper B Fig. B.1.

Building on the previous analysis of wind surge frequency, I explore the physical processes driving these projected changes. I focus on the SSP5-8.5 emission scenario, which shows the strongest increases in winter wind surge frequency. In order to capture the local atmospheric conditions leading to storm surge events (wind surge $\geqslant$ 150 cm), I analyze the mean wind conditions 12 and 3 hours before their onset, as these lead times correspond to the predictor variables used in the statistical storm surge model. For the historical period (1985-2014), I calculate the mean wind conditions from a total of 11,841 storm surge events. For the end of the century under the SSP5-8.5 (2071-2100) scenario, I compute the mean wind conditions from 13,007 storm surge events. Compared to the historical period, when storm surge events were preceded by strong westerly winds 12 hours before and intensified northwesterly winds shortly before the peak, future projections show significant alterations in wind patterns and strength. Under SSP5-8.5, wind speeds increase significantly over the southern North Sea both 12 and 3 hours prior to potential storm surge events, while they decrease to the north and south of this region (Fig. 3.3 a, b). Moreover, the frequency of westerly as well as northwesterly winds, particularly in the German

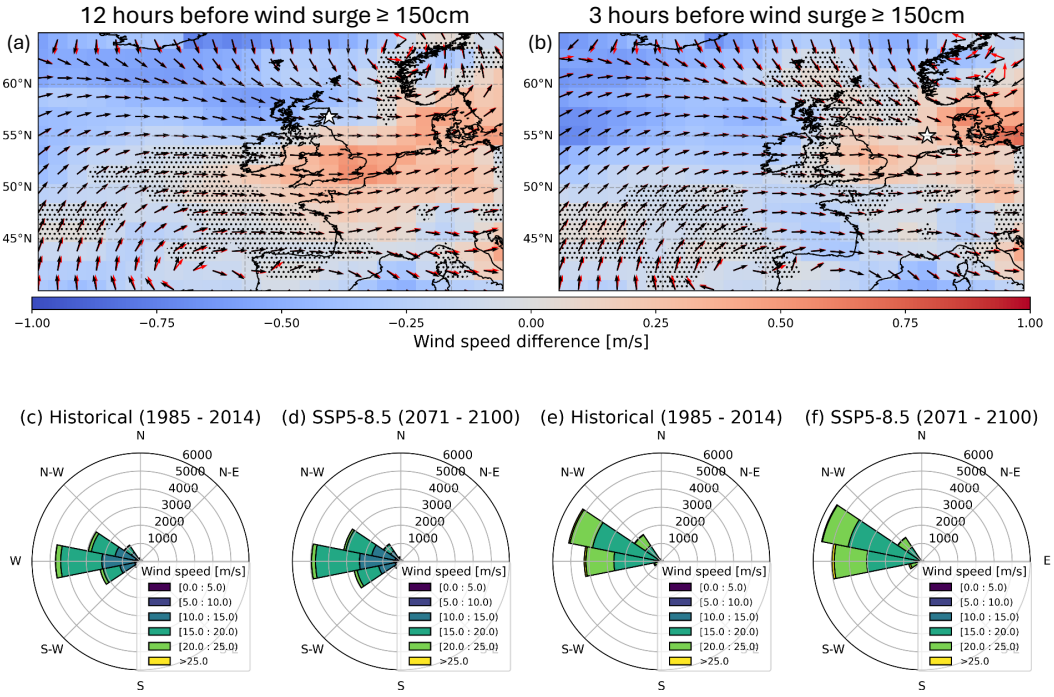


Figure 3.3: Atmospheric conditions associated with $\geqslant$ 150 cm wind surge in Cuxhaven based on the CMIP6 multi-model ensemble. White stars mark the grid cells used as input for the statistical storm surge model. **Top panel:** Projected changes in wind speed associated with wind surges $\geqslant$ 150 cm under SSP5-8.5 by 2071-2100 relative to 1985-2014, shown for 12 (a) and 3 (b) hours before the events. Color shading indicates wind speed differences; black arrows show historical wind direction, and red arrows show projected wind direction (both in unit length). Stippling marks areas with non-significant wind speed changes. **Bottom panel:** Wind roses at the locations marked by white stars in the top panel, 12 (c, d) and 3 (e, f) hours before wind surges $\geqslant$ 150 cm, shown for the historical period (1985-2014) and end of the century (2071-2100) under SSP5-8.5 scenario. Values indicate event counts. Adapted from Paper B Fig. B.2.

Bight, rises significantly (Fig. 3.3 c-f). This combination of enhanced wind speeds and more frequent westerly and northwesterly winds play a central role in driving the higher occurrence of winter storm surge situations projected by the end of the century.

In contrast to Irazoqui Apecechea et al. (2025), who apply a hybrid statistical downscaling model to a large CMIP6 ensemble to project future extreme storm surges across Europe, I find robust changes in surge heights for the German Bight. The region-specific statistical storm surge model developed in Paper A improves agreement among CMIP6 models when applied to climate projections. The projected change in the frequency of positive wind surges is consistent with previous studies focusing on the German Bight (Lang and Mikolajewicz, 2020; Mayer et al., 2022), but using a CMIP6 multi-model ensemble strengthens the robustness of the results. I find a clear seasonal contrast: winter wind surges are projected to become more frequent, while summer wind surges are expected to become less frequent. The reason for this

is mainly due to shifts in wind patterns. In summer, reduced wind speeds (Lang and Mikolajewicz, 2020), more northerly winds (Lang and Mikolajewicz, 2020), and a decline in cyclonic activity (Heinrich et al., 2025) contribute to fewer storm surge events. In winter, more frequent westerly (Heinrich et al., 2025; Mayer et al., 2022; Schade et al., 2025) and northwesterly winds (Krieger and Weisse, 2025; Ortega et al., 2025), a pattern also evident in my analysis, likely explain the increased occurrence of positive wind surge events in the German Bight. In addition, I find that, alongside changes in the frequency of westerly and northwesterly winds, stronger wind speeds over the southern North Sea drive higher storm surge frequency in the German Bight. These changes are linked to large-scale circulation patterns, particularly variations in storm tracks and the NAO. An extension of the North Atlantic storm track into Europe (Harvey et al., 2020; Priestley and Catto, 2022) and an increased occurrence of positive NAO phases (Mitevski et al., 2025) favor westerly winds and associated storm surge risk.

## 3.2 Projected extreme water levels: wind-driven surges and sea-level rise combined

To estimate future coastal water levels in the German Bight, I combine mean sea-level rise (Jensen et al., 2025) with projected wind-driven surges, focusing on winter as the main storm surge season. Using the historical mean high water in Cuxhaven (approximately 650 cm above gauge zero for the period 1995-2014) as a baseline, I add projections of SLR and wind surges for future scenarios. This approach provides a first-order estimate of how combined SLR and wind surges could elevate coastal water levels by the end of the 21st century.

Across all future scenarios, winter high water levels in the German Bight increase significantly by the end of the century compared to the historical period (Fig. 3.4). The frequency of events exceeding today's 800 cm storm surge threshold – corresponding to MHW (650 cm) plus 150 cm – is projected to rise by a factor of 3, 4 or 5 per year under SSP2-4.5, SSP3-7.0, and SSP5-8.5, respectively. Severe storm surges above 900 cm could become up to 6 times more frequent per year by the end of the century. Overall, higher-emission scenarios show stronger increases across most water level ranges, while lower water levels near the MHW become less frequent due to a rising sea level. Importantly, Figure 3.4 indicates that, under a changing climate, sea-level rise is the dominant factor contributing to the increasing frequency of extreme sea levels, rather than wind-induced water level elevations. This finding is consistent with the conclusions of the IPCC's 6th assessment report (Fox-Kemper et al., 2021).

To estimate the combined impact of SLR and projected wind surges on future water levels in Cuxhaven, I make several simplifying assumptions. Although wind surge behavior is known to vary with increasing water depth, I follow Sterl et al. (2009) in assuming a neutral hydrodynamic response to SLR. This assumption allows me to add SLR linearly to the wind surge projections. Moreover, I use regional SLR projections for the North and Baltic Seas, selecting the nearest grid cell to represent Cuxhaven. Finally, I add all results on a constant MHW of 650 cm, even though

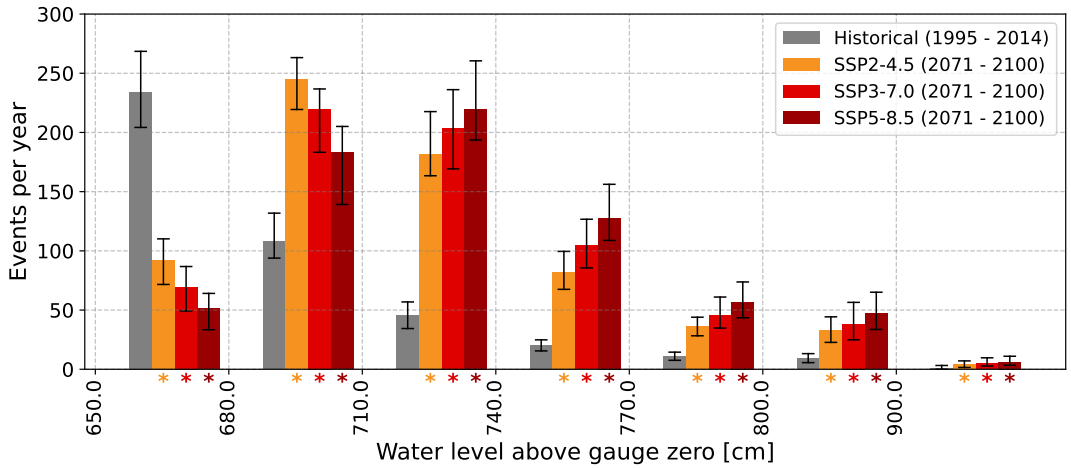


Figure 3.4: Annual counts of winter (DJF) water levels above gauge zero at Cuxhaven for the historical period (1995-2014; gray) and for the end of the century (2071-2100; reddish colors) under different SSP scenarios. Historical water levels combine MHW (650 cm) and historical wind surges, while future projections include historical MHW (650 cm), projected wind surges, and projected SLR. Wind surges are derived from the statistical storm surge model applied to the CMIP6 multi-model ensemble. Water levels are binned in 30 cm intervals from 650–800 cm and 100 cm intervals from 800–900 cm. Stars mark statistically significant changes; vertical error bars show ensemble spread. Taken from Paper B Fig. B.3.

it is expected to rise with sea level. As a result, the combination of SLR and projected wind surges provides a rough estimate of future coastal water levels relative to present-day MHW and existing storm surge thresholds. Although simplified, this approach offers a useful first-order approximation of potential coastal water levels at high tide under climate change.

## 3.3 Answering the Research Questions

Applying the statistical storm surge model developed in Paper A to a CMIP6 multi-model ensemble of climate projections, I find a significant increase in the frequency of positive wind surges during winter, particularly under higher emission scenarios. In contrast, summer wind surge events are projected to decline. Under SSP5-8.5, the frequency of extreme winter wind surges ($\geqslant$ 150 cm) is projected to increase by about 10% annually by the end of the century. This increase is likely driven by more frequent westerly and northwesterly winds, combined with stronger wind speeds over the southern North Sea. These shifts are associated with changes in storm track patterns and a higher occurrence of positive NAO phases under future climate conditions. By combining projected winter wind surges with sea-level rise, I find substantially higher coastal water levels at high tide in Cuxhaven, with both moderate and severe present-day storm surge thresholds being exceeded three to five times more often per year by 2100. Despite simplifications, these results provide a thorough first-order estimate of how climate change may impact extreme coastal water levels in the German Bight.

# 4

# CONCLUSIONS AND OUTLOOK

Storm surges have long been a recurring challenge for the population along the German Bight coast, as well as to coastal protection agencies, critical infrastructure, and emergency management systems. In light of ongoing climate change and the growing need to prepare for future coastal challenges, this dissertation tackles an overarching research question:

**How will climate change affect storm surge risk in the German Bight?**

The overarching goal of this work is to improve our understanding of how storm surge frequency and height may evolve in a warmer climate. To this end, I focused on the two key factors influencing their occurrence: wind and sea-level rise. In order to provide a detailed answer to the dissertation's overarching research question, I formulated three specific research questions (Chapter 1). Each one addresses a different aspect of the topic. In the following, I answer each of these questions.

1. **How well can a simple wind-based regression model predict storm surges in the German Bight?**

To answer the first research question, I developed a simple, wind-based statistical storm surge model for the German Bight. It is based on a multiple linear regression approach using solely 10 m effective wind data as the predictor. I trained and evaluated the statistical model on historical skew surge data from 1959 to 2022 observed in Cuxhaven, employing regularization methods to improve prediction accuracy while keeping the model simple. The final statistical storm surge model consists of only five terms: squared effective wind values at various locations with different lead times across the North Sea region, along with an intercept. Despite its simplicity, the statistical model demonstrates high predictive skill, achieving a correlation of 0.88 – comparable to more complex models. Moreover, I found that the statistical storm surge model offers reliable predictions for both moderate ($\geqslant$ 150 cm) and extreme ($\geqslant$ 250 cm) storm surge events. In summary, a simple wind-based regression model proves well suited for reliably predicting storm surges in the German Bight. These findings are presented and discussed in detail in Paper A (Chapter 2; Schaffer et al., 2025).

The model's strong performance, combined with its simplicity, enables its effective application to climate projections. This makes it a valuable tool for assessing future storm surge heights in the German Bight under changing climate conditions, independent of the ongoing rise in mean sea level. Consequently, I investigated how storm surge heights may change solely due to potential changes in wind conditions.

2. **How will future storm surge heights in the German Bight evolve solely due to potential changes in wind patterns, based on a multi-model assessment?**

To address the second research question, I applied the statistical storm surge model developed in Paper A to a CMIP6 multi-model ensemble under three emission scenarios: SSP2-4.5, SSP3-7.0, and SSP5-8.5. The use of a multi-model ensemble enabled a more robust estimation compared to relying on individual models. When focusing on the winter months (DJF), I found a significant increase of more than 10% per year in the frequency of potential storm surge situations by 2100 under the SSP5-8.5 scenario. This increase is largely driven by more frequent westerly and northwesterly winds and intensified wind speeds over the southern North Sea. These patterns are associated with shifts in storm tracks and more frequent positive NAO phases in a future climate. The results are comprehensively presented and discussed in Paper B (Chapter 3; Schaffer et al., in prep.).

Wind-driven water elevations play a crucial role in assessing extreme coastal water levels, yet they capture only one part of the overall picture. Over longer timescales, the ongoing increase in mean sea level becomes the most critical factor. In this context, I investigated how the interplay between projected sea-level rise and future wind-driven storm surge dynamics shapes extreme coastal water levels in the German Bight.

3. **How will the combined effect of future wind-driven changes in storm surge heights and projected sea-level rise impact extreme water levels in the German Bight?**

To address the third research question, I combined projected local sea-level rise with wind-driven water level changes under three emission scenarios (SSP2-4.5, SSP3-7.0, and SSP5-8.5). This approach allowed me to assess their combined effect on future coastal water levels at high tide. I evaluated changes relative to present-day mean high water and existing storm surge classification thresholds, focusing on the winter months (DJF), which represent the main storm surge season. By the end of the 21st century, I found a significant increase in the frequency of high water levels compared to the historical period. Specifically, winter water levels exceeding the current storm surge threshold of 800 cm at the Cuxhaven tide gauge are projected to occur three to five times more frequently per year by the end of the century. Even the present severe storm surge threshold of 900 cm at the Cuxhaven tide gauge is projected to be exceeded four to six times more frequently per year by 2100. In general, higher-emission scenarios produce stronger increases across most water level ranges, while lower levels near present-day mean high water decline in frequency. These patterns highlight that sea-level rise is the primary driver of future extreme coastal water levels in the German Bight. The findings are fully presented and discussed in Paper B (Chapter 3; Schaffer et al., in prep.).

## 4.1 SETTING THE COURSE: CONTRIBUTIONS AND PERSPECTIVES IN STORM SURGE RESEARCH

Climate change is expected to increase the occurrence of extreme sea levels and, consequently, the risk of coastal flood damage. Estimating storm surge heights is key for understanding changes in extreme sea levels. However, projecting future storm surge heights remains a considerable challenge, as it requires translating changes in atmospheric wind forcing into corresponding water level responses. I addressed this challenge and demonstrated in this dissertation that a simple, purely wind-based statistical storm surge model can reliably predict storm surges heights in the German Bight using 10 m effective wind data. In contrast to complex statistical models designed for detailed, event-specific storm surge prediction (Dangendorf et al., 2014; Jensen et al., 2013; Müller-Navarra and Giese, 1999; Niehüser et al., 2018), I showed that using wind alone provides comparable predictive skill with a much simpler model. The model's simplicity and efficiency make it well suited for application to climate projections. Hence, this approach opens the door to assess future storm surge heights in the German Bight, allowing the use of large multi-model ensembles – an option that was not feasible before. Following this, I demonstrated the model's successful application to a multi-model ensemble of climate simulations. This study provides the first projections of storm surge heights in the German Bight based on a multi-model ensemble across multiple emission scenarios. My findings build on the efforts of Lang and Mikolajewicz (2020) and Mayer et al. (2022) confirming a significant increase in the frequency of storm surge events by 2100 in the German Bight due to changes in wind conditions. In addition, the multi-model assessment provides a more robust estimate of future storm surge heights. Expanding on this approach, I highlighted the importance of incorporating sea-level rise into storm surge projections. I showed that the combined effect of wind-driven surges and rising sea levels leads to substantial increases in the frequency of extreme water levels in Cuxhaven.

The core of these analyses – the statistical storm surge model – offers numerous advantages but also entails certain limitations. During model training, the model identifies and records the wind directions that historically favor storm surges in the German Bight, specifically Cuxhaven. This fixed setup limits its ability to capture potential future shifts in surge-triggering wind directions. However, such changes are unlikely, since the location of Cuxhaven limits storm surge-driving winds to northwesterly directions. Storm surges induced by alternative wind directions, external surges, or pre-filling effects are somewhat underestimated, though still represented within the model. Although I used Cuxhaven as a proxy for the wider German Bight, it is important to emphasize that all results derived from the statistical storm surge model are only valid for this centrally located site. Other coastal areas of the German Bight – particularly the North Frisian and East Frisian coasts – may show different future developments in the frequency of storm surge events. Mayer et al. (2022), for example, report a future overall increase in the frequency of storm surge events throughout the German Bight, comparable in magnitude to the increase projected in my analysis. However, they find that this increase is most pronounced along the North Frisian coast and weakest along the East Frisian coast, highlighting clear spatial differences in storm surge frequency across the German Bight. Such regional

differences are not captured in my Cuxhaven-based approach. Nevertheless, despite this limitation, using the statistical storm surge model with climate projection data offers robust insights into the overall direction of change in storm surge frequency and height in the German Bight. Finally, in this dissertation, I emphasized the importance of incorporating sea-level rise into storm surge projections. While I presented an initial estimate of future extreme coastal water levels under climate change, based on several simplifying assumptions, the proper incorporation of sea-level rise remains a complex and open research challenge.

This work opens new possibilities for investigating storm surge heights in the German Bight across a range of timescales. Thanks to its simplicity and efficiency, the statistical storm surge model is well suited for a variety of applications, such as seasonal or decadal predictions, and even potential integration into operational early warning systems. Beyond the temporal dimension, the underlying approach of developing such a statistical storm surge model is transferable to coastal regions worldwide where wind is the dominant driver of storm surge development. Given the limitations described above, the approach offers clear potential for regionalization within the German Bight: tailored statistical storm surge models can be developed independently for the North Frisian and East Frisian coasts and subsequently applied to large multi-model ensembles of climate projections. Such region-specific models would allow for a more detailed and robust assessment of the spatial variability in future storm surge frequency and height across the German Bight. Moreover, the underlying drivers of the projected increase in storm surge frequency in the German Bight could be further investigated. In particular, future work could focus on quantifying the respective contributions of increasing wind speeds and changing frequencies of surge-favorable wind directions. The findings of this dissertation, together with the conclusions of the IPCC's 6th assessment report (Fox-Kemper et al., 2021), indicate that sea-level rise will be the dominant factor behind increasing occurrences of extreme sea levels. However, the relative contributions of wind-driven changes and sea-level rise to extreme coastal water levels in the German Bight remain poorly quantified. A systematic assessment of these components would provide a more complete understanding of the mechanisms shaping future storm surge risk in the German Bight.

In this dissertation, I investigated long-term projections of storm surge frequency and height in the German Bight until the end of the century. Reliable projections of storm surge risk provide valuable guidance for coastal protection and management agencies, enabling them to improve preparedness, mitigation, and long-term adaptation strategies. They also offer essential input for infrastructure planning and resilience measures, ultimately benefiting communities living along the German Bight coast. Hence, my dissertation bridges scientific insight and societal application, offering knowledge to strengthen coastal safety and resilience in the German Bight in the face of a changing climate.

# PUBLICATIONS

# A

# DEVELOPMENT OF A WIND-BASED STORM SURGE MODEL FOR THE GERMAN BIGHT

The research presented in this chapter has been published as:

Schaffer, L., Boesch, A., Baehr, J., and Kruschke, T. (2025). "Development of a wind-based storm surge model for the German Bight." *Natural Hazards and Earth System Sciences* 25.6, pp. 2081–2096. DOI: 10.5194/nhess-25-2081-2025.

My contributions to the research presented in this chapter include designing and developing the study together with Tim Kruschke. I developed and trained the model, performed the analyses and generated the figures. Together with Johanna Baehr and Tim Kruschke, I interpreted and contextualized the results. I also wrote the manuscript, integrating the contributions of all coauthors.

# DEVELOPMENT OF A WIND-BASED STORM SURGE MODEL FOR THE GERMAN BIGHT

Laura Schaffer[1,2], Andreas Boesch[1], Johanna Baehr[2], and Tim Kruschke[1]

[1]Federal Maritime and Hydrographic Agency (BSH), Hamburg, Germany
[2]Institute of Oceanography, University of Hamburg, Hamburg, Germany

ABSTRACT

Storm surges pose significant threats to coastal regions, including the German Bight, where strong winds from the northwesterly direction drive water levels to extreme heights. In this study, we present a simple, effective storm surge model for the German Bight, utilizing a multiple linear regression approach based solely on 10 m effective wind speed as the predictor variable. We train and evaluate the model using historical skew surge data from 1959 to 2022, incorporating regularization techniques to improve prediction accuracy while maintaining simplicity. The model consists of only five terms, the effective wind at various locations with different lead times within the North Sea region, and an intercept. It demonstrates high predictive skill, achieving a correlation of 0.88. This indicates that, despite its extreme simplicity, the model performs just as well as more complex models. The storm surge model provides robust predictions for both moderate and extreme storm surge events. Moreover, due to its simplicity, the model can be effectively used in climate simulations, making it a valuable tool for assessing future storm surge risks under changing climate conditions, independent of the ongoing and continuous sea-level rise.

## A.1 INTRODUCTION

Many of the world's coasts are endangered by storm surges. These can have devastating consequences, causing widespread destruction and even loss of life (von Storch, 2014). The German Bight, located in the southeastern part of the North Sea (Fig. A.1), is an example of a region that is prone to frequent and severe storm surges. The major driver of storm surges in the German Bight is strong wind from the northwesterly direction associated with intense extratropical cyclones traveling from the North Atlantic into the North Sea region. The co-occurrence of such storms with high tides leads to high coastal water levels, potentially resulting in flooding, erosion and significant damage to infrastructure. Organizations responsible for the planning and construction of protection structures have been confronted with the

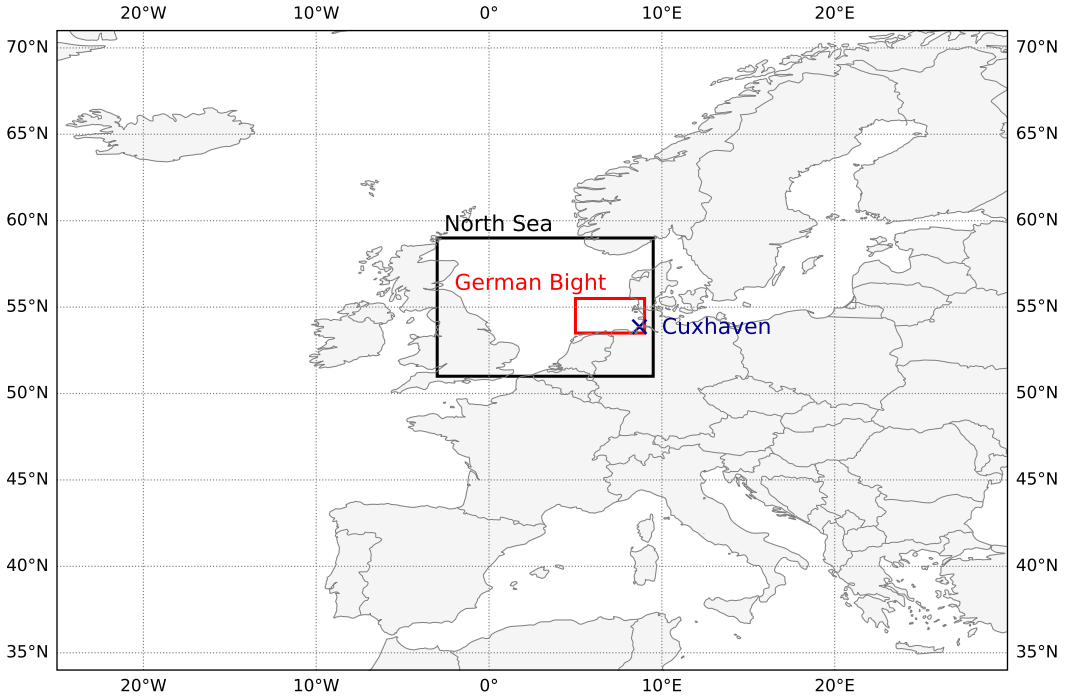


Figure A.1: Map with marked areas of the North Sea (black box) and the German Bight (red box). The blue cross indicates the location of Cuxhaven.

challenge of managing these sudden extreme water-level events for decades. The continuing rise in mean sea level induced by anthropogenic climate change adds even greater urgency to this issue. Assessing the potential of an impending storm surge is therefore important in order to ensure public safety and maintain regional infrastructure.

In addition to other factors such as atmospheric sea-level pressure and external surges (Böhme et al., 2023), wind proves to be the primary driver for sea-level variability in the German Bight (Dangendorf et al., 2013) and therefore plays an important role in estimating the height of storm surges. Various studies investigate the meteorological conditions that caused extreme storm surges in the past. While they focus on just a few case studies, they demonstrate the successful applicability of reanalysis data for recreating these events: the storm surge studies include the well known Hamburg storm surge of 1962 (Jochner et al., 2013; Meyer and Gaslikova, 2024), one of the highest storm surges ever measured in 1976 (Meyer and Gaslikova, 2024) and the storm surge caused by storm "Xaver" in 2013 (Dangendorf et al., 2016; Meyer and Gaslikova, 2024). While these and other studies focus on the analysis of individual historical events, Krieger et al. (2020) concentrate on the statistics and long-term evolution of German Bight storm activity. They find that storm activity over the German Bight is characterized by multidecadal variability. This is in line with the results of Dangendorf et al. (2014), who find that storm surges in the North Sea are characterized by interannual to decadal variability associated with large-scale atmospheric circulation patterns.

Nevertheless, in order to estimate the resulting storm surge levels in the German Bight, a translation of wind speed into water level is required. Hydrodynamic models are the most widely used and reliable method for translating atmospheric conditions into storm surge estimates. While they provide detailed simulations of storm surges, they are computationally expensive and require extensive input data, making them less suitable for climate simulations. In such cases, simpler approaches, such as statistical methods, can serve as more practical alternatives to analyze storm surges. In particular, the skew surge – the difference between the observed water level and the expected astronomical high-water level – provides reliable information about storm surges (Ganske et al., 2018; Williams et al., 2016). Here, two approaches are commonly employed to translate atmospheric conditions into water levels: one uses the so-called effective wind as a proxy, while the second approach involves predicting skew surges using a statistical model.

For the former, a variable – the effective wind – consisting of wind speed and direction is used to objectively assess the conditions for a storm surge in the German Bight (Jensen et al., 2006; Müller-Navarra et al., 2003). Cuxhaven (Fig. A.1), located in the center of the German Bight coast and with its long-gauge data series, is often used as a proxy for that region. For Cuxhaven, the effective wind is defined as the fraction of the 10 m wind blowing from direction 295°. In an empirical study, this wind direction was determined as the one for which the wind-induced increase in water levels in the German Bight is greatest (Jensen et al., 2006; Müller-Navarra et al., 2003). Averaged over the German Bight, the effective wind is therefore a measure of the contribution of wind to storm surges at the German Bight coastline and can be used as an indicator for the storm surge potential of a weather situation (Jensen et al., 2006). Befort et al. (2015) use the effective wind in combination with a storm tracking algorithm to detect storm surges in the German Bight. Using this method, they show an improvement in the identification of storm surge events compared to the sole use of the effective wind. This agrees with findings of Ganske et al. (2018), who state that high effective wind alone is not necessarily linked to a large storm surge height, but that additional parameters such as the storm track need to be taken into account.

Building upon the second approach, namely the use of a statistical model, Müller-Navarra and Giese (1999) re-examined and revised existing studies and similar methods from the 1960s, setting up a statistical model using multiple linear regression in order to determine storm surge situations in the German Bight, i.e., in Cuxhaven. The authors use, as predictors for computing the skew surge in Cuxhaven, wind speed and direction, air and sea surface temperature, air pressure and its 3-hourly change, the water level in Wick on the Scottish east coast 12 h earlier, and water levels in Cuxhaven during the immediately preceding low and high waters. Müller-Navarra and Giese (1999) find that the consideration of external surge and autocorrelation improve the model performance. The result is an empirical model with 14 basic functions that is able to describe the skew surge height in Cuxhaven (Müller-Navarra and Giese, 1999). Several other studies build on this study and base their models on the mathematical approaches by Müller-Navarra and Giese (1999). Jensen et al. (2013), for example, successfully examine the empirical–statistical relationship between wind, air pressure and the skew surge in Cuxhaven for the period 1918

to 2008. As an approximation for external surges, they use air pressure and wind time series at the northern edge of the North Sea. Dangendorf et al. (2014) extend this analysis by reconstructing storm surges in the German Bight back to 1871, but with higher predictive skill from 1910 onward. However, it is worth noting that their model is only based on atmospheric surface forcing as predictors; external surges are excluded from the model setup (Dangendorf et al., 2014). Niehüser et al. (2018) apply a similar model setup for multiple tide gauge locations along the North Sea coast, focusing on the period from 2000 to 2014. In contrast to using wind and air pressure information of the nearest grid cell for each tide gauge location (Dangendorf et al., 2014; Jensen et al., 2013), Niehüser et al. (2018) implement a step wise regression approach, considering time lags up to 24 h. This allows them to determine the location and time lag of relevant predictors for each site. Their model shows comparable skill measures to the more complex model by Jensen et al. (2013). All mentioned statistical modeling approaches require a large number of input variables for very specific locations or regions. Most of these approaches have been employed solely based on observational data or atmospheric reanalysis (Dangendorf et al., 2014; Jensen et al., 2013; Müller-Navarra and Giese, 1999; Niehüser et al., 2018).

In the context of climate change, the assessment of future storm surge risk is of major importance (IPCC, 2023). In order to incorporate necessary climate projections, a less complex statistical model is needed that is applicable to a multi-model ensemble of climate model simulations with only a limited number of variables available and a comparatively coarse spatial resolution.

To fill this gap, this paper seeks to (i) set up a simple storm surge model for Cuxhaven using a multiple linear regression approach based only on the 10 m wind from the ERA5 reanalysis as predictor variable; (ii) improve prediction accuracy and reduce model complexity by applying regularization methods; and (iii) assess the model's performance by using cross-validation methods and classification evaluation. The reason for the restriction to winds is that most climate model simulations provide corresponding information. Thus, this paper introduces a new method for predicting storm surge heights in the German Bight, which can also be applied using data from climate model projections in future studies.

## A.2 METHODS AND DATA

We develop a simple storm surge model for the German Bight, i.e., Cuxhaven, based on a multiple linear regression approach and relying exclusively on the grid-cell-specific 10 m effective wind as the predictor variable. Broadly speaking we follow four steps (Fig. A.2): (a) data preprocessing (Sects. A.2.1.1 and A.2.1.2); (b) the identification of the location and lead time of the predictors across the entire North Sea region (namely certain grid cells of the atmospheric reanalysis used; Sects. A.2.2 and A.3.1); (c) choosing an appropriate threshold value and regularization method for training the model (Sects. A.2.3, A.3.2 and A.3.3); and (d) training and evaluation of the storm surge model (Sects. A.2.3, A.3.4 and A.3.5).

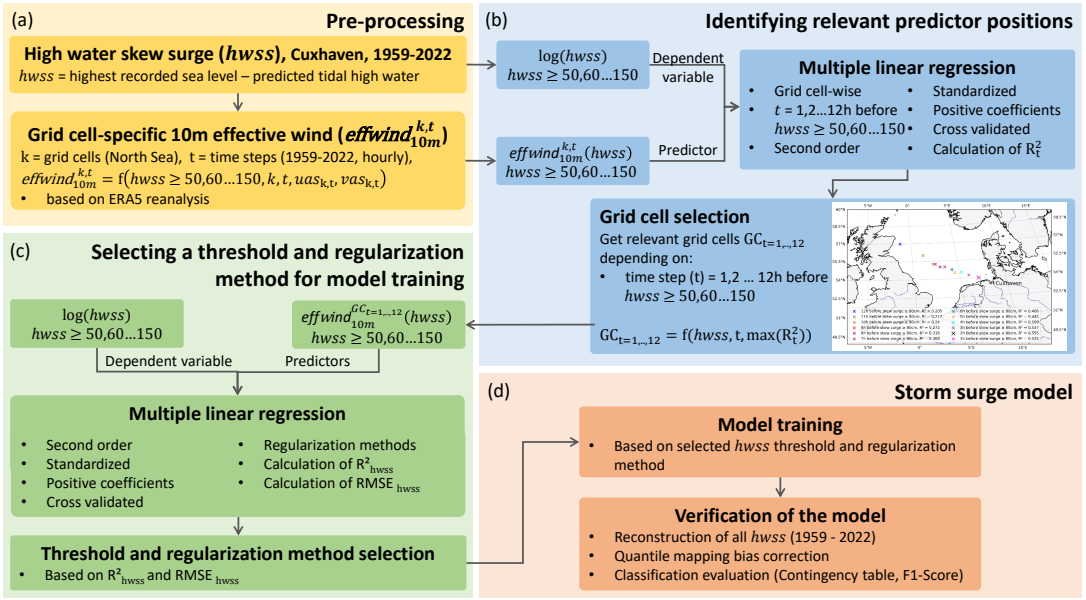


Figure A.2: Schematic representation of the process for developing the wind-based storm surge model. Panel (a) shows the data preprocessing steps; panel (b) shows the identification of relevant predictor positions; panel (c) shows the procedure for selecting a threshold and regularization method for model training; panel (d) shows the final model training and evaluation.

### A.2.1 *Data*

#### A.2.1.1 *Skew surge data*

A valuable metric for storm surge research is the skew surge at high waters (de Vries et al., 1995; Jensen et al., 2013; Williams et al., 2016). It is the height difference between the highest recorded sea level and the predicted tidal high water within a tidal cycle, regardless of the time. We create a time series of high-water skew surge (hwss) at the tide gauge Cuxhaven for the years 1959 to 2022 (Fig. A.8). In order to derive hwss, we calculate consistent tidal predictions for these years based on the observed times and water levels of high waters. The observation data are collected and quality checked by the Waterways and Shipping Office Elbe-Nordsee, which operates the Cuxhaven tide gauge. The height reference is tide gauge zero.

We perform tidal analysis and prediction using the method of "harmonic representation of inequalities". We opt for this method for two reasons: (1) It is a proven operational technique that delivers excellent results under the tidal conditions in the German Bight (Boesch and Jandt-Scheelke, 2020; Boesch and Müller-Navarra, 2019; Horn, 1960), and (2) this technique is applied directly to the heights of the vertices which are needed for this study. For the tidal analysis, we follow the scheme used for the official tide tables: predictions for a given year are based on a tidal analysis of the 19 water-level observation years ending 3 years prior to the prediction year. For example, the prediction for the year 1959 is based on the results of the tidal analysis of the observations from 1938 to 1956. The tidal analysis employs 39 long-period tidal constituents and runs in two iterations, with a three-sigma clipping of outliers before

each iteration. We derive the skew surge for 45 162 high waters compared to 45 169 semidiurnal tidal cycles theoretically present in the studied years. It is worth noting that, due to the calculation process, the skew surge data do not take into account sea-level rise.

Table A.1: Number of data points for each sub-sample based on the selected threshold for the period 1959 to 2022.

| **hwss [cm] ⩾** | **50** | **60** | **70** | **80** | **90** | **100** | **110** | **120** | **130** | **140** | **150** |
|---|---|---|---|---|---|---|---|---|---|---|---|
| Sample size | 3761 | 2730 | 2018 | 1504 | 1161 | 923 | 717 | 551 | 431 | 329 | 253 |

As this study aims for a storm surge model we only use a subsample of high hwss events for training. As part of this study, we test various thresholds as a lower boundary for defining this subsample, specifically ranging from 50 to 150 cm. We decided on this range as it represents a fair compromise between sample size and the official storm surge definition of greater than or equal to 150 cm above mean high water (Sect. A.2.3). In the following we refer to this range as hwss ⩾ 50, 60, . . . , 150 cm. We show the number of available data points for each subsample in Table A.1. We describe the choice of the final threshold in Sects. A.2.3 and A.3.2. As the selected skew surge range is not normally distributed, we apply the natural logarithm to normalize the dataset before using it. Consequently, we train the model based on logarithmic values.

#### A.2.1.2 *Wind data*

ERA5, generated by the European Centre for Medium-Range Weather Forecasts (ECMWF), is the most recent atmospheric reanalysis offering hourly data on various atmospheric, land-surface, and sea-state variables. The data are provided at a horizontal resolution of 31 km and 137 levels in the vertical, covering the period from 1940 onwards (Hersbach et al., 2020).

Based on the 10 m hourly wind components from the ERA5 reanalysis, we use the concept of the effective wind to analyze the wind conditions that contribute to water-level variations in Cuxhaven. The effective wind refers to the combined effect of wind speed and direction. It describes the proportion of the wind projected onto a specific wind direction. Here, the specific wind direction is the one that causes a certain wind-related water level in Cuxhaven. We perform a composite analysis of the zonal (uas) and meridional (vas) components of the 10 m wind, which are associated with hwss ⩾ 50, 60, . . . , 150 cm. For each hour (up to 12 h) prior to the corresponding skew surge event, we use the result of this composite analysis to determine the specific wind direction separately for each hwss training threshold.

As we started our analysis when the backward extension of ERA5 to 1940 was not yet available, we only use the hourly wind components for the period 1959 to 2022. Since our study area is the German Bight, we focus exclusively on the North Sea region, which we define from -5° E to 10.5° E in longitude and from 51° N to 59° N in latitude. For this region, we count 2079 grid cells. For each of these grid cells

($k$) and in hourly time steps ($t$) we calculate the effective wind separately for each hwss training threshold. First, we normalize the mean zonal ($\overline{uas}_k$) and meridional ($\overline{vas}_k$) wind components from the composite analysis by dividing each by the mean wind speed ($\overline{U}_k$). We subsequently calculate the effective wind ($effwind^{k,t}_{10m}$ (hwss)) by projecting the actual wind components ($uas_{k,t}$ and $vas_{k,t}$) onto the corresponding normalized mean components ($\frac{\overline{uas}_k}{\overline{U}_k}$ and $\frac{\overline{vas}_k}{\overline{U}_k}$):

$$effwind^{k,t}_{10m}\,(hwss) = \left(\frac{\overline{uas}_k}{\overline{U}_k}\right) \cdot uas_{k,t} + \left(\frac{\overline{vas}_k}{\overline{U}_k}\right) \cdot vas_{k,t}. \tag{1}$$

The result is the effective wind for the period 1959 to 2022 in hourly time steps and individually for each grid cell in the North Sea region. The particular feature of $effwind^{k,t}_{10m}$ (hwss) is the fact that its value can be negative. This is the case as soon as the wind blows from the opposite direction to the specific wind direction.

### A.2.2 *Statistical model development*

Similar to Niehüser et al. (2018), we apply the approach of non-static predictors, but using a different method. This method only considers predictor locations that are relevant to the observed skew surge variability in Cuxhaven. Thus, instead of just considering the nearest grid cell for the Cuxhaven gauge (Dangendorf et al., 2014; Jensen et al., 2013), we identify grid cells and lead times across the entire North Sea region that are most relevant to the respective subsample (hwss $\geqslant$ 50, 60, ..., 150 cm). Using the effective wind data up to 12 h before each hwss event, we select the grid cells with the highest relevance at each lead time (further details in Sect. A.6.1). This approach enables us to determine the most significant grid cells and lead times for each hwss training threshold (Fig. A.2b). Hereafter, the effective wind in these selected grid cells, along with the corresponding lead times ($effwind^{GC_{t=1,..,12}}_{10m}$(hwss)), serve as predictors. We stress that each of the 12 predictor variables represents a specific position and a lead time in the North Sea region. Separately for every subsample (hwss $\geqslant$ 50, 60...150 cm), we perform multiple linear regression using each of the three regularization techniques - ridge, lasso and elastic net (further details in Sect. A.6.2.1). As we count 11 different hwss training thresholds and three regularization methods, we arrive at 33 models. In the following, we refer to these models as skew surge models. We use the standardized $effwind^{GC_{t=1,..,12}}_{10m}$ (hwss) and set up the skew surge models in quadratic order and with forced positive coefficients (Sect. A.2.3). In addition, we determine the respective regularization parameter $\lambda$ for ridge, lasso and elastic net regression for each skew surge model using cross-validation. Subsequently, we perform a leave-one-out-cross-validation for each skew surge model and regularization technique (Fig. A.2c).

### A.2.3 *Evaluation and setup of the storm surge model*

In order to evaluate the skew surge models (Sect. A.2.2), we calculate $R^2$ and the root-mean-square error (RMSE) (further details in Sect. A.6.2.3). Based on these performance metrics, data availability and the ability of the individual skew surge models to capture even very severe storm surges, we decide on one final hwss threshold for

model training (Sect. A.3.2) and one regularization method (Sect. A.3.3). The model trained on the selected hwss subsample using the chosen regularization method is hereafter referred to as the storm surge model.

We evaluate the storm surge model by predicting all hwss, every 12 hours, for the years from 1959 to 2022. In doing so, we exclude the year to be predicted from the training. As before, we train the storm surge model based on the sub-sample corresponding to the previously selected hwss event threshold. Here, the predictors, namely $effwind_{10m}^{GC_{t=1,..,12}}(hwss)$, are mostly positive, as they correspond to the wind direction relevant to the hwss subsample. For the year that the model is supposed to predict, we have to take all high tides into account. In doing so, we come across skew surge heights that are smaller than the skew surge height with which the model was trained – some even negative. Smaller or sometimes negative hwss indicate a minor water movement or even a water movement away from the coast of Cuxhaven. Here, $effwind_{10m}^{GC_{t=1,..,12}}(hwss)$, which is mainly responsible for this water movement, tends to take on negative values. Since the storm surge model consists of interaction terms and squared terms, negative $effwind_{10m}^{GC_{t=1,..,12}}(hwss)$ as predictors would still lead to positive values. This means that despite negative $effwind_{10m}^{GC_{t=1,..,12}}(hwss)$, the model would predict positive hwss, which is contrary to the physical consequence of negative $effwind_{10m}^{GC_{t=1,..,12}}(hwss)$. To overcome this problem, we create a mathematical condition that we apply solely to the dataset of the year to be predicted. This mathematical condition specifies that whenever a predictor is negative, the coefficient associated with its squared term becomes negative. Furthermore, if both predictors in an interaction term are negative, the coefficient before the term also becomes negative. This mathematical condition, combined with the forced positive coefficients in the training, allows the model to reproduce the physical consequence of negative $effwind_{10m}^{GC_{t=1,..,12}}(hwss)$.

However, since we train the model on logarithmic hwss, the model will always predict hwss greater than zero. In order to address this issue, we apply the quantile mapping bias correction technique based on the equations of Cannon et al. (2015). With this method we aim to minimize distributional biases between predicted and observed hwss time series. Its interval-independent approach considers the entire time series, redistributing predicted values based on the distributions of the observed hwss (Fig. A.2d).

Moreover, we perform a classification evaluation to investigate whether the model correctly classifies the predicted storm surges according to the storm surge definition for the German North Sea coast. The latter is defined by the height of the water level above mean high water (MHW). According to the definition of the Federal Maritime and Hydrographic Agency (BSH), a storm surge event along the German North Sea coast is classified as follows: an increase in water level of 150 to 250 cm above MHW is referred to as a "storm surge"; if the water level reaches between 250 to 350 cm above MHW, it is classified as a "severe storm surge"; and any event exceeding 350 cm above MHW is referred to as a "very severe storm surge" (Müller-Navarra et al., 2012). To assess the extent to which the storm surge model assigns the predicted

hwss to the correct classes, we calculate the F1 score (van Rijsbergen, 1979) (further details in Sect. A.6.2.2). Specifically, we calculate the F1 score for the classes starting from a storm surge ($\geqslant$ 150 cm) and from a severe storm surge ($\geqslant$ 250 cm) for the predicted and bias-corrected high-water skew surges in the years 1959 to 2022.

## A.3 RESULTS

### A.3.1 *Identifying relevant predictor positions*

In the first step for the development of a storm surge model, we determine the location and lead time of the predictors ($effwind_{10m}^{k,t}$ $(hwss)$) in the North Sea region, individually for each hwss training threshold (hwss $\geqslant$ 50,60...150 cm). Figure A.3 shows the location and lead time of the predictors for the training threshold of hwss $\geqslant$ 80 cm. 12 h before skew surge events in Cuxhaven, the effective wind in the northwestern section of the North Sea, near Scotland, shows the highest explained variance ($R^2$ = 0.205) (blue cross in Fig. A.3). With increasing temporal proximity to the skew surge events, the relevance shifts toward the southeastern part of the North Sea. Here, the effective wind in the most southeasterly grid cell, approximately 2 h ($R^2$ = 0.555) and 1 h ($R^2$ = 0.525) before the skew surge events, provides the best description of the resulting water level in Cuxhaven (black and pink cross in Fig. A.3).

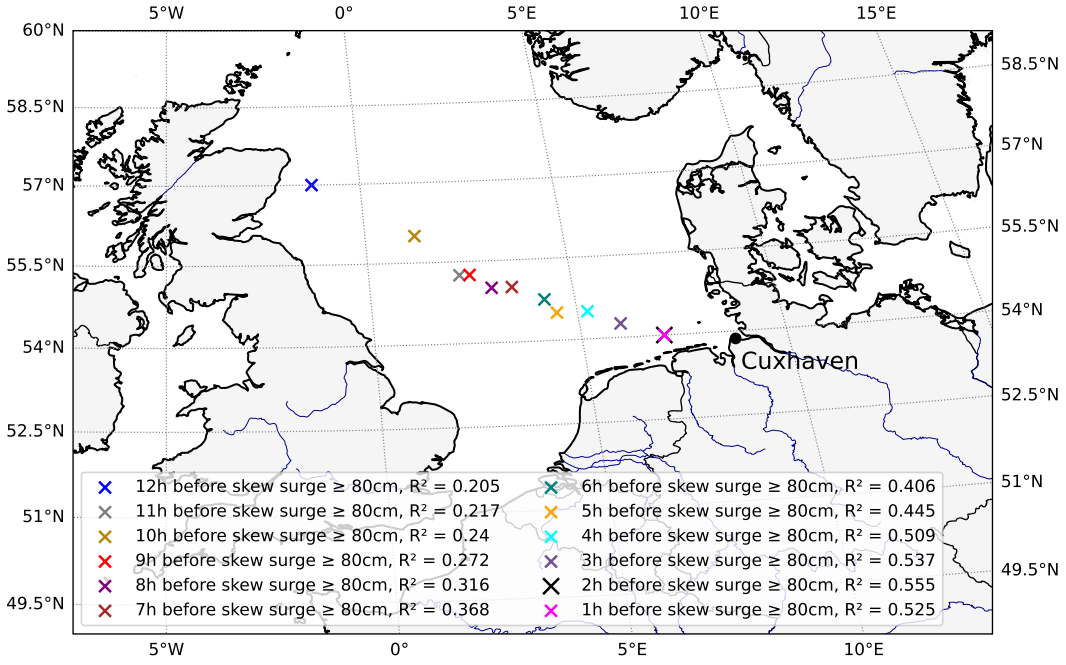


Figure A.3: Map of the North Sea region showing the 12 relevant grid cells highlighted with crosses. Each cross represents a specific grid cell, with the color variations indicating the different time intervals before the skew surge event and the corresponding $R^2$ value (based on a leave-one-out-cross-validation). The threshold for training is hwss $\geqslant$ 80 cm.

Even though the positions in the North Sea region, i.e., the individual grid cells, vary when applying the different hwss subsamples (not shown), the temporal evolution of grid points with maximum $R^2$ consistently follows a northwest to southeast progression. This result is in line with findings of Meyer and Gaslikova (2024) and Gerber et al. (2016), who investigate several storm surges and conclude that the northern storm tracks induce high surges across the southern area of the North Sea.

### A.3.2 *Selecting a threshold for model training*

Once we have determined the location and lead time of the predictors (Sect. A.3.1), we create skew surge models by applying the three regularization methods (further details in Sect. A.6.2.1). We perform a leave-one-out-cross-validation for the models based on ridge, lasso and elastic net regression separately for the training thresholds hwss $\geqslant$ 50, 60, ..., 150 cm, resulting in three models per hwss training threshold. We assess the performance of these skew surge models by computing $R^2$ and RMSE (Fig. A.4). We find a general trend of decreasing $R^2$ values across all three models as

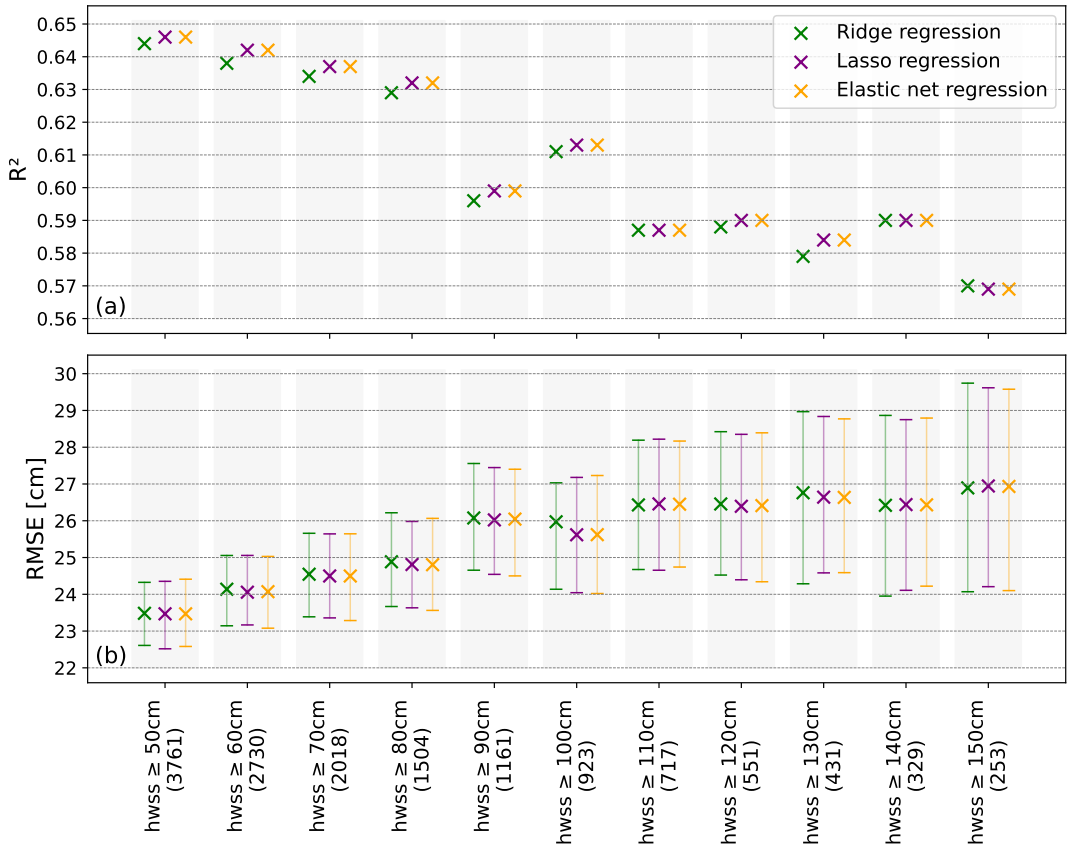


Figure A.4: $R^2$ (a) and RMSE (b) with the corresponding 95 % confidence intervals of the skew surge models including the different regularization methods across different hwss thresholds for training. The training thresholds are shown on the x-axis with the number of available data points in brackets. Each cross represents a specific regularization method (green: ridge regression, purple: lasso regression, orange: elastic net regression). The results are based on a leave-one-out-cross-validation.

the training threshold increases, with the highest $R^2$ value of 0.646 (hwss $\geqslant$ 50 cm) and the lowest being 0.569 (hwss $\geqslant$ 150 cm) (Fig. A.4a). Furthermore, skew surge models using ridge regression have a slightly lower $R^2$ value in most cases compared to models using lasso and elastic net regression. Skew surge models based on lasso and elastic net regression show almost equal $R^2$ values across all hwss training thresholds (Fig. A.4a). This trend is also reflected in the RMSE. When trained with lower hwss thresholds, the RMSE is low and the confidence interval is narrow. Conversely, training with higher hwss thresholds results in higher RMSE values and wider confidence intervals.

Despite lower $R^2$ values for models with ridge regression, we find no significant differences in performance compared to the other regularization methods trained on the same threshold. We see this in the fact that the confidence intervals of the models trained with the same hwss threshold value overlap regardless of the regularization method. The similarity in performance of the three models, each with a different regularization method, is the result of forcing the positive coefficients. By forcing positive coefficients, ridge regression reduces certain coefficients to zero if their impact on the accuracy of the prediction is small. This process is similar to predictor selection and results in model behavior similar to lasso and elastic net regression. Consequently, in our case, the performance of ridge regression is closely related to lasso and elastic net regression.

However, when comparing skew surge models across training thresholds, we find that some models trained with higher thresholds (e.g., hwss $\geqslant$ 110 cm) perform significantly worse compared to those trained with lower thresholds (e.g., hwss $\geqslant$ 50 cm) (Fig. A.4b). Additionally, we observe strong fluctuations in the decrease in $R^2$ values and the increase in RMSE values, which become visible from a hwss training threshold of hwss $\geqslant$ 90 cm (Fig. A.4). One explanation for this phenomenon and the partly resulting significant differences in model performance might be the sample size. As the training threshold increases, the number of events decreases. Having sufficient data is essential for the model to learn patterns accurately and ensure better performance on unseen data.

In our pursuit of developing a storm surge model capable of simulating extreme events, we aim to train it using the highest possible hwss threshold. However, when selecting from the number of possible training thresholds, we face the challenge of striking a balance between sample size, high threshold and model performance. We decide to use a hwss training threshold of greater than or equal to 80 cm. We base our decision on the following reasons: (1) this training threshold does not lead to a significant difference in model performance compared to other thresholds (Fig. A.4b), (2) we have sufficient data to effectively train the model with this threshold, and (3) we find a satisfactory level of accuracy in simulating extreme events (Fig. A.5).

### A.3.3 *Selecting a regularization method*

Following the selection of a hwss training threshold, the next step is to choose a suitable regularization method. Figure A.5 compares the observed and predicted

skew surge heights resulting from a leave-one-out-cross-validation using ridge, lasso and elastic net regression, all related to a training threshold of greater than or equal to 80 cm. As mentioned earlier (Sect. A.3.2), we observe a similarity in model performance. This is also evident when predicting extremes, with most of the extreme values being underestimated. This could be attributed to the limited data on extreme skew surge events. Moreover, the coarse resolution of the atmospheric forcing (ERA5) may contribute to the underestimation of the most extreme events (Dangendorf et al., 2014; Harter et al., 2024). However, even with a relatively low training threshold (hwss $\geqslant$ 80 cm), we still get an appropriate representation of the most extreme events (Fig. A.5). The problem of underestimating extreme events is not unique to this study. Several other studies attempting to reconstruct extreme storm surges using statistical models also encounter similar issues (Dangendorf et al., 2014; Harter et al., 2024; Niehüser et al., 2018).

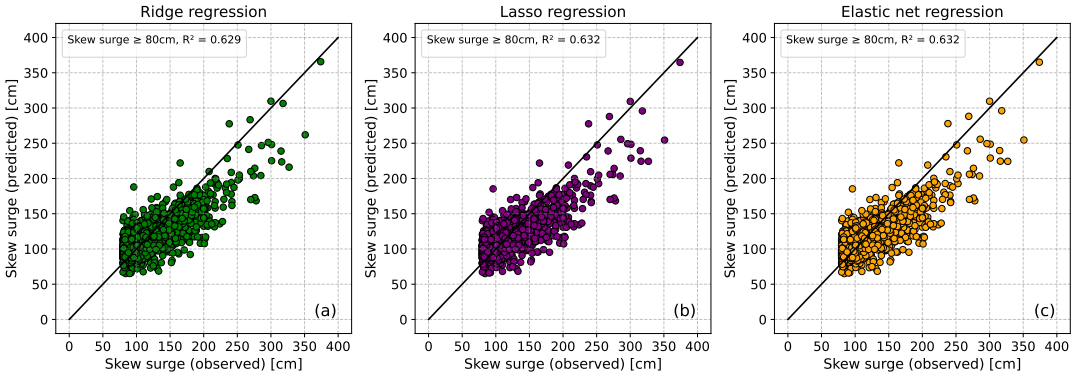


Figure A.5: Comparison between observed skew surge heights and predicted skew surge heights resulting from a leave-one-out-cross-validation using ridge (a), lasso (b) and elastic net regression (c). The black line represents the diagonal, indicating perfect agreement between observed and predicted skew surges. The threshold for training is hwss $\geqslant$ 80 cm.

Furthermore, with regard to the performance of the skew surge models, it is important to evaluate the influence of the predictors. As mentioned above (Sect. A.3.2), due to forced positive coefficients, ridge regression performs a lasso-like predictor selection, resulting in a sparse model with only seven terms including the intercept. However, lasso and elastic net regression models consist of just five terms in total, including the intercept. Both models show similar performance with identical selected predictors but slightly different coefficients.

In summary, in our case, we observe an overall high level of predictive performance with sparse models. Considering the three potential regression methods, we opt for the elastic net regression model (training threshold hwss $\geqslant$ 80 cm) as our final storm surge model (Fig. A.5c):

$$\begin{aligned} \mathrm{hwss}_{\mathrm{StormSurgeModel}} = \mathrm{f}(&\mathit{effwind}_{10\mathrm{m}}^{\mathrm{GC}_{\mathrm{t}=-12}}, \mathit{effwind}_{10\mathrm{m}}^{\mathrm{GC}_{\mathrm{t}=-6}}, \\ &\mathit{effwind}_{10\mathrm{m}}^{\mathrm{GC}_{\mathrm{t}=-2}}, \mathit{effwind}_{10\mathrm{m}}^{\mathrm{GC}_{\mathrm{t}=-1}}) \\ &+ \mathit{intercept} \end{aligned} \tag{2}$$

According to the elastic net regularization, the hwss predicted by the storm surge model is based on the following predictors:

- $effwind_{10m}^{GC_{t=-12}}$: effective wind in the respective grid cell 12 hours prior the skew surge event (squared),
- $effwind_{10m}^{GC_{t=-6}}$: effective wind in the respective grid cell 6 hours prior the skew surge event (squared),
- $effwind_{10m}^{GC_{t=-2}}$: effective wind in the respective grid cell 2 hours prior the skew surge event (squared),
- $effwind_{10m}^{GC_{t=-1}}$: effective wind in the respective grid cell 1 hour prior the skew surge event (squared).

This choice is primarily motivated by its simplicity, as it has even fewer terms compared to the ridge regression model, and unlike the lasso regression model, also includes coefficient shrinkage.

### A.3.4 *Verification of the storm surge model and quantile mapping bias correction*

We eventually verify the storm surge model by using it to predict all high-water skew surge events from 1959 to 2022. By including this broader range of events, we ensure that the model is capable of predicting skew surges on which it was not trained, namely those below 80 cm. In doing so, we train the model based on (hwss $\geqslant$ 80 cm) events of all years except the year we want to predict.

Figure A.6a and b show the probability density function (PDF) and cumulative distribution function (CDF) of the observed and predicted skew surge events from 1959 to 2022. The PDF (Fig. A.6a) reveals that the observed skew surge data have a broader distribution centered around lower skew surge heights, whereas the predicted skew surge data are more concentrated and centered around greater skew surge heights, never falling below zero. We also see the same pattern in the CDF (Fig. A.6b), with the predicted CDF indicating higher skew surges at a given cumulative probability compared to the observed CDF.

Additionally, we plot observed against predicted skew surge heights (Fig. A.7a) and find a strong correlation coefficient of 0.867 and an $R^2$ value of 0.751. However, in the lower range of skew surges (observed values below 80 cm), the model tends to overestimate the values, while in the upper range (observed values above 150 cm), it tends to underestimate the skew surge heights. While the underestimation of extreme skew surges may be due to a lack of data (Sect. A.3.2), the overestimation of low or negative skew surges is a consequence of training on logarithmic values. The reason for this lies in the nature of logarithmic functions which is defined only for positive real numbers.

In order to adjust the model output, we apply bias correction using the quantile mapping method of Cannon et al. (2015). We calculate the transfer function using the observed and reconstructed skew surges, but without performing cross-validation. Figure A.6c and d show the PDF and CDF of the observed and bias-corrected predicted

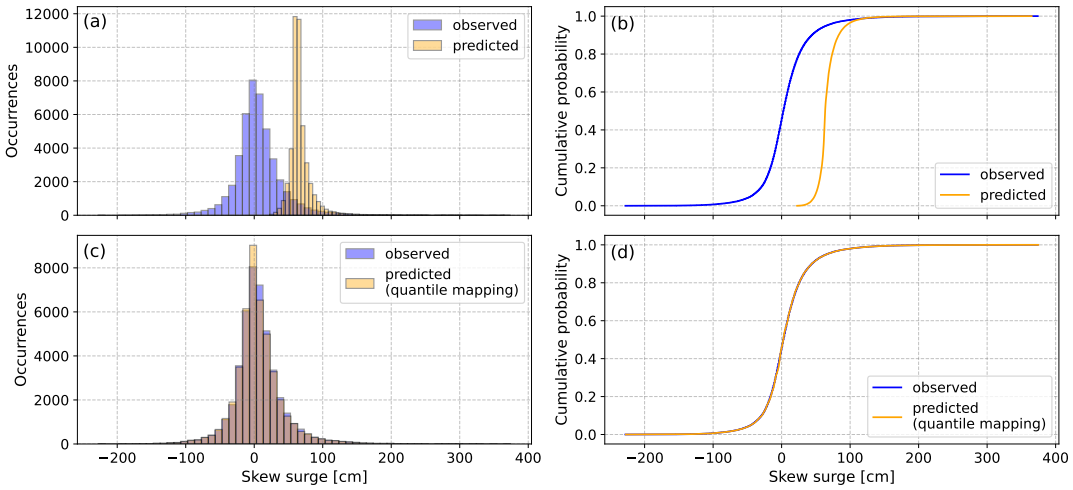


Figure A.6: Comparison of all observed (blue) and predicted (orange) PDFs and CDFs of skew surge events from 1959 to 2022, before (a, b) and after (c, d) bias correction. The threshold for training is hwss $\geqslant$ 80 cm and the regularization method is elastic net, with the year to be predicted being excluded from the training.

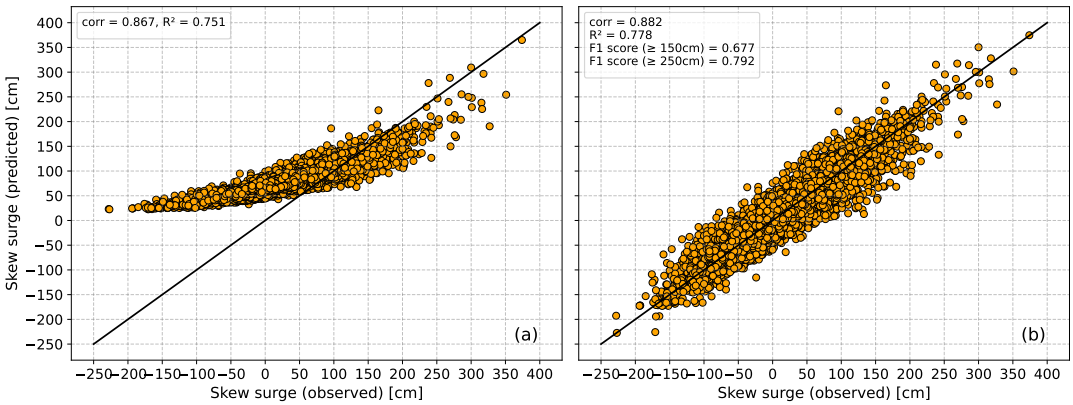


Figure A.7: Scatter plots comparing all observed and predicted skew surge heights from 1959 to 2022 - before (a) and after (b) quantile mapping bias correction. The black line represents the diagonal, indicating perfect agreement between observed and predicted skew surges. The threshold for training is hwss $\geqslant$ 80 cm and the regularization method is elastic net, with the year to be predicted being excluded from the training.

skew surge events. After applying the quantile mapping bias correction, the predicted distribution aligns much more closely with the observed distribution, both in terms of central tendency and spread. Also, the almost overlapping CDFs (Fig. A.6d) and the tighter clustering of points along the diagonal in Fig. A.7b indicate that the quantile mapping method successfully corrects the bias in the model's prediction. Moreover, it effectively reduces both the overestimation of lower skew surges and the underestimation of higher skew surges, resulting in better alignment with the observed values. The corrected prediction exhibit a higher correlation with the observed values (corr = 0.882) and an increase in the $R^2$ value ($R^2$ = 0.778) (Fig. A.7b). Compared to the more complex models developed by Jensen et al. (2013), Dangen-

dorf et al. (2014) and Niehüser et al. (2018), our storm surge model demonstrates equally high skill measures despite its extreme simplicity.

### A.3.5 *Classification evaluation*

To assess the ability of the storm surge model to discriminate extreme storm surge events, we conduct a classification evaluation and calculate the F1 score for two categories: (1) predicting a skew surge of greater than or equal to 150 cm, and (2) predicting a skew surge of greater than or equal to 250 cm. These threshold values are officially used by BSH to define a storm surge and a severe storm surge (Sect. A.2.3). To perform the classification evaluation, we use values from the contingency table based on the model's prediction (Table A.2). The contingency table consists of four values: true negatives, true positives, false negatives and false positives. We use the last three values to calculate precision, recall and ultimately the F1 score (see Sect. A.6.2.2 for details), as shown in Fig. A.7.

Table A.2: Contingency table summarizing model predictions for two categories: skew surge $\geqslant$ 150 cm and skew surge $\geqslant$ 250 cm. Values in bold black represent bias-corrected predictions, while regular black text indicates predictions without bias correction.

| | **Skew surge $\geqslant$ 150 cm** | | **Skew surge $\geqslant$ 250 cm** | |
|---|---|---|---|---|
| True negatives (Correct rejection) | **44829** | 44893 | **45132** | 45136 |
| True positives (Hit) | **170** | 126 | **19** | 6 |
| False negatives (Miss) | **83** | 127 | **5** | 18 |
| False positives (False alarm) | **79** | 15 | **5** | 1 |

In our analysis, the F1 scores for predicting skew surges greater than or equal to 150 and 250 cm demonstrate a clear improvement after applying bias correction. After bias correction, the F1 scores are 0.677 and 0.792, respectively. In contrast, before bias correction, the F1 scores are 0.64 at the 150 cm threshold and 0.387 at the 250 cm threshold. This indicates good model performance at the 150 cm threshold, showing a reasonable balance between precision and recall. For the higher threshold of 250 cm, the model demonstrates even better performance. This improvement suggests that the model is more accurate and reliable in predicting larger skew surges. However, the very small sample size of just 24 events with a skew surge of more than 250 cm (19 hits and 5 misses) plus five false alarms is associated with much higher uncertainty for the respective F1 score. These results underscore the importance of bias correction, as it significantly enhances the model's ability to predict higher skew surge values, improving both precision and recall for extreme events.

## A.4 DISCUSSION

The presented storm surge model, after bias correction, demonstrates a strong correlation between observed and predicted skew surges (Figs. A.7b and A.8). The classification evaluation indicates that the model might be even more accurate in predicting

higher skew surges ($\geqslant$ 250 cm) compared to those above 150 cm. Other studies, such as those by Müller-Navarra and Giese (1999), Niehüser et al. (2018) and Dangendorf et al. (2014) often underestimate these higher skew surges. As previously mentioned, the sample size for calculating the F1 score at the 250 cm threshold is very small, so the F1 score is associated with a much greater uncertainty. Nevertheless, the F1 score underlines that the model is effective in predicting extreme events. It is reasonable to assume that especially severe storm surges are predominantly caused by northwesterly winds, as this pattern aligns with the predictor regions (Sect. A.3.1; Fig. A.3: 12, 6, 2 and 1 h before the storm surge). This assumption is supported by Gerber et al. (2016), who identified, analyzed, and categorized storm surges based on atmospheric conditions. They find that severe storm surges in the German Bight occur more frequently during the northwest type (NWT), characterized by a northwesterly flow from the northern section of the North Sea to the German Bight. Examples of storm surges resulting from an NWT weather situation include the very severe storm surge in February 1962 and the one at the end of January 1976 (Gerber et al., 2016; Jochner et al., 2013; Meyer and Gaslikova, 2024). In these instances, high effective winds (17 to 21 m/s) are recorded at all predictor locations and our storm surge model successfully predicts these storm surges (Fig. A.8).

Another weather situation relevant to storm surges in the German Bight is the west and southwest type (W + SWT), characterized by westerly or southwesterly winds (Gerber et al., 2016). Notable examples of storm surges resulting from W + SWT weather situations include the highest storm surges ever recorded at the beginning of January 1976 (Gerber et al., 2016; Meyer and Gaslikova, 2024) and the storm surge in February 2022 (Mühr et al., 2022). Here, our model shows varying performance. On the one hand, with high effective wind speeds (18 to 23 m/s) at all predictor locations, the storm surge model successfully predicts the storm surge on 3 January 1976 (Fig. A.8b). On the other hand, the model underestimates the storm surge in February 2022 (Fig. A.8a). In this case, effective wind speeds ranged from 15 to 18 m/s in the central (Fig. A.3: 6 h before the storm surge) to southeastern sections of the North Sea (Fig. A.3: 2 and 1 h before the storm surge), but negative effective winds of -7 m/s at the predictor location in the very northwestern section of the North Sea (Fig. A.3: 12 h before the storm surge). The influence of the negative effective wind in the northwestern predictor location results in a lower predicted skew surge.

However, other external factors may also influence the performance of the model. The storm surge in February 2022 was not only the result of predominantly southwesterly winds but also a part of a series of storms (Mühr et al., 2022). This led to a pre-filling of the North Sea (Mühr et al., 2022), causing weaker effective winds to induce a higher skew surge. This pre-filling effect additionally explains why the model underestimates the February 2022 storm surge. Nevertheless, the resulting skew surge prediction still exceeds 150 cm, which means it is still able to identify an event exceeding this critical threshold operationally used for issuing warnings.

When considering the categories for storm-surge-inducing weather situations, the tracks of the NWT and W + SWT categories overlap in certain areas (Gerber et al., 2016). Thus, we cannot conclusively state that our model is better at predicting

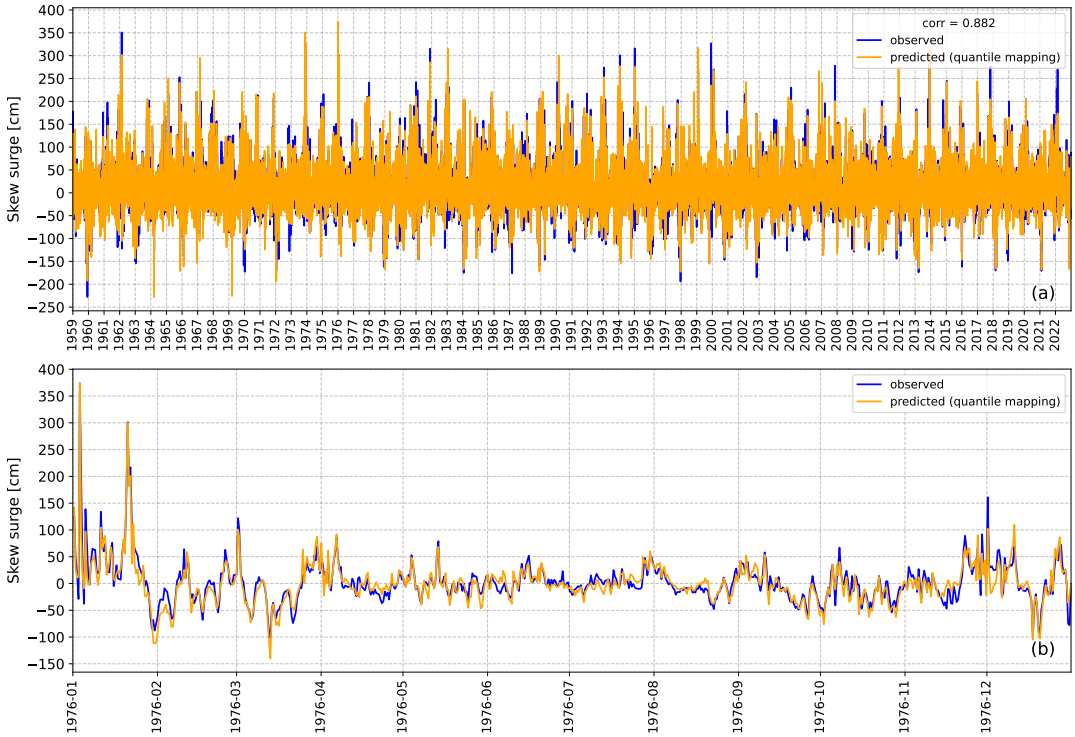


Figure A.8: Time series of all observed and predicted (quantile mapping) skew surges from 1959 to 2022 for the entire period (a) and a zoom into the year 1976 for better visibility of particular events in an example year, containing the highest ever recorded storm surge at Cuxhaven (b). The threshold for training is hwss $\geqslant$ 80 cm and the regularization method is elastic net, with the year to be predicted being excluded from the training.

storm surges from one category over the other. Nevertheless, as long as the triggering weather situation leads to westerly to northwesterly winds, which is mostly the case, the storm surge model is able to predict the resulting storm surge very well.

Another factor contributing to extreme water levels in the North Sea is external surges. These surges are caused by low-pressure systems over the North Atlantic and are amplified at the continental shelf (Böhme et al., 2023). External surges can cause water-level changes exceeding 1 m along the along the British, Dutch, and German coasts (Böhme et al., 2023). When external surges coincide with storm surges, they have the potential to create extreme water levels. Of the 126 external surges recorded between 1971 and 2020, 21% occurred during or close to a storm surge event in the German Bight (Böhme et al., 2023). Notable examples of such co-occurrences include the storm surge in February 1962 and the one in December 2013 (Böhme et al., 2023). For both events, the storm surge model predicted a skew surge of more than 150 cm in December 2013 and even more than 250 cm in February 1962 (Fig. A.8a), leading to storm surge or severe storm surge warnings. However, the actual water levels were underestimated by approximately 50 cm, which roughly corresponds to the average influence of external surges on water levels in Cuxhaven during storm surges (Böhme et al., 2023).

Despite the aforementioned limitations, we find strong model performance in predicting both moderate and extreme storm surges in the German Bight.

## A.5 SUMMARY AND CONCLUSIONS

In this study, we developed a statistical wind-based storm surge model for the German Bight that is able to predict skew surges based solely on the effective wind. Aiming for model simplicity, we identified predictor locations across the entire North Sea, considered numerous training thresholds, and applied three different regularization methods. The resulting storm surge model comprises only five terms: the squared effective wind in certain grid cells at four lead times (12, 6, 2, and 1 h prior to the skew surge event) as robust predictors, along with an intercept.

We validate the model against historical data and find that it achieves high predictive accuracy, rivaling more complex models despite its simplicity. Moreover, our findings underscore the significance of wind as the primary driver of storm surges in the German Bight. The model provides reliable predictions for both moderate and extreme storm surge events, with more accurate predictions for surges preceded by westerly or northwesterly winds. In particular, the good prediction accuracy for storm surges greater than or equal to 250 cm is a unique outcome of this study.

Furthermore, the simplicity of our storm surge model facilitates its application to climate simulations, making it a valuable tool for assessing storm surge risk in the German Bight under changing climate conditions, on top of sea-level rise. Additionally, this approach is not only effective for the German Bight but also adaptable to other coastal regions worldwide.

## A.6 APPENDIX

### A.6.1 *Identifying relevant predictor positions*

To determine the location and lead time of the predictors ($effwind^{k,t}_{10m}\,(hwss)$) within the North Sea region, we create an individual statistical model for each grid cell in the North Sea region at each time step using quadratic regression. In the following, we refer to these models as grid cell models. In a first step, we select all time steps of $effwind^{k,t}_{10m}\,(hwss)$ 12 hours before the respective occurrence of hwss $\geqslant$ 50, 60...150 cm in Cuxhaven. Since $effwind^{k,t}_{10m}\,(hwss)$ is available in hourly resolution, this corresponds to 12 time steps. We choose 12 h, as this is approximately the time between two high tides. Since we count 2079 grid cells in the North Sea region and consider 12 time steps, we have a total of 24 948 grid cell models for each of the 11 hwss training thresholds. The dependent variable in each model is the respective logarithmic hwss height, with the standardized $effwind^{k,t}_{10m}\,(hwss)$ serving as predictor. As the wind stress depends on the square of the wind speed (Olbers et al., 2012), we create the grid cell models with quadratic order.

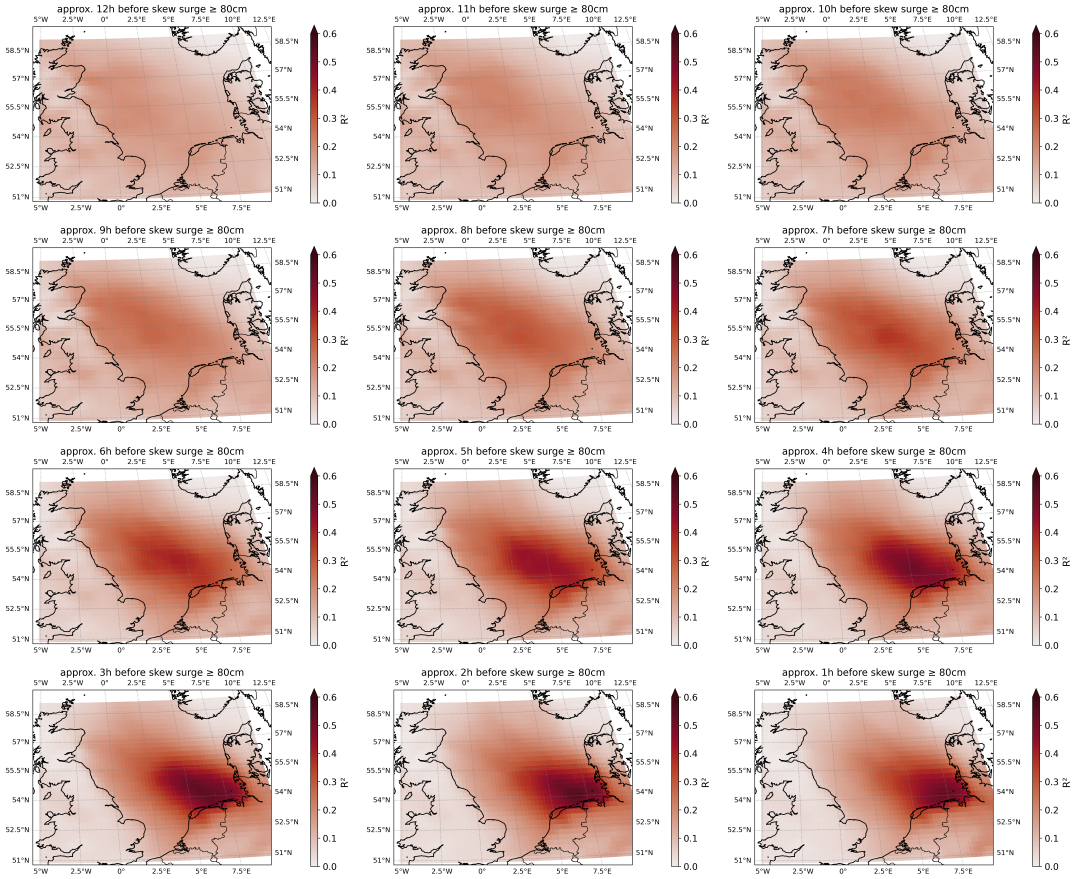


Figure A.9: $R^2$ value (based on a leave-one-out-cross-validation) of each grid cell model within the North Sea region for 12 h before the skew surge event (top left) to 1 h before the skew surge event (bottom right). The darker the color, the greater the $R^2$ value. The event threshold for training is hwss $\geqslant$ 80 cm.

Once we have defined the conditions for the grid-cell models, we perform a leave-one-out-cross-validation and calculate the coefficient of determination ($R^2$) for each grid-cell model. In order to obtain the most relevant grid cells for the respective subsample of events, we select the grid-cell model with the highest $R^2$ value from each time step (Fig. A.9). As we consider the 12 h before the occurrence of hwss $\geqslant$ 50, 60, ..., 150 cm, we obtain 12 grid-cell models and thus grid cells ($GC_{t=1,..,12}$), each of which contains both the relevant lead time and position in the North Sea region for the respective hwss training threshold in Cuxhaven.

### A.6.2 *Performance metrics and model optimization strategies*

#### A.6.2.1 *Regularization methods*

The usual regression procedure for determining the unknown coefficients in a multiple linear regression model is based on the ordinary least squares (OLS) method. Its error criterion is the minimization of the sum of the squared errors, where the error is the difference between the actual and the predicted value (Wilks, 2011). However,

OLS has some known disadvantages. For example, OLS is highly sensitive to outliers in the data and can be prone to overfitting. In addition, OLS performs poorly when it comes to accuracy in predicting unseen data and in interpreting the model (Zou and Hastie, 2005). For the latter, the simpler the model, the more the relationship between the dependent variable and the predictors is highlighted. The model's simplicity is particularly important when the number of predictors is large.

An effective method for overcoming the difficulties of OLS is regularization. It is a method to avoid overfitting and control the complexity of models by adding a penalty term to the model's target function during training. The aim is to keep the model from fitting too closely to the training data and to encourage simpler models that are better suited to unseen data. Here, we consider three different regularization techniques, namely ridge (Hoerl and Kennard, 1970a,b), lasso (Tibshirani, 1996) and elastic net regression (Zou and Hastie, 2005).

The main idea behind ridge regression (Hoerl and Kennard, 1970a,b) is its ability to strike a balance between bias and variance. This is achieved by including a penalty term proportional to the square of the coefficients in the loss function. This approach leads to the coefficient estimates being smaller while still having non-zero values. The target function to be minimized becomes:

$$\text{Loss}_{\text{Ridge}} = \text{Loss}_{\text{OLS}} + \lambda \sum_{j=1}^{n} \beta_j^2, \tag{3}$$

where $\text{Loss}_{\text{OLS}}$ is the loss function of Ordinary Least Squares, $\lambda$ is the regularization parameter that defines the regularization strength and $\sum_{j=1}^{n} \beta_j^2$ is the regularization term - the sum of squared coefficients. Since large coefficients may lead to low bias and high variance, they are penalized by adding the regularization term and effectively shrink toward zero. Consequently the model becomes sensitive to fluctuations in the data. However, ridge regression is unable to create a simple model, in the sense of fewer predictors, as it always retains all predictors in the model. This contrasts with the lasso regression (Tibshirani, 1996).

Lasso regression is a method to reduce overfitting and perform predictor selection by setting some coefficient estimates to exactly zero. For this purpose, a regularization term proportional to the absolute value of the coefficients is added to the loss function. The target function to be minimized becomes:

$$\text{Loss}_{\text{Lasso}} = \text{Loss}_{\text{OLS}} + \lambda \sum_{j=1}^{n} |\beta_j|, \tag{4}$$

where $\text{Loss}_{\text{OLS}}$ is the OLS loss function, $\lambda$ is the regularization parameter and $\sum_{j=1}^{n} |\beta_j|$ is the regularization term - the sum of absolute values of coefficients. Lasso regression simplifies the model by shrinking less important coefficients to zero, effectively eliminating some predictors from the model. This leads to simpler and more interpretable models.

Zou and Hastie (2005) propose a third regularization method whose main principle is to balance ridge and lasso regression by adding both ridge and lasso regularization terms to the loss function. The target function to be minimized becomes:

$$\text{Loss}_{\text{Elastic Net}} = \text{Loss}_{\text{OLS}} + \lambda_1 \sum_{j=1}^{n} |\beta_j| + \lambda_2 \sum_{j=1}^{n} \beta_j^2, \tag{5}$$

where $\text{Loss}_{\text{OLS}}$ is the loss function of OLS, $\lambda_1$ and $\lambda_2$ are the regularization parameters for lasso and ridge penalties respectively, $\sum_{j=1}^{n} |\beta_j|$ is the lasso regularization term and $\sum_{j=1}^{n} \beta_j^2$ is the ridge regularization term. Elastic net regression combines the strength of both lasso and ridge regression by balancing the selection of predictors and coefficient shrinkage, resulting in more robust and reliable predictive models.

#### A.6.2.2 *F1 Score*

The F1 score combines precision and recall into one metric. Precision measures the accuracy of positive predictions made by the model. It is determined by dividing the number of true positive predictions by the total number of samples predicted as positive, regardless of correct identification:

$$\text{Precision} = \frac{TP}{TP + FP}, \tag{6}$$

where TP represents true positive predictions and FP indicates false positive predictions.

Recall measures the fraction of actual positives that were correctly identified by the model. It is computed by dividing the number of true positive predictions by the total number of samples that should have been identified as positive:

$$\text{Recall} = \frac{TP}{TP + FN}, \tag{7}$$

where TP refers to true positive predictions and FN to false negative predictions. The F1 score is defined as the harmonic mean of precision and recall:

$$F1 = 2\frac{PR}{P + R}, \tag{8}$$

where P stands for precision and R for recall. The F1 score has its best value at 1 (perfect precision and recall) and its worst at 0.

#### A.6.2.3 *Root-mean-square error*

The root-mean-square error (RMSE) is a measure of how well the model is performing in terms of prediction accuracy, with lower values indicating better performance. It has the same units as the observed values – in this case cm. We also determine the 95% confidence interval for the RMSE by applying the bootstrap method. This method involves resampling from the original dataset – here 1000 times – with replacements to simulate multiple scenarios.

## DATA AVAILABILITY

Water-level data for the Cuxhaven gauge are available upon request from the Waterways and Shipping Office Elbe-Nordsee via email (wsa-elbe-nordsee@wsv.bund.de). The ERA5 reanalysis products used for this study are available in the Copernicus Data Store at https://doi.org/10.24381/cds.adbb2d47 (Hersbach et al., 2023). The skew surge data used in this study can be accessed at https://doi.bsh.de/10.60751/96dc-te47 (Boesch, 2024).

## AUTHOR CONTRIBUTIONS

LS and TK designed and developed the study. AB computed and provided the skew surge data. LS did the analysis and created the figures. LS, JB and TK discussed the results. LS wrote the manuscript with contributions from all coauthors.


## ACKNOWLEDGMENTS

We thank Daniel Krieger and Claudia Hinrichs for their valuable feedback on this manuscript. Johanna Baehr was funded by the Deutsche Forschungsgemeinschaft (DFG, German Research Foundation) under Germany's Excellence Strategy: EXC 2037 "Climate, Climatic Change, and Society (CLICCS)" (project number: 390683824) and a contribution from the Center for Earth System Research and Sustainability (CEN) of the University of Hamburg. We thank the German Climate Computing Center (DKRZ) for providing their computing resources.

We thank the two reviewers for their valuable comments on the manuscript.

## FINANCIAL SUPPORT

This research has been supported by the German Federal Ministry for Digital and Transport (BMDV) in the context of the BMDV Network of Experts; the Deutsche Forschungsgemeinschaft (DFG, German Research Foundation) under Germany's Excellence Strategy: EXC 2037 "Climate, Climatic Change, and Society (CLICCS)" (project number: 390683824); and a contribution from the Center for Earth System Research and Sustainability (CEN) of the University of Hamburg.

# B

# FUTURE STORM SURGE RISK IN THE GERMAN BIGHT

The research presented in this chapter is complete and is currently in preparation for submission:

Schaffer, L., Baehr, J., and Kruschke, T. (in prep.). "Future Storm Surge Risk in the German Bight."

My contributions to the research presented in this chapter include developing the study concept and design together with Johanna Baehr and Tim Kruschke. I retrained the model, selected and processed the climate model data and performed the analyses. I generated all figures and interpreted the results together with Johanna Baehr and Tim Kruschke. Additionally, I wrote the manuscript, integrating the contributions of all co-authors.

# FUTURE STORM SURGE RISK IN THE GERMAN BIGHT

Laura Schaffer[1,2], Johanna Baehr[2], and Tim Kruschke[1]

[1]Federal Maritime and Hydrographic Agency (BSH), Hamburg, Germany
[2]Institute of Oceanography, University of Hamburg, Hamburg, Germany

## KEY POINTS

- Under SSP5-8.5, we project an increase in the frequency of winter storm surge events by more than 10% by the end of the century
- When combined with sea-level rise, present-day storm surge thresholds are projected to be exceeded three to five times more often by 2100

## ABSTRACT

Storm surges in the German Bight are among the North Sea's most severe coastal hazards. Assessing their future frequency and intensity is essential for evaluating coastal risk under changing climate conditions. We apply a statistical storm surge model for the German Bight to a CMIP6 multi-model ensemble under three emission scenarios (SSP2-4.5, SSP3-7.0, SSP5-8.5). Across all SSP scenarios, potential storm surge situations are projected to become significantly more frequent in winter by 2100. This increase is driven by stronger and more frequent westerly and northwesterly winds, likely linked to storm track shifts and more frequent positive North Atlantic Oscillation phases. In contrast, summer surge frequency is projected to decrease. These seasonal trends intensify under higher-emission scenarios. In combination with local sea-level rise projections, we find both moderate and severe present-day storm surge thresholds being exceeded three to five times more often by 2100, especially under high-emission scenarios.

## PLAIN LANGUAGE SUMMARY

Storm surges – temporary rises in sea level caused by strong winds – pose a serious risk to people and property along the German coast. In this study, we investigate how often and how severe these storm surges might become in the future, depending on the level of future greenhouse gas concentrations. To do this, we use a statistical storm surge model designed for the German Bight and apply it to a large set of

global climate simulations. We find that by the end of the century, potential storm surge situations are likely to become more frequent in winter. This is because winds from the west and northwest are expected to become stronger and more frequent. These changing wind patterns may be linked to shifts of typical storm tracks over the North Atlantic. In contrast, storm surges are expected to happen less often in summer. We also explore the combined effect of rising sea levels and future surges, finding that water levels along the German North Sea Coast will more often exceed today's storm surge thresholds. The higher the emissions in the future, the greater the risk becomes.

## B.1 INTRODUCTION

Storm surges in the German Bight – the southeastern part of the North Sea – are among the most dangerous coastal hazards in the region. These storm surges are caused when strong winds, particularly from northwest, push seawater towards the coast, temporarily raising sea levels well above normal tidal ranges (Pugh and Woodworth, 2014). The wind climate over the North Atlantic plays a central role in shaping the conditions that lead to storm surges in the German Bight and is characterized by the North Atlantic Oscillation (NAO), one of the primary modes of atmospheric variability in the Northern Hemisphere which influences the climate of both the North Atlantic and Europe (Hurrell and Deser, 2010; Wakelin et al., 2003). Wind conditions in the German Bight are predominately characterized by south-westerly and westerly winds, particularly during the winter months, and are strongly influenced by the state of the NAO (Mathis et al., 2015; Rubinetti et al., 2023). Wakelin et al. (2003) examines the sea-level dependence on the NAO, concluding that sea-level variations in the German Bight are primarily driven by wind patterns associated with the NAO. Since wind is the primary driver for sea-level variability – and consequently of storm surges – in the German Bight (Dangendorf et al., 2013), understanding how wind patterns evolve under future climate scenarios is essential in order to assess long-term coastal risks.

Recent studies increasingly focused on projecting future wind conditions in this region. Ortega et al. (2025) investigate future wind patterns under the RCP8.5 emission scenario using the regional coupled ocean-atmosphere model system MPIOM-REMO. Their results indicate an increasing frequency and intensity of westerly winds during the winter months, which may be linked to a predominance of the positive NAO phase. Similarly, Schade et al. (2025) use a CMIP6 multi-model ensemble and project an increase in frequency of westerly wind patterns under the SSP3-7.0 and SSP5-8.5 scenarios towards 2100. These wind patterns are known to favor storm surge events along the German North Sea Coast (Schade et al., 2025). Moreover, Krieger and Weisse (2025) apply both a CMIP6 multi-model ensemble and the Max Planck Institute Grand Ensemble with CMIP6 forcing. They find an increase in frequency of westerly winds over the North Atlantic and northwesterly winds over the German Bight. While their results also show a decrease in overall storm activity, they find that the most extreme storms in the German Bight could become stronger or more frequent under future climate conditions.

Strong winds associated with extra-tropical cyclones along the North Atlantic storm track – a region of frequent cyclone activity – are the primary driver of extreme storm surges in the German Bight (Danard et al., 2004). Several studies have investigated how climate change may affect storms and storm tracks over the North Atlantic and how these changes are connected to changes in atmospheric circulation patterns (Harvey et al., 2020, 2014, 2015; Lee et al., 2021; Lehmann et al., 2014; Priestley and Catto, 2022). The IPCC's 6th assessment report concluded that climate models show generally low agreement regarding changes in extra-tropical cyclone density over the North Atlantic in boreal winter (Lee et al., 2021). Priestley and Catto (2022) analyze projections from a CMIP6 multi-model ensemble and find that the total number of cyclones over the North Atlantic decreased by the end of the century, with a more pronounced decrease under higher emission scenarios. During the Northern Hemisphere winter, their results indicate an extension of the North Atlantic storm track into Europe, along with a reduction in cyclone activity over the Mediterranean. Despite the overall decline in cyclone frequency, Priestley and Catto (2022) project an increase in the number of intense cyclones that impact Northern Europe during winter. These findings are consistent with Harvey et al. (2020), who, based on a comprehensive analysis of 19 CMIP3, 38 CMIP5, and 14 CMIP6 models, conclude that the climate change response of the North Atlantic storm track is a strengthening and extension of the winter storm track into Europe. These projected changes in storm track and cyclone intensity are of particular relevance for the German Bight, where wind fields associated with extra-tropical cyclones largely determine storm surge magnitudes.

While future wind conditions have been increasingly investigated, relatively few studies have focused on how these projections translate into corresponding surge heights. Mayer et al. (2022) used a regionalized ensemble of 30 MPI-ESM1.1-LR members, downscaled with MPIOM-REMO under RCP8.5, to analyze future storm surge characteristics in the German Bight. They find an increase in frequency and duration of storm surges by the end of the century, however extreme events show no clear climate-driven change. They link these changes primarily to the increasing frequency of strong westerly winds. Using MPIOM-REMO, Lang and Mikolajewicz (2020) likewise find an increased frequency of extreme high sea levels under rising $CO_2$ concentrations in the German Bight, even without taking mean sea-level rise into account. They attribute this to enhanced large-scale storm track activity and stronger westerly wind speed extremes over the region. Irazoqui Apecechea et al. (2025) introduce a hybrid statistical downscaling model to project future extreme storm surges across Europe using a large CMIP6 ensemble. In contrast to previous studies, their results show no robust change in surge intensity for the southern North Sea by 2100. This indicates that region-specific models or tailored methods may be required to better capture storm surge dynamics in the southern North Sea.

Estimating future storm surge heights is essential in evaluating potential coastal risks, especially as accelerating sea-level rise in the North Sea (Steffelbauer et al., 2022) raises the baseline for storm surges. However, most existing studies rely on a single climate model or emission scenario, limiting the robustness of their projections. This highlights the need to use multi-model ensembles for predicting storm surge

heights in order to improve the robustness of future projections. Addressing this gap, this study uses a CMIP6 multi-model ensemble combined with a simple statistical storm surge model (Schaffer et al., 2025), specifically tailored for Cuxhaven – a city serving as a proxy for the German Bight – to estimate future storm surge intensity. Specifically, it aims to (i) analyze future frequency of predicted surges, (ii) examine wind conditions driving high surges, and (iii) provide a rough estimate of future high tide water levels in Cuxhaven by combining projected surges with sea-level rise.

## B.2 METHODS AND DATA

### B.2.1 *CMIP6 Multi-Model Ensemble*

In this study, we use the output of climate models from the sixth phase of the Coupled Model Intercomparison Project (Eyring et al., 2016, CMIP6). Specifically, we use the zonal (uas) and meridional (vas) components of the 10-meter wind from the historical simulations covering the period 1960-2014, as well as projections from future scenario simulations under SSP2-4.5, SSP3-7.0 and SSP5-8.5 forcings, which span the years 2015-2100. We include only those CMIP6 models for which wind data are available at three-hourly resolution for both historical and scenario simulations, and where the realization is used across the historical and future periods. Based on these criteria, we select nine different climate models with in total 25 ensemble members for our analysis (Table S1).

### B.2.2 *Sea-Level Rise Data*

We use sea-level rise (SLR) projections for Cuxhaven for the period 2070-2100 under three emission scenarios – SSP2-4.5, SSP3-7.0, and SSP5-8.5 – based on a newly developed dataset by Jensen et al. (2025). This dataset combines IPCC projections of total sea-level change (Garner et al., 2022) with a high-resolution land elevation model for Fennoscandia (Vestøl et al., 2019), resulting in an optimized set of relative sea-level projections for the North Sea and Baltic Sea regions. As the data is available at decadal resolution, we perform linear interpolation to generate a three-hourly time series, enabling us to combine the SLR data with the projected wind surges.

### B.2.3 *Mean High Water Data*

To obtain a rough estimate of future water levels at Cuxhaven during high tide, we combine projected wind surges and SLR with the mean high water level. We calculate the mean high water (MHW) for the reference period 1995-2014 by averaging the annually computed mean high waters over these years (Boesch, 2025).

### B.2.4 *Statistical Storm Surge Model*

Schaffer et al. (2025) developed a simple statistical storm surge model for the German Bight based on multiple linear regression, using the grid cell-specific effective

wind as predictor variable. The simplicity of the statistical model allows its application to climate projections. However, the statistical model is based on an hourly temporal resolution, which limits its direct applicability to climate model output, where the highest available temporal resolution is typically three-hourly. To address this limitation, we re-train the statistical model using three-hourly data. Specifically, we use the same input data as in the hourly model – grid cell-specific effective wind calculated from the zonal and meridional wind components from the ERA5 reanalysis (Hersbach et al., 2020) over the period 1959-2022 – but modify the dataset by first selecting three-hourly time steps. Throughout the re-training process, we follow the same statistical approach described in Schaffer et al. (2025). The statistical storm surge model trained on three-hourly grid cell-specific effective wind speed data performs comparably to the hourly model, demonstrating high predictive skill with a correlation coefficient of 0.88. It achieves this performance with just three terms: the effective wind speed at two locations with different lead times (12 and 3 hours before the surge) within the North Sea region, plus an intercept (Fig. S1).

To apply the statistical storm surge model to climate projections, we use grid cell specific effective wind speed values derived from the CMIP6 multi-model ensemble (Sect. B.2.1) as input. The statistical storm surge model requires these effective wind values at specific North Sea locations and lead times. As climate models differ not only in temporal but also in spatial resolution, we select, for each climate model individually, the grid cells nearest to the original locations to account for their coarser grid. Subsequently, by applying all statistical methods described in Schaffer et al. (2025), we obtain wind surge projections for both the historical period and three future scenarios: SSP2-4.5, SSP3-7.0, and SSP5-8.5. The projected wind surge refers to the wind-driven component of coastal water elevation during high tide, as the statistical model is trained exclusively on high water skew surges (Boesch, 2024). Since climate models do not include tidal information, we calculate the wind surge independently at every three-hour interval.

## B.3 RESULTS

### B.3.1 *Frequency of Projected Wind Surges*

We apply the statistical storm surge model (Sect. B.2.4) to both historical and future wind conditions from the CMIP6 multi-model ensemble (Sect. B.2.1). This allows us to assess future wind surge heights in the German Bight under different SSP scenarios to compare impacts across emission pathways. Figure B.1 shows the projected frequency of wind surge events for the historical period (1985-2014) and the end of the century (2071-2100), separately for winter (Fig. B.1a, b) and summer (Fig. B.1c, d) months, along with changes relative to the historical period. We assess statistically significant changes by bootstrapping (1000 resamples) the historical data for each season and testing whether future scenario values fall outside the 95% confidence interval. We find a significant increase in the frequency of winter wind surge events across all SSP scenarios by 2100, including events exceeding 150 cm, which is the official threshold for storm surges in the German Bight (MHW plus 150 cm) (BSH, 2025a). For events above this threshold, the increase exceeds 10% under the SSP5-8.5

scenario (Fig. B.1b). In contrast, summer projections indicate a decrease in positive wind surge events compared to the historical period, with stronger declines under higher forcing.

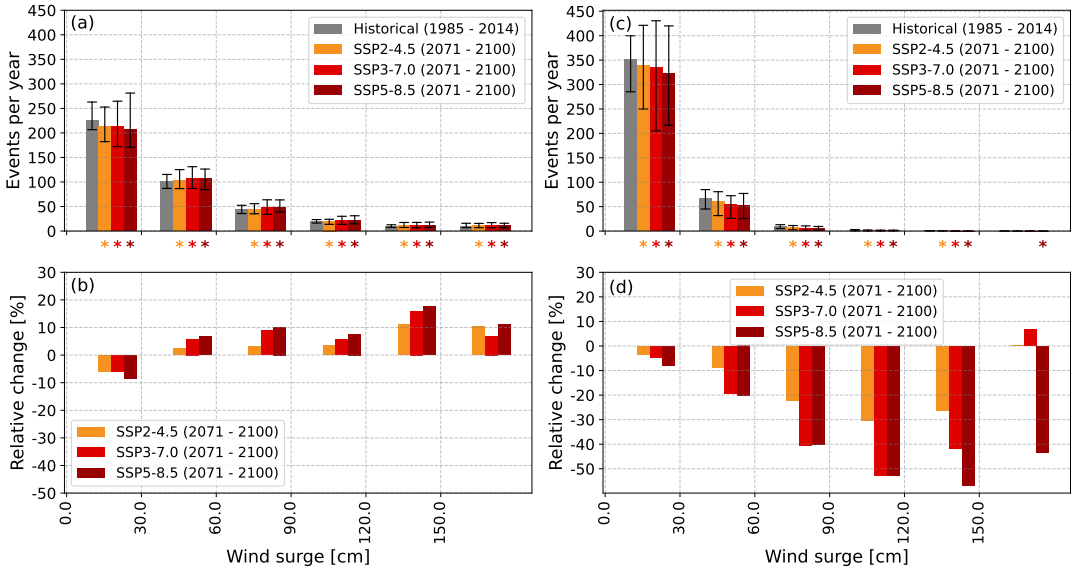


Figure B.1: **Top panel**: Annual counts of positive wind surge events, categorized into 30 cm bins, based on the output of the statistical storm surge model applied to the CMIP6 multi-model ensemble. Results are shown for winter (DJF) (a) and summer (JJA) (c) months during the historical period (1985–2014; gray) and projected for the end of the century (2071–2100; reddish colors) under different SSP scenarios. Vertical error bars represent the ensemble spread. Stars indicate statistically significant changes. **Bottom panel**: Projected changes in event frequency by bin at the end of the century compared to the historical period for DJF (b) and JJA (d).

Additionally, we conduct a seasonality analysis to assess whether climate change affects the timing and distribution of storm surges throughout the year. In contrast to Mayer et al. (2022), who report a shift in seasonality from the last to the first quarter of a year, we do not find significant changes in the overall seasonality of storm surges or mean wind surge events (Fig. S2 and S3).

### B.3.2 *Future Wind Conditions Linked to High Surges*

To investigate the changes in wind conditions that contribute to an increased frequency of storm surge events during winter – defined here as wind surges $\geqslant$ 150 cm – we perform a composite analysis of wind speed and direction 12 and three hours prior to potential storm surge events. We choose these specific lead times as the statistical storm surge model used to compute the wind surges relies on wind information from these points in time (Sect. B.2.4). We conduct this analysis for both the historical period and the future climate projection under the SSP5-8.5 scenario. We provide the number of events from each climate model contributing to this analysis in Table S2.

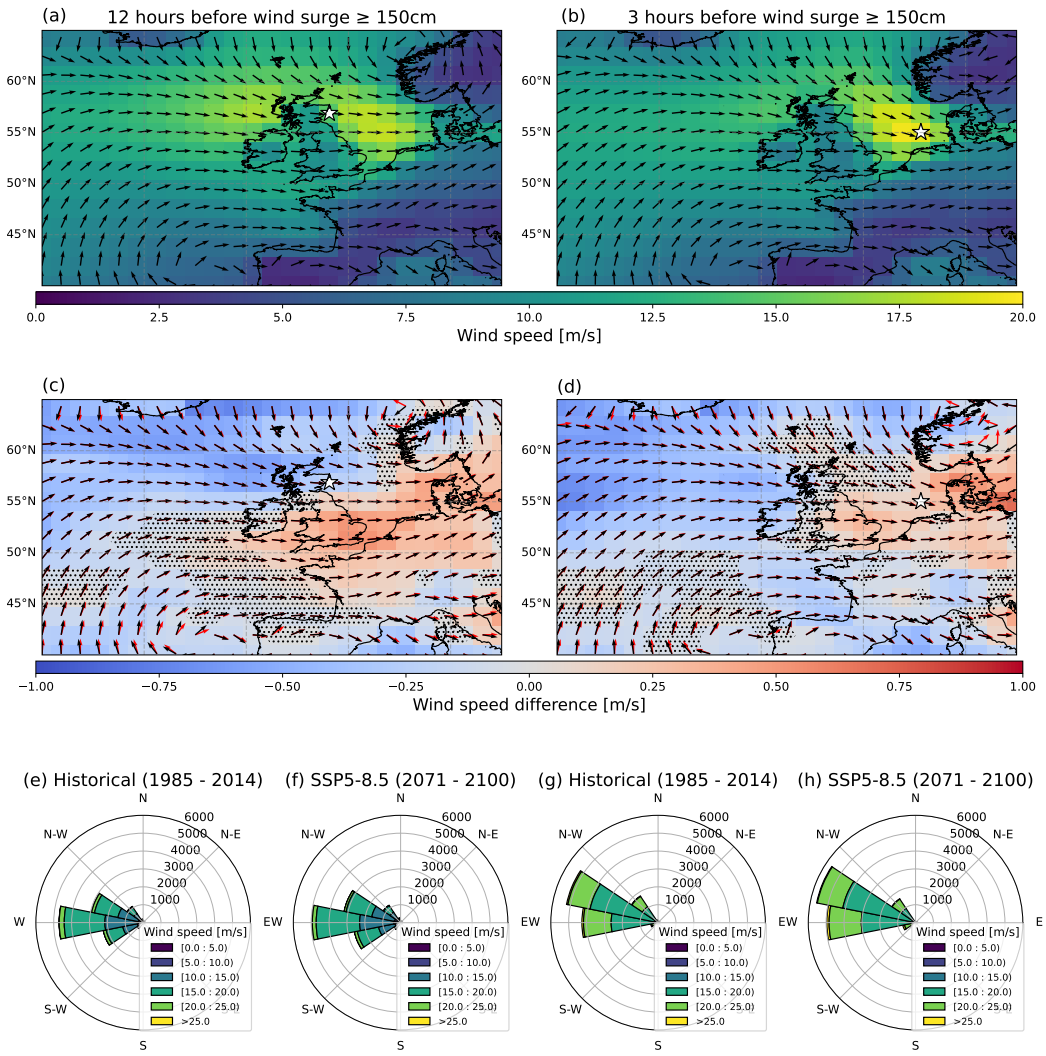


Figure B.2: Atmospheric conditions linked to ⩾ 150 cm wind surges in Cuxhaven based on the CMIP6 multi-model ensemble. White stars indicate the grid cells used as input for the statistical storm surge model. **Top panel**: Composite analysis of wind speed (color shading) and wind direction (black arrows – displayed in unit length) 12 (a) and 3 (b) hours before wind surge events ⩾ 150 cm during the historical period (1985-2014). **Middle panel**: Projected changes in wind speed associated with ⩾ 150 cm wind surges under SSP5-8.5 by 2071-2100, relative to 1985-2014. Shown for 12 (c) and 3 (d) hours before wind surge events. Color shading shows wind speed differences; black arrows indicate historical wind direction; red arrows show projected wind direction – both displayed in unit length. Stippling marks areas with non-significant wind speed changes. **Bottom panel**: Wind roses showing wind conditions at the locations marked by white stars, 12 (e and f) and 3 (g and h) hours before ⩾ 150 cm wind surge events. Results are shown for the historical period (1985-2014) and end of the century (2071-2100) under the SSP5-8.5 scenario. Values indicate event counts.

In the historical period, we find predominantly westerly winds 12 hours before potential storm surge events, along with high wind speeds over the North Sea (Fig. B.2a). Three hours before, winds shift to northwesterly directions, accompanied by a further intensification of wind speeds over the North Sea (Fig. B.2b). Towards the

end of the century, under the SSP5-8.5 scenario, wind speeds increase significantly in the southern North Sea both 12 and three hours prior to the events compared to the historical period (Fig. B.2c, d). In contrast, wind speeds decrease to the north and south of this region. A closer look at the wind conditions used as input in the statistical storm surge model (white stars in Fig. B.2a-d) shows that, despite a significant decrease in wind speed 12 hours before the potential storm surge events, the frequency of westerly winds increases (Fig. B.2e, f). Three hours before the events, wind speed increases significantly, accompanied by a higher frequency of westerly and northwesterly winds in the German Bight (Fig. B.2g, h).

Previous studies report a rise in frequency (Ortega et al., 2025; Schade et al., 2025) and intensity (Ortega et al., 2025) of westerly winds during winter in the German Bight, a trend we similarly observed in our analysis of the mean winter wind climate (Fig. S4 d-f). However, these changes are more pronounced during high surge events (Fig. B.2). Mayer et al. (2022) link the rising frequency of westerly winds to increased storm surge potential. Our analysis supports this interpretation but also suggests that increasing wind speed may raise storm surge frequency. In particular, the combination of more frequent westerly and northwesterly winds, along with a significant increase in wind speed over the southern North Sea, is important in contributing to the higher frequency of winter storm surge events by the end of the century.

### B.3.3 *Combined Effect of SLR and Projected Wind Surges on Water Levels*

While wind-driven water level elevations are a key factor contributing to extreme coastal water levels, they represent only one part of the broader picture. The most critical factor in the long term is the ongoing rise in mean sea level. Here, we combine these two components to provide a rough estimate of potential future coastal water levels during high tide by the end of the 21st century, focusing on winter only, as this represents the main storm surge season. To do so, we add projections of SLR (Sect. B.2.2) and wind surges (Sect. B.3.1) to the historical MHW in Cuxhaven (1995-2014), which is approximately 650 cm above gauge zero. For the historical period, we combine MHW with historical wind surges, while for future scenarios, we add projected wind surges and SLR. This enables assessment of changes relative to the historical water levels. Across all future scenarios, we find a clear increase in high water levels in winter compared to the historical period. Notably, winter water levels exceeding the present storm surge threshold of 800 cm at Cuxhaven – which occurred on average 9 times per year during the historical period – become significantly more frequent by the end of the century, increasing to 33 (SSP2-4.5), 38 (SSP3-7.0), and 47 (SSP5-8.5) events per year (Fig. B.3). Even for the present threshold of a severe storm surge (900 cm), we find a significant increase: while such levels occurred on average once per year during the historical period, they rise to 4 (SSP2-4.5), 5 (SSP3-7.0), and 6 (SSP5-8.5) events per year by the end of the century (Fig. B.3).

A notable feature is the shift in scenario ordering across the water level bins. From 710 cm onward, higher-emission scenarios show a stronger increase in the frequency of water levels within each bin. In contrast, closer to the historical MHW (650 cm),

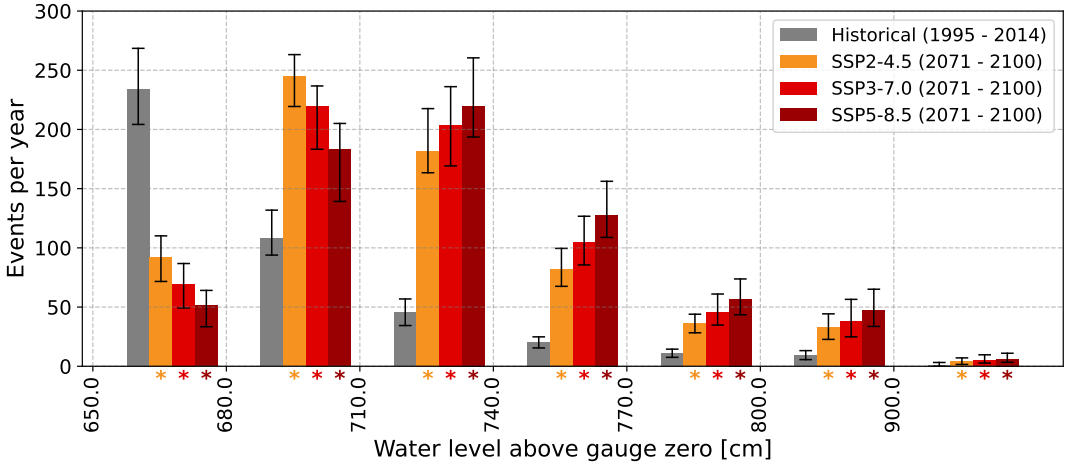


Figure B.3: Annual counts of winter water level above gauge zero at Cuxhaven for the historical period (1995-2014; gray), representing the combined effect of MHW and historical wind surges. Projections for the end of the century (2071-2100; reddish colors) include the combined effect of MHW, projected wind surges, and projected SLR under different SSP scenarios. Wind surges (historical and projected) are based on the output of the statistical storm surge model applied to the CMIP6 multi-model ensemble. Water levels are grouped into 30 cm bins from 650 cm to 800 cm and into 100 cm bins from 800 cm to 900 cm. Stars indicate statistically significant changes. Vertical error bars represent the ensemble spread.

this order is reversed, with lower-emission scenarios showing higher frequencies. We explain this reversal by stronger SLR in higher-emission scenarios, which makes lower water levels less frequent and requires more negative wind surges to reach historical levels.

## B.4 DISCUSSION

While Irazoqui Apecechea et al. (2025) report no robust changes in surge intensity for the southern North Sea, we find significant changes in surge intensity for the German Bight by applying a region-specific statistical storm surge model to climate projections. The projected increase in frequency of wintertime positive wind surges aligns with previous studies focusing on the German Bight (Lang and Mikolajewicz, 2020; Mayer et al., 2022), which, however, rely on single-model experiments. In contrast, we use a CMIP6 multi-model ensemble to strengthen the robustness of the signal. Similar to Lang and Mikolajewicz (2020), we find a clear seasonal contrast, with an increase in positive wind surge events during winter and a decrease in summer. This seasonal divergence appears to be linked to regional shifts in wind patterns. In summer, Lang and Mikolajewicz (2020) report a significant decrease in mean wind speed and more northerly winds in the North Sea, both of which are confirmed by our analysis (Fig. S4 a-c). Supporting this, Heinrich et al. (2025) find a robust decline in the frequency of cyclonic West days over Europe during summer, based on CMIP6 projections. Together, these changes in wind speed, direction, and synoptic conditions likely contribute to the reduced frequency of extreme sea levels in summer (Lang

and Mikolajewicz, 2020), consistent with our findings. In winter, a different pattern emerges. Heinrich et al. (2025)report an increase in westerly wind patterns favorable to storm surges in the German Bight, which is independently confirmed by Schade et al. (2025) using a CMIP6 multi-model ensemble similar to ours. Targeting the German Bight, Ortega et al. (2025) and Krieger and Weisse (2025) identify increasing westerly and northwesterly winds, a trend also evident in our analysis of wind direction and speed during storm surge events. These changes in wind conditions likely explain the increased occurrence of positive wind surges in the German Bight. Furthermore, we find that the increase in storm surge events may not only result from more frequent westerly and northwesterly winds (Mayer et al., 2022), but also from a significant rise in wind speed over the southern North Sea under storm conditions. Changes in wind and storm surge patterns are linked to large-scale circulations, especially storm tracks. In winter, storm track density increases over northwestern Europe, especially around the British Isles, while decreasing over southwestern Europe and the Norwegian Sea, with the strongest changes occurring under SSP5-8.5 (Harvey et al., 2020; Priestley and Catto, 2022). This tri-polar pattern – enhanced activity over northwestern Europe, reduced activity to the south and north – mirrors our analysis of wind conditions associated with storm surges in the German Bight. In contrast, summer shows a broad reduction in storm track density across Northern Europe, especially under higher-emission scenarios (Priestley and Catto, 2022), reducing cyclone activity and associated storm surge risk. These seasonal shifts in storm track density align with our findings on the changing frequency of potential storm surge events.

These changes in storm track behavior and associated storm surge risk are closely linked to the NAO (Mitevski et al., 2025). Using CMIP5 and CMIP6 climate models, Mitevski et al. (2025) isolate the $CO_2$ response of the NAO and find a shift toward more positive and less variable phases, in both winter and summer. This includes an increase in extreme NAO+ events and a decline in extreme NAO- events, especially in winter, resulting in more frequent westerly winds across Europe and the North Atlantic. Our results are consistent with this response, suggesting that the increased occurrence of NAO+ conditions likely contributes to the projected rise in storm surge events in the German Bight.

Nonetheless, our method has certain limitations. Our approach relies on a statistical storm surge model using effective wind from two grid cells. During training, the model identifies and fixes wind directions at each grid cell for the historical time period that favor high surges in Cuxhaven. This fixed setup limits the model's ability to capture future shifts in surge-triggering wind directions. However, such shifts are unlikely in the German Bight, where the coastline shape constrains storm surge-driving winds to predominantly northwesterly directions. Thus, our method can still reliably assess changes in the frequency and magnitude of surge-relevant wind conditions.

Another factor is the three-hourly resolution of the multi-model data. With our approach, we assume high tide at every time step to estimate wind surge frequency. Since high tide occurs only twice daily, this leads to an overestimation of absolute

event counts. However, the relative increase in frequency and change ratios still reflect the expected trends under future climate conditions. This affects not only the projected frequency of wind surges but also our assessment of their combined effect with SLR.

To estimate the joint effect of SLR and projected wind surges on water levels in Cuxhaven, we apply several simplifying assumptions. While it is known that wind surge behavior can change with increasing water depth, we follow Sterl et al. (2009) in assuming that the hydrodynamic response to SLR is neutral, allowing us to add SLR linearly to wind surge projections. We use sea-level projections specifically developed for the North and Baltic Seas, assigning the nearest available grid cell as representative for Cuxhaven. Additionally, we assume a constant MHW level of 650 cm, even though MHW is expected to rise slightly faster than mean sea level. As a result, the combined effect reflects a rough estimate relative to present-day MHW and existing thresholds for storm surge classification. Despite these simplifications, the approach provides a useful first-order estimate of future water level heights under climate change.

## B.5 CONCLUSION

We present a comprehensive assessment of future storm surge risk in the German Bight by applying a simple statistical storm surge model to a CMIP6 multi-model ensemble under three emission scenarios: SSP2-4.5, SSP3-7.0, and SSP5-8.5. By using this multi-model ensemble, we provide a more robust estimate than previous single-model approaches. Our results show a significant increase in the frequency of positive wind surges during winter, particularly under higher-emission scenarios, while summer surge events are projected to decline. These results are consistent with previous single-model studies focusing on the German Bight. Notably, we find that the frequency of extreme wind surge events ($\geqslant$ 150 cm), classified as storm surges, increases by more than 10% under SSP5-8.5 by 2100. This increase is primarily driven by more frequent westerly and northwesterly wind conditions, combined with stronger wind speeds over the southern North Sea. These changes in wind pattern are closely linked to changes in storm track dynamics and increased occurrence of positive NAO phases under future climate conditions.

The combination of projected wind surges and SLR leads to substantial increase in coastal water levels during high tide in Cuxhaven, especially under higher-emission scenarios. We find both moderate and severe present-day storm surge thresholds being exceeded three to five times more often by 2100 compared to the historical period. Despite methodological simplifications, the results offer a rough estimate of how climate change may impact extreme coastal water levels in the German Bight.

## DATA AVAILABILITY STATEMENT

Sea-level rise data were taken from Jensen (2025). Mean high water data are available in Boesch (2025).

## COMPETING INTERESTS

The authors declare there are no conflicts of interest for this manuscript.

## ACKNOWLEDGMENTS

We thank Frank Janssen and Jens Möller for their valuable feedback on this manuscript. This study was funded by the German Federal Ministry of Transport (BMV) in the context of the BMV Research Network. Johanna Baehr received funding by the Deutsche Forschungsgemeinschaft (DFG, German Research Foundation) under Germany's Excellence Strategy, EXC 2037 "Climate, Climatic Change and Society" CLICCS (project no. 390683824), as a contribution to the Center for Earth System Research and Sustainability (CEN) of the University of Hamburg. We thank the German Climate Computing Center (DKRZ) for providing their computing resources.

# SUPPORTING INFORMATION FOR "FUTURE STORM SURGE RISK IN THE GERMAN BIGHT"

Laura Schaffer[1,2], Johanna Baehr[2], and Tim Kruschke[1]

[1]Federal Maritime and Hydrographic Agency (BSH), Hamburg, Germany
[2]Institute of Oceanography, University of Hamburg, Hamburg, Germany

## CONTENTS OF THIS FILE

1. Figures S1 to S4
2. Tables S1 to S2

## INTRODUCTION

Included in this supporting information are:

- Predictor locations and lead times of the three-hourly statistical storm surge model (Figure S1).
- Daily 31-day running mean and 99.45th percentile wind surge values for historical and end-of-century periods across all SSP scenarios, based on multi-model ensemble output (Figure S2).
- Monthly frequency of extreme wind surge events ($\geqslant$ 150 cm) during the historical and end-of-century periods across all SSP scenarios, based on a multi-model ensemble (Figure S3).
- Projected changes in mean wind speed and direction for summer and winter by the end of the century compared to the historical period, shown for all SSP scenarios using CMIP6 multi-model ensemble data (Figure S4).
- List of the nine different CMIP6 models used in the analysis, including associated ensemble sizes (Table S1).
- Number of extreme wind surge events ($\geqslant$ 150 cm) and ensemble sizes for each climate model included in the composite analysis (Table S2).

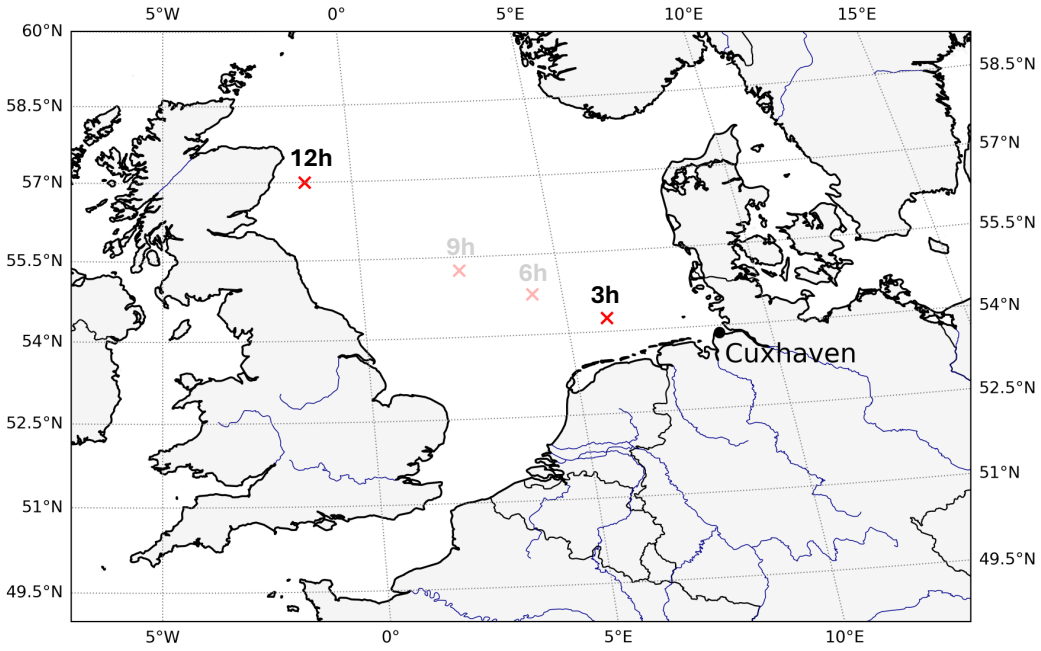


Figure S1: Predictor locations used in the statistical storm surge model, trained on three-hourly data for high water skew surges ($\geqslant$ 80 cm) across the North Sea. Red crosses indicate grid cells retained after elastic net regression, with lead times (in hours) labeled above each location; non-selected grid cells are shown faded.

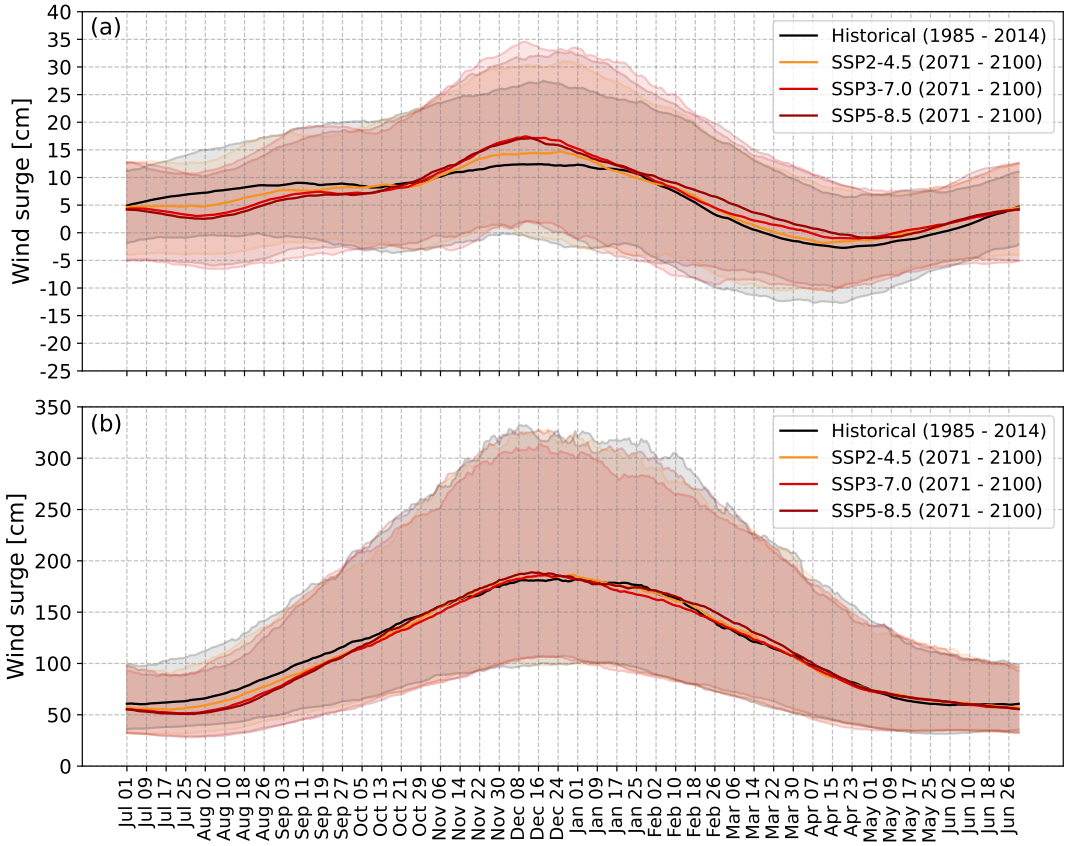


Figure S2: 31-day running mean wind surge (a) and 99.45th percentile wind surge (b) for the historical period (1985-2014; gray) and the end of the century (2071-2100; reddish colors), shown for all three SSP scenarios: SSP2-4.5, SSP3-7.0, and SSP5-8.5. All values are shown for each day of the year. Wind surge values are based on the output of the statistical storm surge model applied to the multi-model ensemble. The bold lines represent the ensemble mean, with the shaded areas indicating the 95% confidence interval.

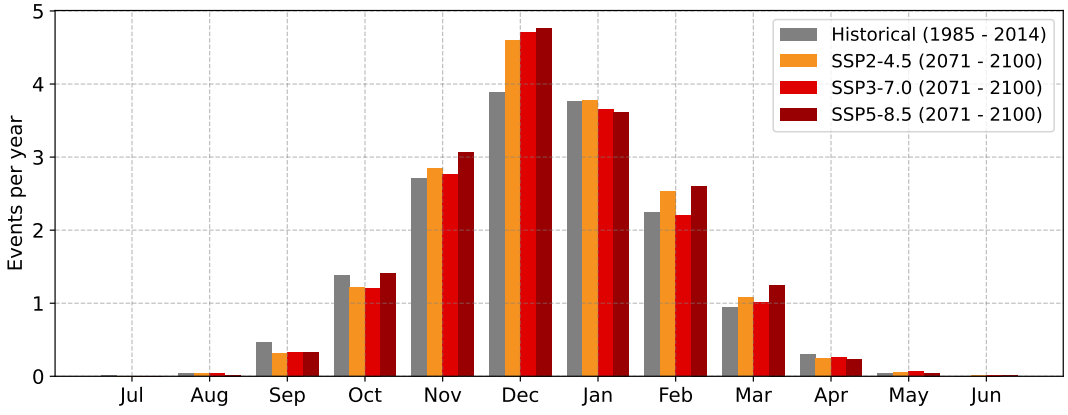


Figure S3: Number of wind surge events $\geqslant$ 150 cm for each month of the year during the historical period (1985-2014; gray) and at the end of the century (2071-2100; reddish colors), shown for all three SSP scenarios: SSP2-4.5, SSP3-7.0, and SSP5-8.5. Wind surge values are based on the output of the statistical storm surge model applied to the multi-model ensemble.

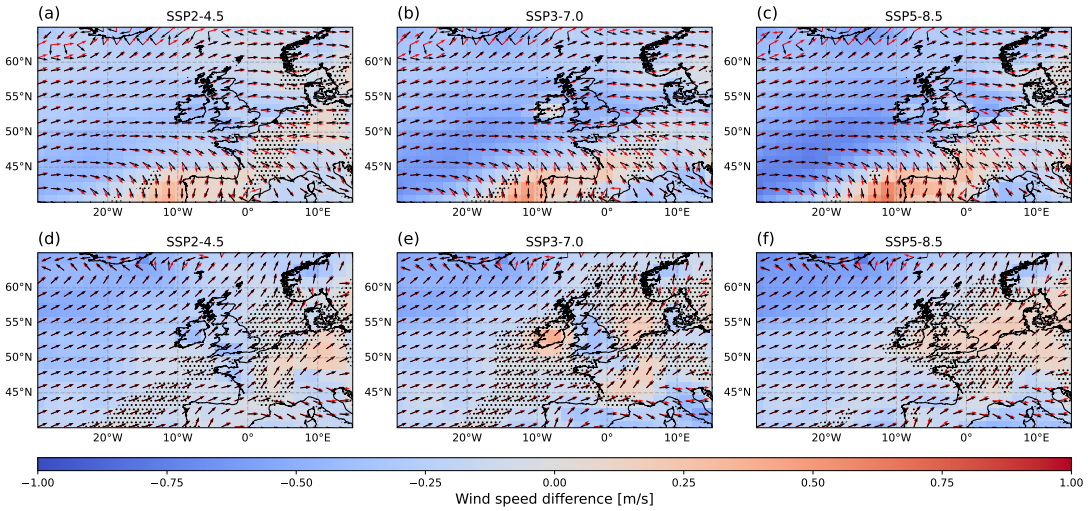


Figure S4: Changes in mean wind speed during the summer months (a-c) and the winter months (d-f) by the end of the century (2071-2100) compared to the historical period (1985-2014). Changes are indicated by color shading and are shown for the three SSP scenarios, based on the wind data from the CMIP6 multi-model ensemble. Black arrows represent the mean wind direction during the historical period, while red arrows show the projected wind direction at the end of the century. Stippling indicates areas where wind speed changes are not statistically significant.

Table S1: List of the nine CMIP6 models used in this study, along with their ensemble sizes.

| | Number of Ensemble Members | | | | |
|---|---|---|---|---|---|
| Model | Historical | SSP2-4.5 | SSP3-7.0 | SSP5-8.5 | Reference |
| AWI-CM-1-1-MR | 1 | 1 | 1 | 1 | Semmler et al. (2018) |
| BCC-CSM2-MR | 1 | 1 | 1 | 1 | Wu et al. (2019) |
| CMCC-CM2-SR5 | 1 | 1 | 1 | 1 | Cherchi et al. (2019) |
| CNRM-CM6-1-HR | 1 | 1 | 1 | 1 | Voldoire et al. (2019) |
| EC-Earth3 | 1 | 1 | 1 | 1 | Döscher et al. (2022) |
| IPSL-CM6A-LR | 6 | 6 | 6 | 6 | Boucher et al. (2020) |
| MIROC6 | 3 | 3 | 3 | 3 | Tatebe et al. (2019) |
| MPI-ESM1-2-LR | 10 | 10 | 10 | 10 | Mauritsen et al. (2019) |
| MRI-ESM2-0 | 1 | 1 | 1 | 1 | Yukimoto et al. (2019) |

Table S2: Number of wind surge events ($\geqslant$ 150 cm) from each climate model contributing to the composite analysis, along with the corresponding ensemble size.

| | | Number of Wind Surge Events ($\geqslant$ 150 cm) | |
|---|---|---|---|
| Model | Ensemble size | Historical (1985-2014) | SSP5-8.5 (2071-2100) |
| AWI-CM-1-1-MR | 1 | 595 | 697 |
| BCC-CSM2-MR | 1 | 366 | 615 |
| CMCC-CM2-SR5 | 1 | 420 | 499 |
| CNRM-CM6-1-HR | 1 | 424 | 484 |
| EC-Earth3 | 1 | 440 | 370 |
| IPSL-CM6A-LR | 6 | 2874 | 3533 |
| MIROC6 | 3 | 1212 | 1124 |
| MPI-ESM1-2-LR | 10 | 4921 | 5279 |
| MRI-ESM2-0 | 1 | 589 | 406 |

# BIBLIOGRAPHY

# BIBLIOGRAPHY


Befort, D., Peter, M., Leckebusch, G., Ulbrich, U., Ganske, A., Rosenhagen, G., and Heinrich, H. (2015). "Identification of storm surge events over the German Bight from atmospheric reanalysis and climate model data." *Nat. Hazard Earth Sys.* 15. DOI: 10.5194/nhess-15-1437-2015.

Bernier, N. B. et al. (2024). "Storm surges and extreme sea levels: Review, establishment of model intercomparison and coordination of surge climate projection efforts (SurgeMIP)." *Weather and Climate Extremes* 45, p. 100689. ISSN: 2212-0947. DOI: https://doi.org/10.1016/j.wace.2024.100689.

Blender, R., Fraedrich, K., and Lunkeit, F. (1997). "Identification of cyclone-track regimes in the North Atlantic." *Quarterly Journal of the Royal Meteorological Society* 123.539, pp. 727–741. DOI: https://doi.org/10.1002/qj.49712353910.

Boesch, A. and Jandt-Scheelke, S. (2020). "A comparison study of tidal prediction techniques for applications in the German Bight." *EGU General Assembly 2020*. DOI: 10.5194/egusphere-egu2020-1640.

Boesch, A. and Müller-Navarra, S. (2019). "Reassessment of long-period constituents for tidal predictions along the German North Sea coast and its tidally influenced rivers." *Ocean Sci.* 15.5, pp. 1363–1379. DOI: 10.5194/os-15-1363-2019.

Boesch, A. (2024). *Skew surge for tide gauge Cuxhaven (1959-2022)*. DOI: 10.60751/96dc-te47.

– (2025). "Calculation of tidal parameters by analysing the semi-monthly inequality." *Reports of the Federal Maritime and Hydrographic Agency; No. 57*. DOI: https://doi.bsh.de/10.57802/t88x-g031.

Böhme, A., Gerkensmeier, B., Bratz, B., Krautwald, C., Müller, O., Goseberg, N., and Gönnert, G. (2023). "Improvements to the detection and analysis of external surges in the North Sea." *Nat. Hazard Earth Sys.* 23.5, pp. 1947–1966. DOI: 10.5194/nhess-23-1947-2023.

Boucher, O. et al. (2020). "Presentation and Evaluation of the IPSL-CM6A-LR Climate Model." *Journal of Advances in Modeling Earth Systems* 12.7, e2019MS002010. DOI: https://doi.org/10.1029/2019MS002010.

Bundesamt für Seeschifffahrt und Hydrographie (2024). *Fact Sheet: Sturmfluten*. URL: https://www.bsh.de/DE/PUBLIKATIONEN/_Anlagen/Downloads/BSH-Informationen/Fact-Sheets/FactSheet_Sturmfluten.html (visited on 08/29/2025).

– (2025a). *Storm surges*. URL: https://www.bsh.de/EN/TOPICS/Water_levels_and_tides/Storm_surges/Storm_surges_node.html (visited on 08/29/2025).

– (2025b). *Tides*. URL: https://www.bsh.de/EN/TOPICS/Water_levels_and_tides/Tides/tides_node.html (visited on 08/29/2025).

Cannon, A. J., Sobie, S. R., and Murdock, T. Q. (2015). "Bias Correction of GCM Precipitation by Quantile Mapping: How Well Do Methods Preserve Changes in Quantiles and Extremes?": *J. Climate* 28.17, pp. 6938–6959. DOI: 10.1175/JCLI-D-14-00754.1.

Cherchi, A. et al. (2019). "Global Mean Climate and Main Patterns of Variability in the CMCC-CM2 Coupled Model." *Journal of Advances in Modeling Earth Systems* 11.1, pp. 185–209. DOI: https://doi.org/10.1029/2018MS001369.

Cosby, A. G., Lebakula, V., Smith, C. N., Wanik, D. W., Bergene, K., Rose, A. N., Swanson, D., and Bloom, D. E. (2024). "Accelerating growth of human coastal populations at the global and continent levels: 2000-2018." *Scientific Reports* 14.1, p. 22489. ISSN: 2045-2322. DOI: 10.1038/s41598-024-73287-x.

Dacre, H. F., Hawcroft, M. K., Stringer, M. A., and Hodges, K. I. (2012). "An Extratropical Cyclone Atlas: A Tool for Illustrating Cyclone Structure and Evolution Characteristics." *Bulletin of the American Meteorological Society* 93.10, pp. 1497–1502. DOI: 10.1175/BAMS-D-11-00164.1.

Danard, M. B., Dube, S. K., Gönnert, G., Munroe, A., Murty, T. S., Chittibabu, P., Rao, A. D., and Sinha, P. C. (2004). "Storm surges from extra-tropical cyclones." *Natural Hazards* 32.2, pp. 177–190. DOI: 10.1023/B:NHAZ.0000031312.98231.81.

Dangendorf, S., Arns, A., Pinto, J., Ludwig, P., and Jensen, J. (2016). "The exceptional influence of storm " Xaver " on design water levels in the German Bight." *Environ. Res. Lett.* 11. DOI: 10.1088/1748-9326/11/5/054001.

Dangendorf, S., Mudersbach, C., Wahl, T., and Jensen, J. (2013). "Characteristics of intra-, inter-annual and decadal sea-level variability and the role of meteorological forcing: the long record of Cuxhaven." *Ocean Dynamics* 63, pp. 209–224. DOI: 10.1007/s10236-013-0598-0.

Dangendorf, S., Müller-Navarra, S., Jensen, J., Schenk, F., Wahl, T., and Weisse, R. (2014). "North Sea Storminess from a Novel Storm Surge Record since AD 1843." *J. Climate* 27.10, pp. 3582–3595. DOI: 10.1175/JCLI-D-13-00427.1.

Dangendorf, S., Sun, Q., Gamage, P. M. M., Wahl, T., Marcos, M., Marzeion, B., Slangen, A., and Mitrovica, J. (2025). "Human-driven sea-level rise has tripled the frequency of coastal sea-level extremes since 1900." *Research Square*. DOI: 10.21203/rs.3.rs-7491013/v1.

de Guttry, C. and Ratter, B. (2022). "Expiry date of a disaster: Memory anchoring and the storm surge 1962 in Hamburg, Germany." *International Journal of Disaster Risk Reduction* 70, p. 102719. ISSN: 2212-4209. DOI: https://doi.org/10.1016/j.ijdrr.2021.102719.

de Vries, H., Breton, M., de Mulder, T., Krestenitis, Y., Ozer, J., Proctor, R., Ruddick, K., Salomon, J. C., and Voorrips, A. (1995). "A comparison of 2D storm surge models applied to three shallow European seas." *Environ. Softw.* 10.1, pp. 23–42. ISSN: 0266-9838. DOI: 10.1016/0266-9838(95)00003-4.

Döscher, R. et al. (2022). "The EC-Earth3 Earth system model for the Coupled Model Intercomparison Project 6." *Geoscientific Model Development* 15.7, pp. 2973–3020. DOI: 10.5194/gmd-15-2973-2022.

Eyring, V., Bony, S., Meehl, G. A., Senior, C. A., Stevens, B., Stouffer, R. J., and Taylor, K. E. (2016). "Overview of the Coupled Model Intercomparison Project Phase 6 (CMIP6) experimental design and organization." *Geoscientific Model Development* 9.5, pp. 1937–1958. DOI: 10.5194/gmd-9-1937-2016.

Fox-Kemper, B. et al. (2021). "Ocean, Cryosphere and Sea Level Change." *Climate Change 2021: The Physical Science Basis. Contribution of Working Group I to the Sixth Assessment Report of the Intergovernmental Panel on Climate Change*. Ed. by Masson-

Delmotte, V. et al. Cambridge, United Kingdom and New York, NY, USA: Cambridge University Press, pp. 1211–1362. DOI: 10.1017/9781009157896.011.

Ganske, A., Fery, N., Gaslikova, L., Grabemann, I., Weisse, R., and Tinz, B. (2018). "Identification of extreme storm surges with high-impact potential along the German North Sea coastline." *Ocean Dynam.* 68, pp. 1371–1382. DOI: 10.1007/s10236-018-1190-4.

Garner, G. G. et al. (2022). *IPCC AR6 Sea Level Projections*. DOI: 10.5281/zenodo.6382554.

Gerber, M., Ganske, A., Müller-Navarra, S., and Rosenhagen, G. (2016). "Categorisation of Meteorological Conditions for Storm Tide Episodes in the German Bight." *Meteorol Z.* 25.4, pp. 447–462. DOI: 10.1127/metz/2016/0660.

Gönnert, G. (2003). "Sturmfluten und Windstau in der Deutschen Bucht - Charakter, Veränderungen und Maximalwerte im 20. Jahrhundert." ger. *Die Küste* 67, p. 185. URL: https://hdl.handle.net/20.500.11970/101500.

Harter, L., Pineau-Guillou, L., and Chapron, B. (2024). "Underestimation of extremes in sea level surge reconstruction." *Sci. Rep-UK* 14.1. Ed. by Science, S. and LLC, B. M., 14875 (12p.) DOI: 10.1038/s41598-024-65718-6.

Harvey, B. J., Cook, P., Shaffrey, L. C., and Schiemann, R. (2020). "The Response of the Northern Hemisphere Storm Tracks and Jet Streams to Climate Change in the CMIP3, CMIP5, and CMIP6 Climate Models." *Journal of Geophysical Research: Atmospheres* 125.23, e2020JD032701. DOI: https://doi.org/10.1029/2020JD032701.

Harvey, B. J., Shaffrey, L. C., and Woollings, T. J. (2014). "Equator-to-pole temperature differences and the extra-tropical storm track responses of the CMIP5 climate models." *Climate Dynamics* 43.5, pp. 1171–1182. DOI: 10.1007/s00382-013-1883-9.

– (2015). "Deconstructing the climate change response of the Northern Hemisphere wintertime storm tracks." *Climate Dynamics* 45.9, pp. 2847–2860. DOI: 10.1007/s00382-015-2510-8.

Heinrich, P., Hagemann, S., and Weisse, R. (2025). "Automated classification of atmospheric circulation types for compound flood risk assessment: CMIP6 model analysis utilising a deep learning ensemble." *Environmental Research Letters* 20.7, p. 074018. DOI: 10.1088/1748-9326/adddcb.

Hersbach H.and Bell, B. et al. (2023). *ERA5 hourly data on single levels from 1940 to present. Copernicus Climate Change Service (C3S) Climate Data Store (CDS)*. data set. DOI: 10.24381/cds.adbb2d47.

Hersbach, H. et al. (2020). "The ERA5 global reanalysis." *Q. J. Roy. Meteor. Soc.* 146.730, pp. 1999–2049. DOI: 10.1002/qj.3803.

Hoerl, A. E. and Kennard, R. W. (1970a). "Ridge Regression: Applications to Nonorthogonal Problems." *Technometrics* 12, pp. 69–82.

– (1970b). "Ridge Regression: Biased Estimation for Nonorthogonal Problems." *Technometrics* 12.1, pp. 55–67. ISSN: 00401706. (Visited on 03/22/2024).

Horn, W. (1960). "Some recent approaches to tidal problems." *Int. Hydrogr. Rev.* 37, pp. 65–84.

Hurrell, J. W. and Deser, C. (2010). "North Atlantic climate variability: The role of the North Atlantic Oscillation." *Journal of Marine Systems* 79.3, pp. 231–244. ISSN: 0924-7963. DOI: https://doi.org/10.1016/j.jmarsys.2009.11.002.

Hurrell, J. W., Kushnir, Y., Ottersen, G., and Visbeck, M. (2003). *The North Atlantic Oscillation: Climatic Significance and Environmental Impact*. Vol. 134. ISBN: 0-87590-994-9. DOI: 10.1029/GM134.

IPCC (2023). "Climate Change 2023: Synthesis Report. Contribution of Working Groups I, II and III to the Sixth Assessment Report of the Intergovernmental Panel on Climate Change. [Core Writing Team, H. Lee and J. Romero (eds.)]" Pp. 35–115. DOI: 10.59327/IPCC/AR6-9789291691647.

Irazoqui Apecechea, M., Melet, A., Menendez, M., Lobeto, H., and Valle-Rodriguez, J. B. (2025). "Projections of changes in extreme storm surges for European coasts using statistical downscaling." *EGUsphere* 2025, pp. 1–29. DOI: 10.5194/egusphere-2025-3558.

Jensen, C. (2025). *DASNordicSLR. Sea Level Projections for Northern Europe (2020-2150). Based on IPCC AR6 SSP Scenarios and NKG Land Uplift Data*. DOI: https://doi.bsh.de/10.60751/3x97-gp60.

Jensen, C., Janssen, F., and Kruschke, T. (2025). "DASNordicSLR - Sea Level Projections for Northern Europe." *EarthArXiv*. DOI: 10.31223/X5TJ24.

Jensen, J., Mudersbach, C., and Dangendorf, S. (2013). "Untersuchungen zum Einfluss der Astronomie und des lokalen Windes auf sich verändernde Extremwasserstände in der Deutschen Bucht." *KLIWAS Schriftenreihe* 25. DOI: 10.5675/Kliwas_25.2013_ExtremwasserstÃd'nde.

Jensen, J., Mudersbach, C., Mueller-Navarra, S. H., Bork, I., Koziar, C., and Renner, V. (2006). "Modellgestützte Untersuchungen zu Sturmfluten mit sehr geringen Eintrittswahrscheinlichkeiten an der deutschen Nordseeküste." URL: https://api.semanticscholar.org/CorpusID:111537190.

Jensen, J. and Müller-Navarra, J. (2008). "Storm surges on the German Coast." *Die Küste* 74, pp. 92–124.

Jochner, M., Schwander, M., and Brönnimann, S. (2013). "Reanalysis of the Hamburg Storm Surge of 1962." *Geographica Bernensia* G89, pp. 19–26. DOI: 10.4480/GB2013.G89.02.

Koopmann, G. (1962). "Wasserstandserhöhungen in der Deutschen Bucht infolge von Schwingungen und Schwallerscheinungen und deren Bedeutung bei der Sturmflut vom 16./17. Februar 1962." *Deutsche Hydrografische Zeitschrift* 15.5, pp. 181–198. ISSN: 0012-0308. DOI: 10.1007/BF02021678.

Krieger, D. and Weisse, R. (2025). "CMIP6 Multi-model Assessment of Northeast Atlantic and German Bight Storm Activity." *EGUsphere* 2025, pp. 1–30. DOI: 10.5194/egusphere-2025-111.

Krieger, D., Krueger, O., Feser, F., Weisse, R., Tinz, B., and Storch, H. von (2020). "German Bight storm activity, 1897–2018." *Int. J. Climatol.* 41.S1, E2159–E2177. DOI: 10.1002/joc.6837.

Krieger, D., Weisse, R., Baehr, J., and Borchert, L. F. (2025). "Machine Learning-Driven Skillful Decadal Predictions of German Bight Storm Surges." *Geophysical Research Letters* 52.4, e2024GL111558. DOI: https://doi.org/10.1029/2024GL111558.

Kron, W. (2013). "Coasts: the high-risk areas of the world." *Natural Hazards* 66.3, pp. 1363–1382. ISSN: 1573-0840. DOI: 10.1007/s11069-012-0215-4.

Lang, A. and Mikolajewicz, U. (2020). "Rising extreme sea levels in the German Bight under enhanced CO2 levels: a regionalized large ensemble approach for the North

Sea." *Climate Dynamics* 55, pp. 1829–1842. DOI: https://doi.org/10.1007/s00382-020-05357-5.

Lee, J.-Y. et al. (2021). "Future Global Climate: Scenario-Based Projections and Near-Term Information." *Climate Change 2021: The Physical Science Basis. Contribution of Working Group I to the Sixth Assessment Report of the Intergovernmental Panel on Climate Change*. Ed. by Masson-Delmotte, V. et al. Cambridge, UK and New York, NY, USA: Cambridge University Press. Chap. 4, pp. 553–672. DOI: 10.1017/9781009157896.006.

Lehmann, J., Coumou, D., Frieler, K., Eliseev, A. V., and Levermann, A. (2014). "Future changes in extratropical storm tracks and baroclinicity under climate change." *Environmental Research Letters* 9.8, p. 084002. DOI: 10.1088/1748-9326/9/8/084002.

Mathis, M., Elizalde, A., Mikolajewicz, U., and Pohlmann, T. (2015). "Variability patterns of the general circulation and sea water temperature in the North Sea." *Progress in Oceanography* 135, pp. 91–112. ISSN: 0079-6611. DOI: https://doi.org/10.1016/j.pocean.2015.04.009.

Mauritsen, T. et al. (2019). "Developments in the MPI-M Earth System Model version 1.2 (MPI-ESM1.2) and Its Response to Increasing CO2." *Journal of Advances in Modeling Earth Systems* 11.4, pp. 998–1038. DOI: https://doi.org/10.1029/2018MS001400.

Mayer, B., Mathis, M., Mikolajewicz, U., and Pohlmann, T. (2022). "RCP8.5-projected changes in German Bight storm surge characteristics from regionalized ensemble simulations for the end of the twenty-first century." *Frontiers in Climate* Volume 4 - 2022. ISSN: 2624-9553. DOI: 10.3389/fclim.2022.992119.

Meyer, E. M. I. and Gaslikova, L. (2024). "Investigation of historical severe storms and storm tides in the German Bight with century reanalysis data." *Natural Hazards and Earth System Sciences* 24.2, pp. 481–499. DOI: 10.5194/nhess-24-481-2024.

Mitevski, I., Lee, S. H., Vecchi, G., Orbe, C., and Polvani, L. M. (2025). "More positive and less variable North Atlantic Oscillation at high CO2 forcing." *npj Climate and Atmospheric Science* 8, p. 171. DOI: 10.1038/s41612-025-01051-7.

Mühr, B., Eisenstein, L., Pinto, J. G., Knippertz, P., Mohr, S., and Kunz, M. (2022). *CEDIM Forensic Disaster Analysis Group (FDA): Winter storm series: Ylenia, Zeynep, Antonia (int: Dudley, Eunice, Franklin) - February 2022 (NW & Central Europe)*. Tech. rep. Karlsruher Institut für Technologie (KIT). 21 pp. DOI: 10.5445/IR/1000143470.

Müller-Navarra, S. H. and Giese, H. (1999). "Improvements of an empirical model to forecast wind surge in the German Bight." *Deutsche Hydrographische Zeitschrift* 51, pp. 385–405. DOI: 10.1007/BF02764162.

Müller-Navarra, S. H., Lange, W., Dick, S., and Soetje, K. C. (2003). "Über die Verfahren der Wasserstands- und Sturmflutvorhersage: hydrodynamisch-numerische Modelle der Nord- und Ostsee und ein empirisch-statistisches Verfahren für die Deutsche Bucht." *Promet* 29, pp. 117–124.

Müller-Navarra, S. H., Seifert, W., Lehmann, H.-A., and Maudrich, S. (2012). "Sturmflutvorhersage für Hamburg 1962 und heute." *Bundesamt für Seeschifffahrt und Hydrographie, Hamburg und Rostock*.

Niehüser, S., Dangendorf, S., Arns, A., and Jensen, J. (2018). "A high resolution storm surge forecast for the German Bight."

O'Neill, B. C. et al. (2016). "The Scenario Model Intercomparison Project (ScenarioMIP) for CMIP6." *Geoscientific Model Development* 9.9, pp. 3461–3482. DOI: 10.5194/gmd-9-3461-2016.

O'Halloran, C. and Silver, M. (2022). "Awareness of ocean literacy principles and ocean conservation engagement among American adults." *Frontiers in Marine Science* Volume 9 - 2022. ISSN: 2296-7745. DOI: 10.3389/fmars.2022.976006.

Olbers, D., Willebrand, J., and Eden, C. (2012). "Forcing of the Ocean." *Ocean Dynamics*. Berlin, Heidelberg: Springer Berlin Heidelberg, pp. 433–444. ISBN: 978-3-642-23450-7. DOI: 10.1007/978-3-642-23450-7_13.

Ortega, M., Rubinetti, S., Konyssova, G., Mayer, B., Sánchez, E., Gutiérrez, C., Wiltshire, K. H., and Sidorenko, V. (2025). "Future Wind Conditions in the German Bight Under RCP8.5 Emissions Scenario (2006–2099) From Regional Coupled Ocean–Atmosphere Model System MPIOM-REMO." *International Journal of Climatology* 45.7, e8814. DOI: https://doi.org/10.1002/joc.8814.

Priestley, M. D. K. and Catto, J. L. (2022). "Future changes in the extratropical storm tracks and cyclone intensity, wind speed, and structure." *Weather and Climate Dynamics* 3.1, pp. 337–360. DOI: 10.5194/wcd-3-337-2022.

Pugh, D. and Woodworth, P. (2014). *Sea-Level Science: Understanding Tides, Surges, Tsunamis and Mean Sea-Level Changes*. Cambridge University Press.

Rubinetti, S., Fofonova, V., Arnone, E., and Wiltshire, K. H. (2023). "A Complete 60-Year Catalog of Wind Events in the German Bight (North Sea) Derived From ERA5 Reanalysis Data." *Earth and Space Science* 10.10, e2023EA003020. DOI: https://doi.org/10.1029/2023EA003020.

Schade, N. H., Jensen, C., and Kruschke, T. (2025). "Large scale atmospheric conditions favoring storm surges in the North and Baltic Seas and possible future changes." *Frontiers in Environmental Science* Volume 13 - 2025. ISSN: 2296-665X. DOI: 10.3389/fenvs.2025.1601836.

Schaffer, L., Baehr, J., and Kruschke, T. (in prep.). "Future Storm Surge Risk in the German Bight."

Schaffer, L., Boesch, A., Baehr, J., and Kruschke, T. (2025). "Development of a wind-based storm surge model for the German Bight." *Natural Hazards and Earth System Sciences* 25.6, pp. 2081–2096. DOI: 10.5194/nhess-25-2081-2025.

Semmler, T., Danilov, S., Rackow, T., Sidorenko, D., Barbi, D., Hegewald, J., Sein, D., Wang, Q., and Jung, T. (2018). *AWI AWI-CM1.1MR model output prepared for CMIP6 CMIP*. DOI: 10.22033/ESGF/CMIP6.359.

Seneviratne, S. (2021). "Weather and Climate Extreme Events in a Changing Climate." *Climate Change 2021 – The Physical Science Basis: Working Group I Contribution to the Sixth Assessment Report of the Intergovernmental Panel on Climate Change*. Cambridge University Press, pp. 1513–1766. DOI: 10.1017/9781009157896.013.

Steffelbauer, D. B., Riva, R. E. M., Timmermans, J. S., Kwakkel, J. H., and Bakker, M. (2022). "Evidence of regional sea-level rise acceleration for the North Sea." *Environmental Research Letters* 17.7, p. 074002. DOI: 10.1088/1748-9326/ac753a.

Sterl, A., Brink, H. van den, Vries, H. de, Haarsma, R., and Meijgaard, E. van (2009). "An ensemble study of extreme storm surge related water levels in the North Sea in a changing climate." *Ocean Science* 5.3, pp. 369–378. DOI: 10.5194/os-5-369-2009.

Tatebe, H. et al. (2019). "Description and basic evaluation of simulated mean state, internal variability, and climate sensitivity in MIROC6." *Geoscientific Model Development* 12.7, pp. 2727–2765. DOI: 10.5194/gmd-12-2727-2019.

Tibshirani, R. (1996). "Regression Shrinkage and Selection Via the Lasso." *Journal of the Royal Statistical Society: Series B (Methodological)* 58.1, pp. 267–288. DOI: 10.1111/j.2517-6161.1996.tb02080.x.

van Rijsbergen, C. (1979). "Information Retrieval." London: Butterworths. URL: http://www.dcs.gla.ac.uk/Keith/Preface.html.

Vestøl, O., Ågren, J., Steffen, H., Kierulf, H., and Tarasov, L. (2019). "NKG2016LU: a new land uplift model for Fennoscandia and the Baltic Region." *Journal of Geodesy* 93, pp. 1759–1779. DOI: 10.1007/s00190-019-01280-8.

Voldoire, A. et al. (2019). "Evaluation of CMIP6 DECK Experiments With CNRM-CM6-1." *Journal of Advances in Modeling Earth Systems* 11.7, pp. 2177–2213. DOI: https://doi.org/10.1029/2019MS001683.

von Storch, H. (2014). "Storm Surges: Phenomena, Forecasting and Scenarios of Change." *Proc. IUTAM* 10, pp. 356–362. ISSN: 2210-9838. DOI: 10.1016/j.piutam.2014.01.030.

von Storch, H., Gönnert, G., and Meine, M. (2008). "Storm surges—An option for Hamburg, Germany, to mitigate expected future aggravation of risk." *Environmental Science Policy* 11.8, pp. 735–742. ISSN: 1462-9011. DOI: https://doi.org/10.1016/j.envsci.2008.08.003.

von Storch, H. and Woth, K. (2008). "Storm surges: perspectives and options." *Sustainability Science* 3.1, pp. 33–43. ISSN: 1862-4057. DOI: 10.1007/s11625-008-0044-2.

Wakelin, S. L., Woodworth, P. L., Flather, R. A., and Williams, J. A. (2003). "Sea-level dependence on the NAO over the NW European Continental Shelf." *Geophysical Research Letters* 30.7. DOI: https://doi.org/10.1029/2003GL017041.

Wilks, D. S. (2011). "Chapter 7 - Statistical Forecasting." *International Geophysics* 100. URL: https://api.semanticscholar.org/CorpusID:125404165.

Williams, J., Horsburgh, K. J., Williams, J. A., and Proctor, R. N. F. (2016). "Tide and skew surge independence: New insights for flood risk." *Geophys. Res. Lett.* 43.12, pp. 6410–6417. DOI: 10.1002/2016GL069522.

Wu, T. et al. (2019). "The Beijing Climate Center Climate System Model (BCC-CSM): the main progress from CMIP5 to CMIP6." *Geoscientific Model Development* 12.4, pp. 1573–1600. DOI: 10.5194/gmd-12-1573-2019.

Yukimoto, S. et al. (2019). "The Meteorological Research Institute Earth System Model Version 2.0, MRI-ESM2.0: Description and Basic Evaluation of the Physical Component." *Journal of the Meteorological Society of Japan. Ser. II* 97.5, pp. 931–965. DOI: 10.2151/jmsj.2019-051.

Zou, H. and Hastie, T. (2005). "Regularization and Variable Selection Via the Elastic Net." *Journal of the Royal Statistical Society Series B: Statistical Methodology* 67.2, pp. 301–320. ISSN: 1369-7412. DOI: 10.1111/j.1467-9868.2005.00503.x.

# EIDESSTATTLICHE VERSICHERUNG

**Eidesstattliche Versicherung**
*Declaration on Oath*

Hiermit erkläre ich an Eides statt, dass ich die vorliegende Dissertationsschrift selbst verfasst und keine anderen als die angegebenen Quellen und Hilfsmittel benutzt habe. Sofern im Zuge der Erstellung der vorliegenden Dissertationsschrift generative Künstliche Intelligenz (gKI) basierte elektronische Hilfsmittel verwendet wurden, versichere ich, dass meine eigene Leistung im Vordergrund stand und dass eine vollständige Dokumentation aller verwendeten Hilfsmittel gemäß der Guten wissenschaftlichen Praxis vorliegt. Ich trage die Verantwortung für eventuell durch die gKI generierte fehlerhafte oder verzerrte Inhalte, fehlerhafte Referenzen, Verstöße gegen das Datenschutz- und Urheberrecht oder Plagiate.

*I hereby declare and affirm that this doctoral dissertation is my own work and that I have not used any aids and sources other than those indicated. If electronic resources based on generative artificial intelligence (gAI) were used in the course of writing this dissertation, I confirm that my own work was the main and value-adding contribution and that complete documentation of all resources used is available in accordance with good scientific practice. I am responsible for any erroneous or distorted content, incorrect references, violations of data protection and copyright law or plagiarism that may have been generated by the gAI.*

Hamburg, den 26.11.2025

Laura Schaffer

## DECLARATION ON CONFORMITY
## ÜBEREINSTIMMUNGSERKLÄRUNG

---

Ich versichere, dass dieses gebundene Exemplar der Dissertation und das in elektronischer Form eingereichte Dissertationsexemplar (über den Docata-Upload) und das bei der Fakultät zur Archivierung eingereichte gedruckte gebundene Exemplar der Dissertationsschrift identisch sind.

*I, the undersigned, declare that this bound copy of the dissertation and the dissertation submitted in electronic form (via the Docata upload) and the printed bound copy of the dissertation submitted to the faculty for archiving are identical.*

Hamburg, den 26.11.2025

Laura Schaffer